JELS

ISSN 2087-2852

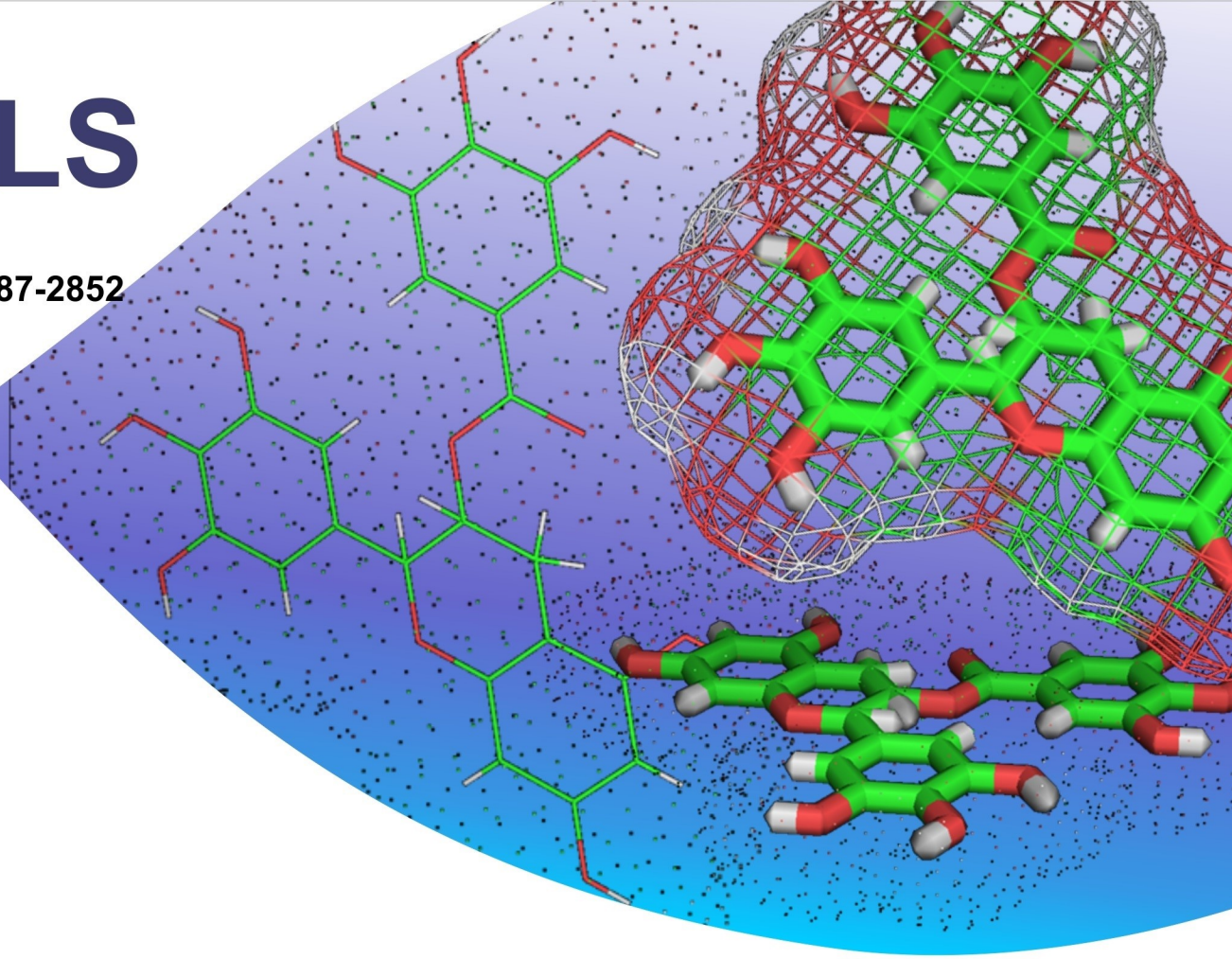

The Journal of EXPERIMENTAL LIFE SCIENCE

J.Exp. Life Sci.	Vol. 10	No. 2	pages. 72-149	June 2020

Published by :
Graduate Program, Universitas Brawijaya

jels.ub.ac.id

ISSN. 2087-2852
E-ISSN. 2338-1655

The Journal of Experimental Life Science

Discovering Living System Concept through Nano, Molecular and Cellular Biology

Editorial Board

Chief Editor
Wenny Bekti Sunarharum, STP., M.Food.St., Ph.D

Editorial Board
Aida Sartimbul, M.Sc. Ph.D - UB
Adi Santoso, M.Sc. Ph.D - LIPI
Nurul Taufiq, M.Sc. Ph.D - BPPT
Arifin Nur Sugiharto, M.Sc. Ph.D -UB
Sukoso, Prof. MSc. Ph.D-UB
Etik Mardliyati, Dr. - BPPT
Soemarno, Ir., MS., Dr., Prof. - UB
M. Sasmito Djati, Ir., MS., Dr., Prof. - UB

Reviewers
Ekwan N. Wiratno, S.Si., M.Si.– UB
Jayarani Fatimah Putri, S.Si., M.Si, Ph.D – UB
Moch. Sasmito Djati, Ir., MS, Dr., Prof. – UB
Irfan Mustafa, S.Si.,M.Si.,Ph.D - UB
Mufidah Afiyanti, Ph.D. – UB
Attabik Mukhammad Amrillah, S.Pi., M.Si - UB
Indah Yanti, S.Si., M.Si. - UB

Editorial Assistant
Jehan Ramdani Haryati, S.S.i, M.Si.

Illustrator
M. Qomaruddin, S.Si., M.M.

Address
The Journal of Experimental Life Science
Building B, 1st Floor, Postgraduate School, University of Brawijaya
Jl. Mayor Jenderal Haryono 169, Malang, 65145
Telp: (0341) 571260 ; Fax: (0341) 580801
Email: jels@ub.ac.id
Web: http://www.jels.ub.ac.id

ISSN. 2087-2852
E-ISSN. 2338-1655

Table of Content

Optimal Control of Cervical Cancer Model with Vaccination and Screening

Karunia Theda Kristanti[1*], Trisilowati[2], Agus Widodo[2]

[1]Master Program of Mathematics, Faculty of Mathematics and Natural Sciences, University of Brawijaya, Malang, Indonesia

[2]Department of Mathematics, Faculty of Mathematics and Natural Sciences, University of Brawijaya, Malang, Indonesia

Abstract

In this paper, an optimal control problem of a cervical cancer model with vaccination and screening as controls is discussed. This vaccine can stimulate the immune system to produce antibodies that can prevent the occurrence of human papillomavirus (HPV) infections, while screening is used as secondary prevention of early detection of cervical cancer cells so that treatment can begin immediately. The models were divided into two compartments, females and males. The female's compartment consists of susceptible, vaccinated, infected, screening, cervical cancer, and recovered females. Meanwhile, the male's compartment consists of susceptible, infected, and recovered males. The purpose of this optimal control was to minimize the number of infected females, infected males, and cervical cancer, as well as to minimize the cost of the controls. Optimal control was obtained by using the Pontryagin principle. Furthermore, an optimal control problem was solved numerically using the Forward-Backward Sweep method to determine the effect of vaccination and screening on the model. The results indicate that vaccination and screening as controls are effective in reducing the subpopulation of HPV infection, which can further reduce the occurrence of cervical cancer.

Keywords: cervical cancer, vaccination, screening, optimal control

INTRODUCTION

Cervical cancer is abnormal growth and development of cervix cells and causes some abnormal organ function [1]. Cervical cancer generally attacks the sexually active female. The cause of cervical cancer is Human Papillomavirus (HPV) infection, especially types 16 and 18. This virus can be transmitted through sexual activity changing partners [2]. The occurrence of cervical cancer is also increased in the population with several factors, including late diagnosis, low socioeconomic status, limited resources, limited infrastructure, and low degrees of education [3].

Cervical cancer can be prevented by HPV vaccinations and screening examinations, such as the Pap smear test or IVA [4]. Vaccination is given to stimulate the immune system to produce antibodies. Further, these antibodies will prevent HPV from infecting cervical cells. Three types of vaccines can be used, namely bivalent, quadrivalent, and nonavalent. Meanwhile, the Pap smear test and the IVA test are also crucial in suppressing the incidence of cervical cancer immediately. This test is an early attempt to find out the presence of cervical cancer cells so that treatment can be done.

Related to the transmission of HPV infection and cervical cancer, in 2014, Pongsumpun [5] modeled the spread of cervical cancer in the female population. This study found that every woman could be infected by HPV when the occurrence of HPV infection is high. Therefore, a woman's risk of cervical cancer will also be high. In contrast to the model discussed by Pongsumpun, Malik *et al.* in 2016 [6] examined the optimal control of the spread of HPV in the presence of vaccination. The model consists of the female's compartment and the male's compartment. It is assumed that only the population of the susceptible female who gets vaccinated. There are three types of vaccines used as controls, namely bivalent, quadrivalent, and nonavalent vaccines.

Furthermore, Sado [7] discussed the model of the spread of cervical cancer in the female population by adding the parameters of vaccination. Based on these results, the vaccine can reduce and control the transmission of cervical cancer due to HPV infection. Regarding the model involving vaccination and screening, Saldana *et al.* [8] discussed the optimal control of HPV infection transmission models without involving cervical cancer. The results of the study of Saldana et al. explain that vaccination and

* Correspondence address:
Karunia Theda Kristanti
Email : kristantikarunia@gmail.com
Address : Dept. Mathematics, University of Brawijaya, Veteran Malang, Malang 65145

screening can reduce the level of infected individuals in both the female and male subpopulations.

This research constructs a mathematical model of cervical cancer by vaccination and screening that modify the model of Malik et al. and Saldana et al. It was assumed that every susceptible female can have only one type of vaccine. In this model, cervical cancer can occur due to sexual interactions between female and male. Next, we investigated the effect of this interaction on both the female and male populations. Therefore, the population was divided into female and male compartments.

MATERIAL AND METHOD

The model of cervical cancer was constructed by involving control vaccination ($\boldsymbol{u_1}$) and screening ($\boldsymbol{u_2}$). Next, an optimal control problem was carried out with the following steps.

a. Construct a cervical cancer model with vaccination and screening as controls.
b. Define the objective functional to minimize the number of populations infected with HPV infection.
c. Apply the Pontryagin principle to solve the optimal control problem.
d. Determine the state, adjoint, and stationary conditions.
e. Perform numerical simulations using the Sweep Forward and Backward method using MATLAB software.

RESULT AND DISCUSSION

Construction Model

In the cervical cancer model, the population was divided into the female population and the male population. The female population was divided into six subpopulation: susceptible female (S_f) consists of individuals who have not vaccinated, vaccinated females (V) consists of individuals who carry out vaccinations, infected females (I_h) consists of individuals infected with HPV, screening female (I_{sc}) consists of individuals who carry out prevention with Pap smear or IVA test, cervical cancer females (C) consists of individuals with cervical cancer, recovered females (R_f) consists of individuals who recover from the infection and having cleared from infection due to treatment or leaving the sexual activity.

Meanwhile, the male population is divided into three subpopulations: susceptible male (S_m) consists of individuals who have a chance of being infected with HPV, infected male (J) consists of individual infected with HPV, and recovered male (R_m) consists of individuals recovering from infection and having cleared from infection. The model is constructed under the assumptions,

1. Only a subpopulation of the susceptible female is given vaccination using one type of vaccine, such as bivalent, quadrivalent, or nonavalent vaccine.
2. Screening is also only done by a subpopulation of infected females.
3. The transmission of HPV infection is caused by an interaction between susceptible subpopulation and infected subpopulation.
4. Individual of recovered subpopulation who has been cleared of HPV infection will be able to lose the immunity and move to a susceptible population.

The diagram of the model can be described as in Figure 1. Based on the assumption above, the model can be written in the form of differential equations:

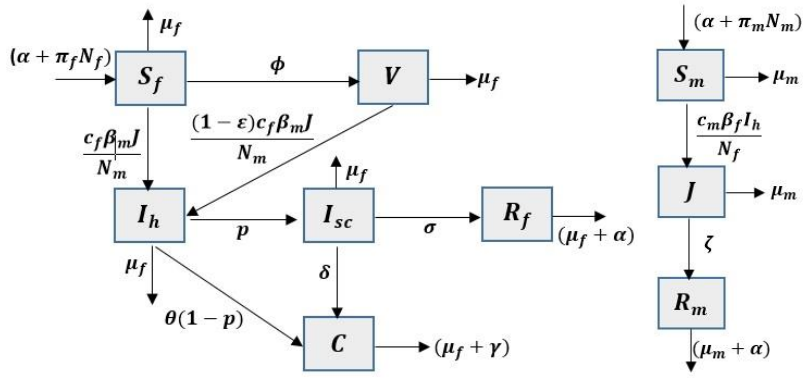

Figure 1. Flow diagram of the model

(1)

$$\frac{dS_f(t)}{dt} = \pi_f N_f(t) - \phi S_f(t) - \frac{c_f\beta_m J(t)S_f(t)}{N_m(t)} - \mu_f S_f(t) + \alpha R_f(t),$$
$$\frac{dV(t)}{dt} = \phi S_f(t) - \mu_f V(t) - (1-\varepsilon)\frac{c_f\beta_m J(t)V(t)}{N_m},$$
$$\frac{dI_h(t)}{dt} = \frac{c_f\beta_m J(t)S_f(t)}{N_m(t)} + (1-\varepsilon)\frac{c_f\beta_m J(t)V(t)}{N_m(t)} - pI_h(t) - \mu_f I_h(t) - \theta(1-p)I_h(t),$$
$$\frac{dI_{sc}(t)}{dt} = pI_h(t) - \sigma I_{sc}(t) - \mu_f I_{sc}(t) - \delta I_{sc}(t),$$
$$\frac{dC(t)}{dt} = \delta I_{sc}(t) + \theta(1-p)I_h(t) - (\mu_f + \gamma)C(t),$$
$$\frac{dR_f(t)}{dt} = \sigma I_{sc}(t) - \mu_f R_f(t) - \alpha R_f(t),$$
$$\frac{dS_m(t)}{dt} = \pi_m N_m(t) - \frac{c_m\beta_f I_h(t)S_m(t)}{N_f(t)} - \mu_m S_m(t) + \alpha R_m(t),$$
$$\frac{dJ(t)}{dt} = \frac{c_m\beta_f I_h(t)S_m(t)}{N_f(t)} - \zeta J(t) - \mu_m J(t),$$
$$\frac{dR_m(t)}{dt} = \zeta J(t) - \mu_m R_m(t) - \alpha R_m(t),$$

where

$N_f(t) = S_f(t) + V(t) + I_h(t) + I_{sc}(t) + C(t) + R_f(t)$, and

$N_m(t) = S_m(t) + J(t) + R_m(t)$.

The description of the parameters used in the model is described in Table 1. We normalize the equations (1) in terms of the proportions

$$\bar{S}_f(t) = \frac{S_f(t)}{N_f(t)}, \bar{V}(t) = \frac{V(t)}{N_f(t)}, \bar{I}_h(t) = \frac{I_h(t)}{N_f(t)},$$
$$\bar{I}_{sc}(t) = \frac{I_{sc}(t)}{N_f(t)}, \bar{C}(t) = \frac{C(t)}{N_f(t)}, \bar{R}_f(t) = \frac{R_f(t)}{N_f(t)},$$
$$\bar{S}_m(t) = \frac{S_m(t)}{N_m(t)}, \bar{J}(t) = \frac{J(t)}{N_m(t)}, \bar{R}_m(t) = \frac{R_m(t)}{N_m(t)}.$$

Then normalized system becomes,

$$\begin{aligned}
\frac{d\bar{S}_f(t)}{dt} &= \pi_f - \phi\bar{S}_f(t) - c_f\beta_m\bar{J}(t)\bar{S}_f(t) - \pi_f\bar{S}_f(t) + \alpha\bar{R}_f(t),\\
\frac{d\bar{V}(t)}{dt} &= \phi\bar{S}_f(t) - (1-\varepsilon)c_f\beta_m\bar{J}(t)\bar{V}(t) - \pi_f\bar{V}(t),\\
\frac{d\bar{I}_h(t)}{dt} &= c_f\beta_m\bar{J}(t)\bar{S}_f(t) + (1-\varepsilon)c_f\beta_m\bar{J}(t)\bar{V}(t) - p\bar{I}_h(t) - \theta(1-p)\bar{I}_h(t) - \pi_f\bar{I}_h(t),\\
\frac{d\bar{I}_{sc}(t)}{dt} &= p\bar{I}_h - \sigma\bar{I}_{sc}(t) - \delta\bar{I}_{sc}(t) - \pi_f\bar{I}_{sc}(t),\\
\frac{d\bar{C}(t)}{dt} &= \delta\bar{I}_{sc}(t) + \theta(1-p)\bar{I}_h(t) - \gamma\bar{C}(t) - \pi_f\bar{C}(t),\\
\frac{d\bar{R}_f(t)}{dt} &= \sigma\bar{I}_{sc}(t) - \pi_f\bar{R}_f(t) - \alpha\bar{R}_f(t),\\
\frac{d\bar{S}_m(t)}{dt} &= \pi_m - c_m\beta_f\bar{I}_h(t)\bar{S}_m(t) - \pi_m\bar{S}_m(t) + \alpha\bar{R}_m(t),\\
\frac{d\bar{J}(t)}{dt} &= c_m\beta_f\bar{I}_h(t)\bar{S}_m(t) - \zeta\bar{J}(t) - \pi_m\bar{J}(t),\\
\frac{d\bar{R}_m(t)}{dt} &= \zeta\bar{J}(t) - \pi_m\bar{R}_m(t) - \alpha\bar{R}_m(t).
\end{aligned} \tag{2}$$

Providing control in the form of vaccination as primary prevention is carried out in susceptible populations to prevent the occurrence of HPV infection. Meanwhile, secondary prevention in the form of screening was done as an early effort to find out the presence of abnormal cells that can cause cervical cancer. The formulation model of cervical cancer transmission with controls in the form of vaccination (u_1) and screening (u_2) is presented as follows.

$$\begin{aligned}
\frac{d\bar{S}_f(t)}{dt} &= \pi_f - u_1(t)\bar{S}_f(t) - c_f\beta_m\bar{J}(t)\bar{S}_f(t) - \pi_f\bar{S}_f(t) + \alpha\bar{R}_f(t),\\
\frac{d\bar{V}(t)}{dt} &= u_1(t)\bar{S}_f(t) - (1-\varepsilon)c_f\beta_m\bar{J}(t)\bar{V}(t) - \pi_f\bar{V}(t),\\
\frac{d\bar{I}_h(t)}{dt} &= c_f\beta_m\bar{J}(t)\bar{S}_f(t) + (1-\varepsilon)c_f\beta_m\bar{J}(t)\bar{V}(t) - u_2(t)\bar{I}_h(t) - \theta\big(1-u_2(t)\big)\bar{I}_h(t) - \pi_f\bar{I}_h(t),\\
\frac{d\bar{I}_{sc}(t)}{dt} &= u_2(t)\bar{I}_h - \sigma\bar{I}_{sc}(t) - \delta\bar{I}_{sc}(t) - \pi_f\bar{I}_{sc}(t),\\
\frac{d\bar{C}(t)}{dt} &= \delta\bar{I}_{sc}(t) + \theta\big(1-u_2(t)\big)\bar{I}_h(t) - \gamma\bar{C}(t) - \pi_f\bar{C}(t),\\
\frac{d\bar{R}_f(t)}{dt} &= \sigma\bar{I}_{sc}(t) - \pi_f\bar{R}_f(t) - \alpha\bar{R}_f(t),\\
\frac{d\bar{S}_m(t)}{dt} &= \pi_m - c_m\beta_f\bar{I}_h(t)\bar{S}_m(t) - \pi_m\bar{S}_m(t) + \alpha\bar{R}_m(t),\\
\frac{d\bar{J}(t)}{dt} &= c_m\beta_f\bar{I}_h(t)\bar{S}_m(t) - \zeta\bar{J}(t) - \pi_m\bar{J}(t),\\
\frac{d\bar{R}_m(t)}{dt} &= \zeta\bar{J}(t) - \pi_m\bar{R}_m(t) - \alpha\bar{R}_m(t).
\end{aligned} \tag{3}$$

Objective Functional

The aim of optimal control in this study was to minimize the number of populations infected with HPV and cervical cancer, as well as to minimize the control costs, namely

$$Z[u_1, u_2] = \int_0^T [I_h + J + C + w_1{u_1}^2(t) + w_2{u_2}^2(t)]dt. \tag{4}$$

w_1 is the weight of control costs in the form of vaccines with ${u_1}^2(t)$ indicates the level of vaccination cost. w_2 is the weight of control costs in the form of screening with ${u_2}^2(t)$ indicates the

level of *screening* cost. Vaccination was given to susceptible female populations, while screening was carried out by populations of females infected with HPV with the appearance of several symptoms. Based on equation (4), we will look for u_1^*, u_2^* which results in minimizing the objective functional value that is

$$Z[u_1^*, u_2^*] = \min\{Z[u_1, u_2]|u_1, u_2 \epsilon \mathbb{V}\}$$

with

$$\mathbb{V} = \{(u_1(t), u_2(t)): 0 \le u_1(t) \le 1, 0 \le u_2(t) \le 1\}.$$

Hamiltonian Function

Based on the objective functional (4) and the constraints on the equation (3) to get the optimal system, the Hamiltonian function is formed as follows.

$$\begin{aligned}H &= I_h + J + C + w_1 {u_1}^2(t) + w_2 {u_2}^2(t)\\ &+\lambda_{\bar{S}_f}(\pi_f - u_1(t)\bar{S}_f(t) - c_f\beta_m\bar{J}(t)\bar{S}_f(t) - \pi_f\bar{S}_f(t)\\ &\quad +\alpha\bar{R}_f(t))\\ &+\lambda_{\bar{V}}\left(u_1(t)\bar{S}_f(t) - (1-\varepsilon)c_f\beta_m\bar{J}(t)\bar{V}(t) - \pi_f\bar{V}(t)\right)\\ &+\lambda_{\bar{I}_h}(c_f\beta_m\bar{J}(t)\bar{S}_f(t) + (1-\varepsilon)c_f\beta_m\bar{J}(t)\bar{V}(t)\\ &\quad -u_2(t)\bar{I}_h(t) - \theta(1-u_2(t))\bar{I}_h(t) - \pi_f\bar{I}_h(t))\\ &+\lambda_{\bar{I}_{sc}}\left(u_2(t)\bar{I}_h - \sigma\bar{I}_{sc}(t) - \delta\bar{I}_{sc}(t) - \pi_f\bar{I}_{sc}(t)\right)\\ &+\lambda_{\bar{C}}\left(\delta\bar{I}_{sc}(t) + \theta(1-u_2(t))\bar{I}_h(t) - \gamma\bar{C}(t) - \pi_f\bar{C}(t)\right)\\ &+\lambda_{\bar{R}_f}\left(\sigma\bar{I}_{sc}(t) - \pi_f\bar{R}_f(t) - \alpha\bar{R}_f(t)\right)\\ &+\lambda_{\bar{S}_m}\left(\pi_m - c_m\beta_f\bar{I}_h(t)\bar{S}_m(t) - \pi_m\bar{S}_m(t) + \alpha\bar{R}_m(t)\right)\\ &+\lambda_{\bar{J}}\left(c_m\beta_f\bar{I}_h(t)\bar{S}_m(t) - \zeta\bar{J}(t) - \pi_m\bar{J}(t)\right)\\ &+\lambda_{\bar{R}_m}(\zeta\bar{J}(t) - \pi_m\bar{R}_m(t) - \alpha\bar{R}_m(t)).\end{aligned} \quad (5)$$

The Hamilton function reaches an optimal solution if the state equation, adjoint equation, and stationary conditions are fulfilled.

State Equations

The state equation for optimal control problems (4) with constraints (3) was obtained by differentiating the Hamiltonian function (5) with respect to each adjoint variable as follows.

$$\begin{aligned}\frac{d\bar{S}_f}{dt} &= \frac{\partial H}{d\lambda_{\bar{S}_f}} = \pi_f - u_1(t)\bar{S}_f(t) - c_f\beta_m\bar{J}(t)\bar{S}_f(t)\\ &\quad -\pi_f\bar{S}_f(t) + \alpha\bar{R}_f(t),\\ \frac{d\bar{V}}{dt} &= \frac{\partial H}{d\lambda_{\bar{V}}} = u_1(t)\bar{S}_f(t) - (1-\varepsilon)c_f\beta_m\bar{J}(t)\bar{V}(t)\\ &\quad -\pi_f\bar{V}(t),\\ \frac{d\bar{I}_h}{dt} &= \frac{\partial H}{d\lambda_{\bar{I}_h}} = c_f\beta_m\bar{J}(t)\bar{S}_f(t) + (1-\varepsilon)c_f\beta_m\bar{J}(t)\bar{V}(t)\\ &\quad -u_2(t)\bar{I}_h(t) - \theta(1-u_2(t))\bar{I}_h(t) - \pi_f\bar{I}_h(t),\end{aligned} \quad (6)$$

$$\begin{aligned}\frac{d\bar{I}_{sc}}{dt} &= \frac{\partial H}{d\lambda_{\bar{I}_{sc}}} = u_2(t)\bar{I}_h - \sigma\bar{I}_{sc}(t) - \delta\bar{I}_{sc}(t)\\ &\quad -\pi_f\bar{I}_{sc}(t),\\ \frac{d\bar{C}}{dt} &= \frac{\partial H}{d\lambda_{\bar{C}}} = \delta\bar{I}_{sc}(t) + \theta(1-u_2(t))\bar{I}_h(t)\\ &\quad -\gamma\bar{C}(t) - \pi_f\bar{C}(t),\\ \frac{d\bar{R}_f}{dt} &= \frac{\partial H}{d\lambda_{\bar{R}_f}} = \sigma\bar{I}_{sc}(t) - \pi_f\bar{R}_f(t) - \alpha\bar{R}_f(t),\\ \frac{d\bar{S}_m}{dt} &= \frac{\partial H}{d\lambda_{\bar{S}_m}} = \pi_m - c_m\beta_f\bar{I}_h(t)\bar{S}_m(t)\\ &\quad -\pi_m\bar{S}_m(t) + \alpha\bar{R}_m(t),\\ \frac{d\bar{J}}{dt} &= \frac{\partial H}{d\lambda_{\bar{J}}} = c_m\beta_f\bar{I}_h(t)\bar{S}_m(t) - \zeta\bar{J}(t) - \pi_m\bar{J}(t),\\ \frac{d\bar{R}_m}{dt} &= \frac{\partial H}{d\lambda_{\bar{R}_m}} = \zeta\bar{J}(t) - \pi_m\bar{R}_m(t) - \alpha\bar{R}_m(t),\end{aligned}$$

with initial condition $\bar{S}_f(0) = \bar{S}_{f_0}, \bar{V}(0) = \bar{V}_0,$
$\bar{I}_h(0) = \bar{I}_{h_0}, \bar{I}_{sc}(0) = \bar{I}_{sc_0}, \bar{C}(0) = \bar{C}_0, \bar{R}_f(0) = \bar{R}_{f_0},$
$\bar{S}_m(0) = \bar{S}_{m_0}, \bar{J}(0) = \bar{J}_0, \bar{R}_m(0) = \bar{R}_{m_0}.$

Adjoint Equations

The adjoint equation for the optimal control problem (4) with the constraint (3) was obtained by differentiating the Hamiltonian function (5) with respect to each state variable as follows.

$$\begin{aligned}\frac{d\lambda_{\bar{S}_f}}{dt} &= -\frac{\partial H}{\partial \bar{S}_f} = \left(u_1(t) + c_f\beta_m\bar{J}(t) + \pi_f\right)\lambda_{\bar{S}_f}\\ &\quad - u_1(t)\lambda_{\bar{V}} - c_f\beta_m\bar{J}(t)\lambda_{\bar{I}_h},\\ \frac{d\lambda_{\bar{V}}}{dt} &= -\frac{\partial H}{\partial \bar{V}} = \left(\pi_f + (1-\varepsilon)c_f\beta_m\bar{J}(t)\right)\lambda_{\bar{V}}\\ &\quad - (1-\varepsilon)c_f\beta_m\bar{J}(t)\lambda_{\bar{I}_h},\\ \frac{d\lambda_{\bar{I}_h}}{dt} &= -\frac{\partial H}{\partial \bar{I}_h} = -1 + \left(u_2(t) + \theta(1-u_2(t)) + \pi_f\right)\lambda_{\bar{I}_h}\\ &\quad -u_2(t)\lambda_{\bar{I}_{sc}} - \theta(1-u_2(t))\lambda_{\bar{C}}\\ &\quad +c_m\beta_f\bar{S}_m(t)\lambda_{\bar{S}_m} - c_m\beta_f\bar{S}_m(t)\lambda_{\bar{J}},\\ \frac{d\lambda_{\bar{I}_{sc}}}{dt} &= -\frac{\partial H}{\partial \bar{I}_{sc}} = \left(\sigma + \delta + \pi_f\right)\lambda_{\bar{I}_{sc}} - \delta\lambda_{\bar{C}} - \sigma\lambda_{\bar{R}_f},\\ \frac{d\lambda_{\bar{C}}}{dt} &= -\frac{\partial H}{\partial \bar{C}} = -1 + \left(\pi_f + \gamma\right)\lambda_{\bar{C}},\\ \frac{d\lambda_{\bar{R}_f}}{dt} &= -\frac{\partial H}{\partial \bar{R}_f} = \pi_f\lambda_{\bar{R}_f} - \alpha\lambda_{\bar{S}_f} + \alpha\lambda_{\bar{R}_f},\\ \frac{d\lambda_{\bar{S}_m}}{dt} &= -\frac{\partial H}{\partial \bar{S}_m} = \left(c_m\beta_f\bar{I}_h(t) + \pi_m\right)\lambda_{\bar{S}_m} - c_m\beta_f\bar{I}_h(t)\lambda_{\bar{J}},\\ \frac{d\lambda_{\bar{J}}}{dt} &= -\frac{\partial H}{\partial \bar{J}} = -1 + c_f\beta_m\bar{S}_f(t)\lambda_{\bar{S}_f}\\ &\quad +(1-\varepsilon)c_f\beta_m\bar{V}(t)\lambda_{\bar{V}}\\ &\quad -\left(c_f\beta_m\bar{S}_f(t) + (1-\varepsilon)c_f\beta_m\bar{V}(t)\right)\lambda_{\bar{I}_h}\\ &\quad +(\zeta + \pi_m)\lambda_{\bar{J}} - \zeta\lambda_{\bar{R}_m},\\ \frac{d\lambda_{\bar{R}_m}}{dt} &= -\frac{\partial H}{\partial \bar{R}_m} = \pi_m\lambda_{\bar{R}_m} - \alpha\lambda_{\bar{S}_m} + \alpha\lambda_{\bar{R}_m},\end{aligned} \quad (7)$$

with transversality conditions $\lambda_{\bar{S}_f}(T) = \lambda_{\bar{V}}(T) = \lambda_{\bar{I}_h}(T) = \lambda_{\bar{I}_{sc}}(T) = \lambda_{\bar{C}}(T) = \lambda_{\bar{R}_f}(T) = \lambda_{\bar{S}_m}(T) = \lambda_{\bar{J}}(T) = \lambda_{\bar{R}_m}(T) = 0$.

Stationer Conditions

Stationer conditions for optimal control problems (4) with constraints (3) was obtained by differentiating the Hamiltonian function (5) toward variables u_1, u_2 as follows.

$$\frac{\partial H}{\partial u_1} = 2w_1u_1(t) - \bar{S}_f(t)\lambda_{\bar{S}_f} + \bar{S}_f(t)\lambda_{\bar{V}} = 0,$$
$$u_1^*(t) = \frac{(\lambda_{\bar{S}_f} - \lambda_{\bar{V}})\bar{S}_f^*(t)}{2w_1},$$
$$\frac{\partial H}{\partial u_2} = 2w_2u_2(t) - \bar{I}_h(t)\lambda_{\bar{I}_h} + \theta\bar{I}_h(t)\lambda_{\bar{I}_h} + \bar{I}_h(t)\lambda_{\bar{I}_{sc}} - \theta\bar{I}_h(t)\lambda_{\bar{C}} = 0,$$
$$u_2^*(t) = \frac{(\lambda_{\bar{I}_h} - \lambda_{\bar{I}_{sc}})\bar{I}_h^*(t) + (\lambda_{\bar{C}} - \lambda_{\bar{I}_h})\theta\bar{I}_h^*(t)}{2w_2}.$$

Given that $0 \le u_1(t) \le 1$ and $0 \le u_2(t) \le 1$, thus we get the equation as follows.

$$u_1^*(t) = \begin{cases} 0, & u_1(t) \le 0, \\ u_1(t), & 0 < u_1(t) < 1, \\ 1, & u_1(t) \ge 1. \end{cases}$$
$$u_2^*(t) = \begin{cases} 0, & u_2(t) \le 0, \\ u_2(t), & 0 < u_2(t) < 1, \\ 1, & u_2(t) \ge 1. \end{cases}$$

In compact notation,

$$u_1^*(t) = \min\left\{\max\left[0, \frac{\left(\lambda_{\bar{S}_f} - \lambda_{\bar{V}}\right)\bar{S}_f^*(t)}{2w_1}\right], 1\right\},$$
$$u_2^*(t) = \min\left\{\max\left[0, \frac{(\lambda_{\bar{I}_h} - \lambda_{\bar{I}_{sc}})\bar{I}_h^*(t) + (\lambda_{\bar{C}} - \lambda_{\bar{I}_h})\theta\bar{I}_h^*(t)}{2w_2}\right], 1\right\}$$

Optimal Solution

The optimal solution was obtained by substituting the optimal control $\vec{u}^*$ to the system of state equations (6) and adjoint equations (7) so that the equation system was obtained as follows.

$$\frac{d\bar{S}_f^*(t)}{dt} = \pi_f - u_1^*(t)\bar{S}_f^*(t) - c_f\beta_m\bar{J}^*(t)\bar{S}_f^*(t) - \pi_f\bar{S}_f^*(t) + \alpha\bar{R}_f^*(t),$$
$$\frac{d\bar{V}^*(t)}{dt} = u_1^*(t)\bar{S}_f^*(t) - (1-\varepsilon)c_f\beta_m\bar{J}^*(t)\bar{V}^*(t) - \pi_f\bar{V}^*(t),$$
$$\frac{d\bar{I}_h^*(t)}{dt} = c_f\beta_m\bar{J}^*(t)\bar{S}_f^*(t) + (1-\varepsilon)c_f\beta_m\bar{J}^*(t)\bar{V}^*(t) - u_2^*(t)\bar{I}_h^*(t) - \theta\left(1-u_2^*(t)\right)\bar{I}_h^*(t) - \pi_f\bar{I}_h^*(t),$$
$$\frac{d\bar{I}_{sc}^*(t)}{dt} = u_2^*(t)\bar{I}_h^* - \sigma\bar{I}_{sc}^*(t) - \delta\bar{I}_{sc}^*(t) - \pi_f\bar{I}_{sc}^*(t),$$
$$\frac{d\bar{C}^*(t)}{dt} = \delta\bar{I}_{sc}^*(t) + \theta\left(1-u_2^*(t)\right)\bar{I}_h^*(t) - \gamma\bar{C}^*(t) - \pi_f\bar{C}^*(t),$$
$$\frac{d\bar{R}_f^*(t)}{dt} = \sigma\bar{I}_{sc}^*(t) - \pi_f\bar{R}_f^*(t) - \alpha\bar{R}_f^*(t),$$
$$\frac{d\bar{S}_m^*(t)}{dt} = \pi_m - c_m\beta_f\bar{I}_h^*(t)\bar{S}_m^*(t) - \pi_m\bar{S}_m^*(t) + \alpha\bar{R}_m^*(t),$$
$$\frac{d\bar{J}^*(t)}{dt} = c_m\beta_f\bar{I}_h^*(t)\bar{S}_m^*(t) - \zeta\bar{J}^*(t) - \pi_m\bar{J}^*(t),$$
$$\frac{d\bar{R}_m^*(t)}{dt} = \zeta\bar{J}^*(t) - \pi_m\bar{R}_m^*(t) - \alpha\bar{R}_m^*(t),$$
$$\frac{d\lambda_{\bar{S}_f}}{dt} = \left(u_1^*(t) + c_f\beta_m\bar{J}^*(t) + \pi_f\right)\lambda_{\bar{S}_f} - u_1^*(t)\lambda_{\bar{V}} - c_f\beta_m\bar{J}^*(t)\lambda_{\bar{I}_h},$$
$$\frac{d\lambda_{\bar{V}}}{dt} = \left(\pi_f + (1-\varepsilon)c_f\beta_m\bar{J}^*(t)\right)\lambda_{\bar{V}} - (1-\varepsilon)c_f\beta_m\bar{J}^*(t)\lambda_{\bar{I}_h},$$
$$\frac{d\lambda_{\bar{I}_h}}{dt} = -1 + \left(u_2^*(t) + \theta\left(1-u_2^*(t)\right) + \pi_f\right)\lambda_{\bar{I}_h} - u_2^*(t)\lambda_{\bar{I}_{sc}} - \theta\left(1-u_2^*(t)\right)\lambda_{\bar{C}} + c_m\beta_f\bar{S}_m^*(t)\lambda_{\bar{S}_m} - c_m\beta_f\bar{S}_m^*(t)\lambda_{\bar{J}},$$
$$\frac{d\lambda_{\bar{I}_{sc}}}{dt} = \left(\sigma + \delta + \pi_f\right)\lambda_{\bar{I}_{sc}} - \delta\lambda_{\bar{C}} - \sigma\lambda_{\bar{R}_f},$$
$$\frac{d\lambda_{\bar{C}}}{dt} = -1 + \left(\pi_f + \gamma\right)\lambda_{\bar{C}},$$
$$\frac{d\lambda_{\bar{R}_f}}{dt} = \pi_f\lambda_{\bar{R}_f} - \alpha\lambda_{\bar{S}_f} + \alpha\lambda_{\bar{R}_f},$$
$$\frac{d\lambda_{\bar{S}_m}}{dt} = \left(c_m\beta_f\bar{I}_h^*(t) + \pi_m\right)\lambda_{\bar{S}_m} - c_m\beta_f\bar{I}_h^*(t)\lambda_{\bar{J}},$$
$$\frac{d\lambda_{\bar{J}}}{dt} = -1 + c_f\beta_m\bar{S}_f^*(t)\lambda_{\bar{S}_f} + (1-\varepsilon)c_f\beta_m\bar{V}^*(t)\lambda_{\bar{V}} - \left(c_f\beta_m\bar{S}_f^*(t) + (1-\varepsilon)c_f\beta_m\bar{V}^*(t)\right)\lambda_{\bar{I}_h} + (\zeta + \pi_m)\lambda_{\bar{J}} - \zeta\lambda_{\bar{R}_m},$$
$$\frac{d\lambda_{\bar{R}_m}}{dt} = \pi_m\lambda_{\bar{R}_m} - \alpha\lambda_{\bar{S}_m} + \alpha\lambda_{\bar{R}_m},$$

with boundary conditions $\bar{S}_f(0) = \bar{S}_{f_0}, \bar{V}(0) = \bar{V}_0,$
$\bar{I}_h(0) = \bar{I}_{h_0}, \bar{I}_{sc}(0) = \bar{I}_{sc_0}, \bar{C}(0) = \bar{C}_0, \bar{R}_f(0) = \bar{R}_{f_0},$
$\bar{S}_m(0) = \bar{S}_{m_0}, \bar{J}(0) = \bar{J}_0, \bar{R}_m(0) = \bar{R}_{m_0}, \lambda_{\bar{S}_f}(T) = \lambda_{\bar{V}}(T) = \lambda_{\bar{I}_h}(T) = \lambda_{\bar{I}_{sc}}(T) = \lambda_{\bar{C}}(T) = \lambda_{\bar{R}_f}(T) = \lambda_{\bar{S}_m}(T) = \lambda_{\bar{J}}(T) = \lambda_{\bar{R}_m}(T) = 0.$

Numerical method and simulations

Numerical simulations are conducted by using initial value $\bar{S}_f(0) = 0.3, \bar{V}(0) = 0.2, \bar{I}_h(0) = 0.1, \bar{I}_{sc}(0) = 0.1, \bar{C}(0) = 0.2, \bar{R}_f(0) = 0.1, \bar{S}_m(0) = \bar{S}_m(0) = 0.5, \bar{J}(0) = 0.3, \bar{R}_m(0) = 0.2.$

The simulation result with and without control is presented in Figure 2. The graph solution is shown with the weight values of controls $w_1 = 0.5$, $w_2 = 0.2$, and parameter values, as presented in Table 1. Based on Figure 2, giving a combination of vaccination and screening control have a positive effect on the spread of HPV infection. It appears that the combination of controls can reduce the spread of HPV infection. It can be seen by decreasing the number of subpopulations of females infected with HPV. Before being given control, the number of females infected with HVP is increased. However, after being given control, the number of infected females decreases very significantly. It also results in a decreasing number of cervical cancers. Meanwhile, the combination of controls also has an impact on male subpopulation. These controls are also able to reduce the infected male subpopulation.

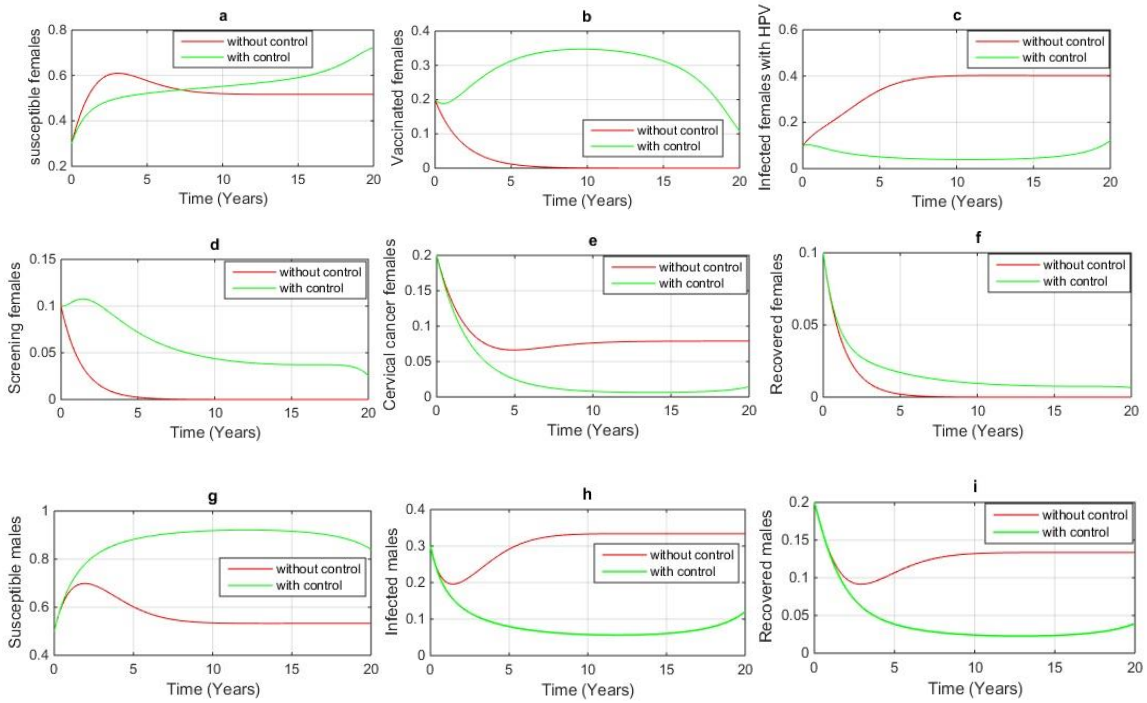

Figure 2. The behavior of cervical cancer model for $t\epsilon[0,20]$

Table 1. Parameter values

Parameter	Description	Value	References
$\pi_f(\pi_m)$	Number of recruitment rate of a sexually-active subpopulation of female (male)	0.5	assumed
$\mu_f(\mu_m)$	The death rate of the subpopulation of female (male)	0.1	assumed
$\beta_f(\beta_m)$	Probability of transfer infection from females to males (males to females)	0.7	[6]
$c_f(c_m)$	The average number of sexual contacts of female for males (male for females)	2	[6]
ϕ	Vaccination rate	0	assumed
ε	Efficacy vaccines	0.8	[6]
p	*Screening* rate	0	assumed
θ	Probability of infected males with HPV can be infected with cervical cancer	0.1	assumed
σ	The recovery rate of females infected	0.2	assumed
ζ	The recovery rate of males infected	0.4	assumed
δ	Probability of *screening* females can be infected with cervical cancer	0.05	assumed
γ	Cervical cancer-induced mortality rate in females	0.01	assumed
α	The rate of immune loss	0.5	assumed

Furthermore, Figure 3 shows the control profile in the form of vaccination and screening. Both of them were used in reducing the number of infected female subpopulations and the infected male subpopulations, as well as the number of cervical cancers. It appears that the vaccination control given is lower than the screening control. It can be influenced by the ability of vaccination given, which has enough impact to reduce the number of infected subpopulations. Meanwhile, screening control must be given in a higher dose to effectively help in suppressing the occurrence of infection.

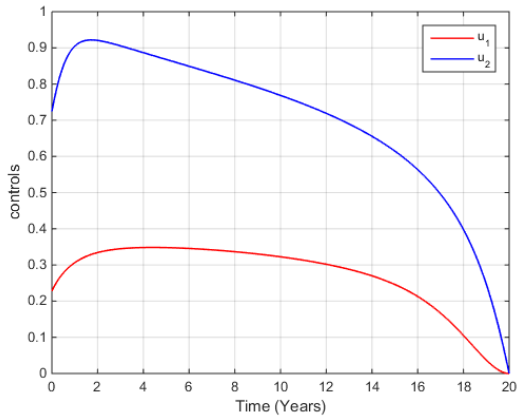

Figure 3. The control profile of cervical cancer model

CONCLUSION

In this study, optimal control of the cervical cancer model has been carried out. Two controls were used in this model, namely vaccination and screening. Based on the results of the study, the provision of these two controls has a positive impact as it can reduce the number of infected subpopulations, both in the subpopulation of infected females and in the subpopulation of infected males. In addition, the administration of this control also leads to a reduced rate of cervical cancer in the female population.

REFERENCES

[1]. Diananda, R. 2008. Mengenal seluk beluk kanker. Katahati. Yogyakarta.

[2]. Centers for Disease Control and Prevention (CDC). 2015. Prevention Human Papillomavirus (HPV). Available at: https://www.cdc.gov/std/HPV/STDFact-HPV.htm.

[3]. Rasjidi, I. 2009. Epidemiologi kanker serviks. *Indonesian Journal of Cancer*. 3. 103-108.

[4]. *Centers for Disease Control and Prevention* (CDC). 2019. Cervical cancer awareness month social media toolkit. *Cancer Center*. The George Washington University.

[5]. Pongsumpun, P. 2014. Mathematical model of cervical cancer due to human papillomavirus infection. Available at: http://www.inase.org/library/2014/athens/bypaper/MMCTSE/MMCTSE-28.pdf

[6]. Malik, T.M., Imran., R. Jayaraman. 2016. Optimal control with multiple human papillomavirus vaccines. *J. Theor. Biol*. 393. 179-193.

[7]. Sado, E.A. 2019. Mathematical modeling of cervical cancer with HPV transmission and vaccination. *Sci. J. Appl. Math. Stat.* 7. 21-25.

[8]. Saldana, F., A. Korobeinikov, I. Barradas, 2019. Optimal control against the human papillomavirus protection versus eradication of the infection. *Abstr. Appl. Anal*. 10. 1-13.

[9]. Lenhart, S., J.T. Workman. 2007. Optimal control applied to biological models. CRC Press. London.

[10]. Bzhalava, D., P. Guan, S. Franceschi, J. Dillner, G. Clifford. 2013. A systematic review of the prevalence of mucosal and cutaneous human papillomavirus types. *J. Virol*. 445. 224-23.

ISSN. 2087-2852
E-ISSN. 2338-1655

Different Intestinal Microbiota Composition Inhibits the *Lactobacillus* Growth in Rheumatoid Arthritis Patients in Malang, Indonesia

Mufidah Mufidah[1,3], Eko Suyanto[1,3], Viranda Susanti[2,3], Hazna Noor Meidinna[1,3], Fatchiyah Fatchiyah[1,3*]

[1]Department of Biology, Faculty of Mathematics and Natural Sciences, Brawijaya University, Malang, Indonesia
[2]Faculty of Dentistry, Brawijaya University , Malang, Indonesia
[3]Research Center of Smart Molecule of Natural Genetics Resource, Brawijaya University, Malang, Indonesia

Abstract

Rheumatoid arthritis (RA) is an autoimmune disease that can cause progressive damage to the joints of patients. The number of patients is expected to increase, along with the exact cause of this disease remains unknown. However, there are several risk factors associated with RA, including dysbiosis. The purpose of this study was to characterize the composition of intestinal microbiota in the RA and control groups through fecal analysis and reveal the association of microbiota composition with RA disease in Indonesia, especially Malang. Fecal samples were obtained from RA patients and controls. Fecal analysis was carried out through several stages, namely the calculation of total bacterial colonies, isolation and characterization of anaerobic bacteria, calculation of the Simpson diversity index, and DNA isolation. Analysis of bacterial composition profiles in fecal was carried out using 6 specific primer sets through PCR analysis. The results of the 16S rRNA PCR analysis showed different microbiota compositions between RA patients and controls. The number of *Enterococcus* bacterial group was lower in the control patients than the RA group, whereas the *Lactobacillus* bacteria decreased in RA patients. In addition, our study found that the existence of bacterial isolate 11 changed the composition of microbiota in RA patients, and the DNA band only appeared in Universal primers. The diversity of bacterial species can provide symbiotic and pathogenetic effects in RA patients.

Keywords: Dysbiosis, intestinal microbiota, PCR, rheumatoid arthritis.

INTRODUCTION

Rheumatoid arthritis (RA) is an autoimmune disease in humans, which is characterized by metabolic disorders and damage to several joints [1]. This disease has received serious attention in Indonesia since the prevalence increased from 6.12% in 2013 [2] to 11.9% in 2018 [3]. The exact cause of RA disease is still unknown hitherto. This phenomenon is caused by RA including in group of multifactor disease. Therefore, the incidence of RA is expected to increase continously.

Previous studies have reported that several factors increase the risk of RA, including age, sex, ethnicity, genetics, and environment [4]. One factor that has been a concern of researchers is the relationship between the emergence of this disease with abnormalities of microbiota (dysbiosis) in the intestinal tract. Dysbiosis may be involved with RA pathogenicity [5]. The condition of dysbiosis in the human digestive tract causes changes in the lining of the intestinal epithelial cells leading to inflammation [6].

Inflammation can trigger the synovial tissue of the joints to form pannus tissue. Pannus tissue will invade bone resulting in damage to the cartilage in the joints [7]. Synovial tissue inflammation can be initiated by several factors, namely immunological and microbial disorders, including oral bacterial DNA in the mouth, increased expression of the peptidylarginine deiminase (PAD) enzyme, unmethylated CpG oligonucleotide, and lipopolysaccharide in bacterial membranes [8].

The human digestive tract contains an abundant and diverse microbial community. Bacterial abundance in the digestive tract is estimated to reach 10^{11} to 10^{12} per-milliliter [9]. In normal condition, the dominant intestinal microbiota originates from the phyla *Firmicutes, Bacteroidetes, Actinobacteria,* and *Verrucomicrobia* [10]. Besides being involved in the digestion and absorption of food, bacteria are also known to be involved in the modulation of the immune system [11-13]. Previous studies have reported changes in the composition of microbiota in the intestine with the immune system lead to autoimmune diseases, which is rheumatoid arthritis [14].

The intestinal microbiota composition of RA patients and controls showed a difference, wherein RA patients, there was a reduction of certain bacteria in the *Bifidobacterium* and *Bacteroides* family [15]. Other studies showed the increase of *Lactobacillus salivarius* species in RA [16]. However, the correlation of the

*Correspondence address:
Prof. Dra. Fatchiyah, M.Kes., Ph.D
Email : fatchiya@ub.ac.id
Address : Faculty of Mathematics and Natural Sciences, Brawijaya University, Veteran Malang, 65145

ISSN. 2087-2852
E-ISSN. 2338-1655

intestinal microbiota composition in affecting the development of RA in humans is still unclear due to various factors of the disease. Therefore, this study was conducted to characterize the composition of intestinal microbiota in RA and control (Non-RA) patients in Indonesia, especially Malang city, through fecal bacteria analysis based on 16S rRNA using PCR. Fecal bacterial analysis can describe the microbial community in the intestine that initiates the emergence of disease in humans because it is related to the fact that fecal is the final product of the digestive process that occurs in the intestine [17]. This research is expected to reveal new things about the composition of microbiota in the intestines of RA sufferers in Indonesia.

MATERIAL AND METHOD

Ethics Clearance

This study was approved with the code of ethics (ethical clearance) No. 051/EC/KEPK-FKIK/ 2019 by the Health Research Ethics Commission (KEPK) Faculty of Medicine and Health Sciences UIN Maulana Malik Ibrahim Malang.

Sampling

Fecal samples were obtained from the hospital with a doctor's intermediary. Patients were recruited based on the sampling method after obtaining an explanation and agreement through the signing of informed consent. Fecal samples were divided into two groups, namely the control (non-RA) and RA group, which consists of three patients as replicates in each. Recruitment of patients as control (Non-RA) and RA group was based on medical records from the hospital with several inclusion criteria of not taking antibiotics, not consuming yogurt during the last four weeks before sampling, and having Indonesian citizenship based on an identity card. Fecal sampling was done by giving patients a sterile set of sampling equipment. Furthermore, fecal samples were stored at 4°C for further analysis [18].

Culture and Determination of Aerobic Mesophilic Bacteria

The 0.5 grams of fecal samples from each patient were collected and then put into NaCl 0.9% using the serial dilution technique. Dilution was carried out to the desired concentration. The suspension was cultured in plate count agar (PCA) media and then aerobically incubated at 37°C for 48 hours. The aerobic bacterial colonies were counted using a colony counter. The calculation was established in triplicate for each control (Non-RA) and the RA group.

Isolation and Characterization of Anaerobic Bacteria

Anaerobic bacterial isolation was done using the serial dilution technique with peptone yeast glucose (PYG) agar. A diluted sample solution of 0.1 mL was put into a sterile petri dish using the pour plate technique and then incubated in the anaerobic jar at room temperature for 48 hours. Anaerobic bacterial colonies were counted and observed for the morphological characteristics. They were purified using the four-way streak plate technique until the pure culture was obtained.

Simpson index calculation

The diversity index used in this study was the Simpson index. The total number of colonies and the number of different species' colonies found in each sample were calculated. The data obtained were analyzed using the Id formula [19]. The Simpson diversity index ranged from 0 to 1. Id values could be calculated using the following formula [20]:

$$Id = \frac{\Sigma\, Ni(Ni-1)}{N(N-1)}$$

Description:
Id = Diversity index
Ni = Number of specific individuals / species found
N = Total number of individuals found

The representation of the index value is as follows:
0.00 - 0.3 = Low dominance, high diversity
0.31 - 0.6 = Moderate dominance, moderate diversity
0.61 - 1.0 = High dominance, low diversity

Bacterial DNA isolation

Anaerobic bacteria were grown in 3 mL of Luria Bertani (LB) broth media for 16 hours at 37°C. Bacterial culture in LB media was centrifuged at 10,000 rpm, 25°C for 5 minutes. The pellets obtained were added with buffer lysis (25 mM EDTA pH 8, 10 mM Tris-HCl pH 8, 100 mM NaCl, 1% SDS, 5 $mg.mL^{-1}$ proteinase-K, and distilled water) and then incubated at 37°C for an hour. Furthermore, the isolation steps of anaerobic bacterial DNA in fecal samples followed the previous method with several modifications [21]. The obtained DNA was stored at -20°C until used.

Bacterial DNA amplification

The PCR technique was based on the previous method with several modifications [21]. The PCR was performed using a thermal cycler with the PCR program set up as follows: hot start at 95°C for 3 minutes; 31 cycles of denaturation at 95°C for 30 seconds, annealing at 55°C for 30 seconds, extension at 72°C for 1 minute; and post

ISSN. 2087-2852
E-ISSN. 2338-1655

extension at 72°C for 5 minutes. Primers used for amplifying the DNA of digestive tract bacteria were the primary set of Universal, *Bacteroides, Clostridium, Bifidobacterium, Enterococcus,* and *Lactobacillus* (Table 1) [22]. The amplification results were detected using 1.5% agarose gel and visualized using the UVP Biodoc-IT Imaging System.

Table 1. Primers used in bacterial DNA amplification

Primer	Primer sequences (5'-3')	Ref
Uni-F	TACGGGAGGCAGCAG	23, 24
Uni-R	ATTAACCGCGGCTGCTGG	
g-Bifid F	CTCCTGGAAACGGGTGG	23
g-Bifid R-	GGTGTTCTTCCCGATATCTACA	
Ent.1017F	CCTTTGACCACTCTAGAG	23
Ent.1263R-	CTTAGCCTCGCGACT	
Lac1-F	AGCAGTAGGGAATCTTCCA	23
Lac2-R	ATTYCACCGCTACACATG	
Bact_F	TCAGTTGTGAAAGTTTGCG	23
Bact_R-	GTRTATCGCMAACAGCGA	
Ccoc_F	TGACGGTACCTGACTAA	24
Ccoc_R-	CTTTGAGTTTYATTCTTGCGAA	

Source: Scientific jounnal [22]

Statistical data analysis

Data were analyzed through descriptive statistics using Microsoft Excel and one-way ANOVA using SPSS 16.0 for windows. Statistical tests performed normality and homogeneity tests with a significance level of 5% ($p < 0.05$).

RESULT AND DISCUSSION

The Amount of Aerobic Mesophilic Microbiota in the Fecal Samples of Control and RA Patients

The aerobic mesophilic count (AMC) performed in three control groups and three RA patients showed differences. The calculation results on Control C1, C2, and C3 were $0.84 \times 10^8 \pm 0.34$, $43800 \times 10^8 \pm 4.79$, and $2.58 \times 10^8 \pm 0.10$, respectively (Table 2). This value indicated that the amount of AMC of C2 was higher than that of C1 and C3. AMC values of RA patients RA1, RA2 and RA3 were $550 \times 10^8 \pm 0.23$, $8.13 \times 10^8 \pm 0.36$ and $0.37 \times 10^8 \pm 0.04$, respectively.

Table 2. Aerobic mesophilic count of bacterial colonies in control and RA patients

No	Sample	Total bacteria (x 10^8 CFU.mL^{-1})	
		P < 0.01	P < 0.05
1	C1	0.84 ± 0.34^{ab}	0.84 ± 0.34^{a}
2	C2	43800 ± 4.79^{abc}	43800 ± 4.79^{abcd}
3	C3	2.58 ± 0.10^{ab}	2.58 ± 0.10^{b}
4	RA1	550 ± 0.23^{abc}	550 ± 0.23^{c}
5	RA2	8.13 ± 0.36^{cd}	8.13 ± 0.36^{d}
6	RA3	0.37 ± 0.04^{bc}	0.37 ± 0.04^{a}

Notes: Values indicate the mean ± standard deviation. Values with the same notation in the column do not differ significantly ($p < 0.01$ and $p < 0.05$).

The RA1 had a higher AMC value than that of RA2 and RA3. The AMC value of C1 was significantly lower than RA2 ($p < 0.01$). There were no significant differences between C2, C3, RA1, and RA3. However, the AMC values of C1, C3, RA1, RA2, and RA3 showed significant differences with a significance level of 5% ($p < 0.05$) (Table 2).

Morphological Characters and Diversity of Microbiota

The most abundant type of microbes found in the human digestive tract was anaerobic bacteria. Previous data reported that the total number of bacteria in each individual's fecal sample consisted of aerobic and anaerobic bacteria. The results of anaerobic bacterial isolation showed the presence of bacterial colonies with 30 different morphological characters. Morphological characters observed included shape, configuration, elevation, optical characteristics, texture, and color. A total of 30 isolates were screened representing each group until eight selected isolates were obtained. The selection was based on characters, including the bacterial isolates found in the control group and RA, found only in the control group, and found only in the RA group (Fig. 1, Table 3).

Our study reported differences in bacterial composition in RA and control patients. The data were used to analyze the diversity index using the Simpson index, so that bacterial dominance could be investigated in each group.

The microbial diversity index in RA and control patients showed variations. The Simpson index values of C1, C2, and C3 were 0.79, 0.68, and 0.73, respectively. However, the Simpson index values of RA1, RA2, and RA3 were 0.63, 0.71, and 0.65, respectively (Table 4). The higher Simpson index value indicated the dominating bacterial group, so it could be inferred that several species of bacteria predominated in each RA and control patients.

Our study observed that isolate 1 dominated in C3, RA1, and RA2. Isolate 10 dominated in C2, RA1, and RA2, while isolate 9 dominated C1. Of the three isolates found in C3, isolate 16 was the least. This indicated that there was a competition between each isolate in C3, which caused the different numbers of each isolate. Differences in the abundance of isolates found in the control and RA group could also represent dysbiosis in the RA group (Table 4).

ISSN. 2087-2852
E-ISSN. 2338-1655

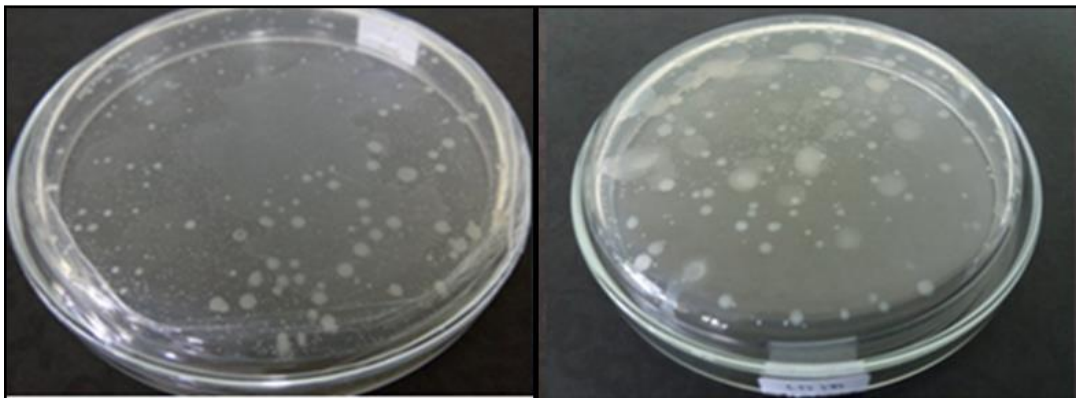

a) **b)**

Figure 1. Morphology of anaerobic bacterial colonies found in fecal samples. a) Control, b) RA patient

Table 3. Morphological characterization of anaerobic bacterial colonies in fecal samples of control and RA patients

Isolate	Shape	Configuration	Elevation	Optical Characteristics	Texture	Color
3*	Oval	Entire	Flat	Clear	Smooth	Clear & White
7*	Round	Entire	Flat	Clear	Smooth	Clear & White
16*	Round	Entire	Pulvinate	Oblique Steep	Smooth	White Milk
18**	Round	Entire	Flat	In diameter	Smooth	Clear, Cloudy & White
1**	Round	Entire	Flat	Clear	Smooth	Clear & White
9**	Round	Entire	Flat	Small	Smooth	White Milk
10**	Round	Entire	Pulvinate	Oblique	Smooth	White Milk
11***	Irregular	Entire	Flat	Oblique	Rough	Clear & White

Description: C = control; RA= RA patient; *= only found in control; **= found in control and RA; ***= only found in RA.

Table 4. Data interpretation on the level of bacterial dominance using the Simpson index in each fecal sample

Isolate	C1	C2	C3	RA1	RA2	RA3
Isolate 1	5	12	124	248	52	27
Isolate 3	1	0	0	0	0	0
Isolate 7	17	0	0	0	0	0
Isolate 9	31	3	0	0	7	0
Isolate 10	2	19	0	207	56	17
Isolate 11	0	0	0	2	4	5
Isolate 16	0	0	23	0	0	0
Isolate 18	0	0	62	3	0	0
Id Simpson	0.79	0.68	0.73	0.63	0.71	0.65

Description: C = control; RA= RA patient

16S rRNA gene analysis

The 16S rRNA gene analysis showed that all selected isolates were successfully amplified at 200bp using universal primers (Fig. 2). Isolate 1, isolate 9, and isolate 18 were identified as *Enterococcus* group with a band size of 300bp. Isolate 3, isolate 7, and isolate 16 were *Lactobacillus* with a band size of 400bp (Fig. 2). However, isolate 10 and isolate 11 were not identified in all markers used in this study.

DISCUSSION

This study showed a significant difference in the amount of aerobic mesophilic number of microbes in the RA and control groups. The amount of aerobic mesophilic number of microbes in the RA group was higher significantly than in the control group ($P<0.01$). Among the 3 control groups, C2 was the sample that had the highest number of microbes. It can be influenced by various factors, such as age, diet, and the disease being suffered [9]. In addition, these factors can cause dysbiosis [25]. This condition results in an imbalance amount of microbes in the digestive tract [26]. Previous studies reported a link between food protein consumption and intestinal microbiota composition based on 16S rRNA gene sequencing analysis [27]. Subjects who consumed beef food showed a reduction in the number of groups of *Bifidobacterium*, *Bacteroides*, and *Clostridium*

bacteria compared with subjects who consumed meatless food [28]. It is known that consumption of peas can increase the group of *Bifidobacterium* and *Lactobacillus* bacteria, while consumption of whey protein can reduce pathogenic *Bacteroides fragilis* and *Clostridium perfringens* [29-30]. This causes the majority of researchers to reveal that protein consumption is positively correlated with microbial diversity [30-32]. We assume the types of food and nutrients consumed are some of the factors that cause the diversity of microbiota composition in the intestine to change, so that it can lead to the emergence of RA disease.

Previous research revealed that the condition of dysbiosis can trigger RA disease through mucosal immune responses induced by collagen-induced arthritis (CIA) [33]. The intestinal microbiota composition correlates with the overall increase in RA symptoms in CIA mice [34]. The susceptibility and severity of arthritis in some rodents kept in a germ-free environment has shown to be reduced compared to rodents induced by the CIA [35]. The part that plays an important role in the interaction between the host and the external environment is the surface of the mucosa, one of which is found in the digestive tract [36]. The mucous layer is continuously exposed to microorganisms that are both commensal and pathogenic [37].

The mucosal immune response is initiated through the introduction of bacterial antigens by mucosa-associated lymphoid tissue (MALT) [38]. MALT follicles containing various immunocompetent cells (T cells, B cells, and APCs) subsequently initiate an immune response [39]. In the RA condition, the barrier which becomes the defense site in the intestine is damaged [40]. This causes bacterial antigen to penetrate the mucosa. The incoming antigen can be eliminated by regulator T cells with specific functions [41].

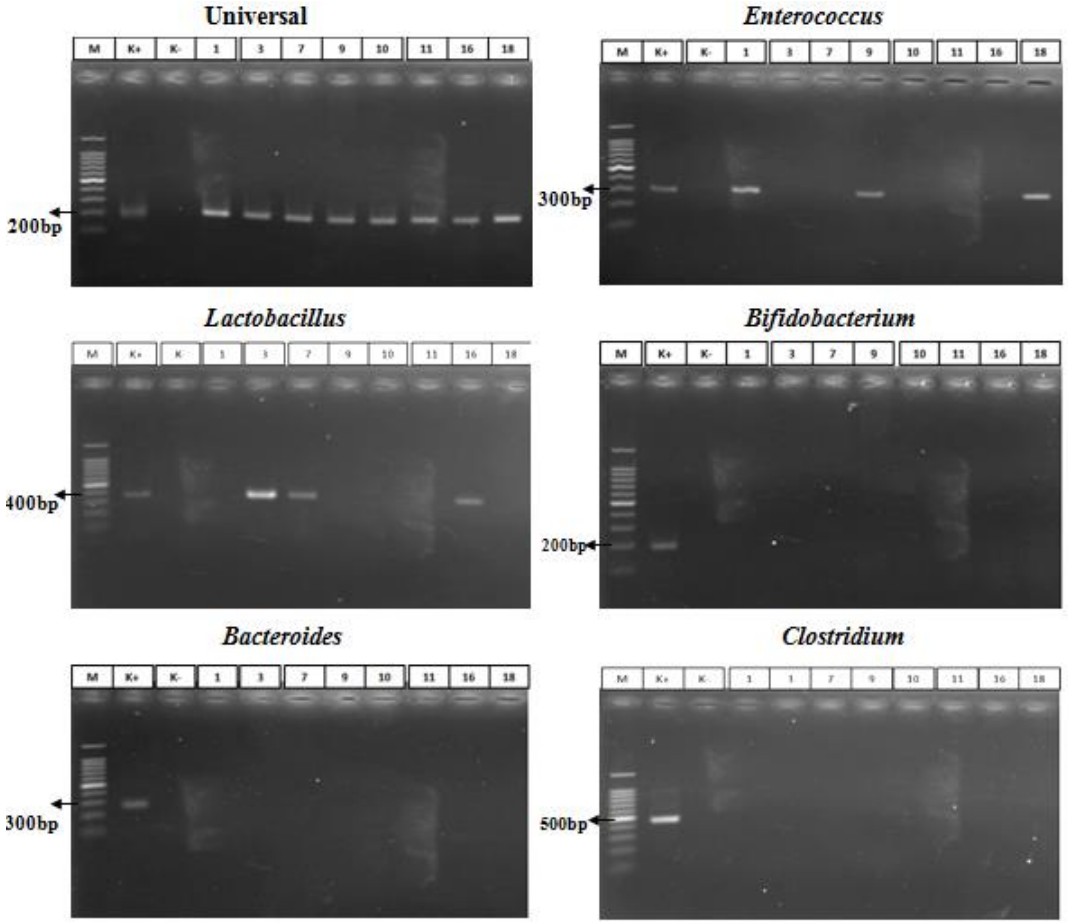

Figure 2. DNA amplification showed bacterial profiling of Universal, *Enterococcus*, *Lactobacillus*, *Bifidobacterium*, *Bacteroides*, and *Clostridium*.

ISSN. 2087-2852
E-ISSN. 2338-1655

Table 5. Interpretation of 16S rRNA PCR products in selected isolates

Isolate	Universal Bacteria	*Enterococcus*	*Lactobacillus*	*Bifidobacterium*	*Bacteroides*	*Clostridium*
	±200bp	±300bp	±400bp	±200bp	±300bp	±500bp
Isolate 1	+	+	-	-	-	-
Isolate 3	+	-	+	-	-	-
Isolate 7	+	-	+	-	-	-
Isolate 9	+	+	-	-	-	-
Isolate 10	+	-	-	-	-	-
Isolate 11	+	-	-	-	-	-
Isolate 16	+	-	+	-	-	-
Isolate 18	+	+	-	-	-	-

Description: + = present; - = absent

In patients with RA, dysregulation of immune system is characterized by the appearance of autoantibodies and autoreactive T cells. RA patients experience dysfunction in circulating regulatory T (Treg) cells as well as an increase of T helper 17 (Th17) in synovial tissue [42]. In this case, macrophages and dendritic cells provide an environment that supports Th17 differentiation and suppresses Treg cell differentiation, which can shift T cell homeostasis toward inflammation [43]. Increasing autoantibody production triggers the formation of more proinflammatory cytokines. The secretion of proinflammatory cytokines stimulates B cells to produce antibodies [44].

One of the factors causing damage to mucosal sites is changes in diversity and abundance of microbes [45]. This triggers inflammation through an imbalance of T cell subpopulations (Th1, Th2, Th17 and Treg cells) [46]. The diversity and abundance of microbes can be analyzed using the Simpson index [47]. The Simpson index analysis results indicate the presence of microbial dominance in the RA and control groups. Overall, the control group had a higher dominance value than the RA group. This showed that the types of microbes in the digestive tract of the RA group were more diverse. High bile acid concentration in the digestive tract is one of the factors that cause the diversity of bacteria. The anatomical structure of the intestine, pH, oxygen pressure, availability of substrate and food flow rate are also the elements that lead to the diversity of bacteria in the digestive tract [48]. The data also showed that the structure of the intestinal microbiota could change periodically.

Changes in microbial diversity in the control and RA group can be evaluated through 16S rRNA gene analysis using PCR. The results of the 16S rRNA gene analysis showed a group of *Enterococcus* found in both the RA and control group (Table 5). The abundance of *Enterococcus* in the control group was lower than in the RA group. *Enterococcus* is one of the pathogenic bacteria that often causes bloodstream infections (BSI) [49]. The common species of *Enterococcus* found in the digestive tract are *E. faecalis* and *E. faecium*. However, *E. faecium* was reported to have a higher level of antibiotic resistance [50]. Previous studies had also found that patients with inflammatory bowel disease and rheumatoid arthritis have a high risk of being infected with *E. faecium* [51]. Infection by various bacteria and viruses often manifests arthritis. Other bacteria associated with infections of the digestive tract are *Salmonella* and *Shigella,* which can cause oligoarticular inflammation or polyarticular arthritis within four weeks of infection [52].

The results of this study reported that *Lactobacillus* bacteria dominated the control group, which was not found in the RA group. Some studies showed the opposite, where *Lactobacillus* was more common in RA patients than in the healthy control group [53,54]. Previous studies mentioned several species of *Lactobacillus*, such as *L. bifidus*, can cause joint swelling in mice [55]. *Lactobacillus* is a normal bacterial flora that has a role as a probiotic. The presence of probiotic microorganisms in the intestinal mucosal layer can prevent the presence of pathogenic bacterial colonization [56]. The presence of *Lactobacillus* bacteria, which acts as probiotic bacteria, causes the *Enterococcus* bacterial group in control patients to be found in small amounts. This bacterium has an immunoregulatory function and plays a role in maintaining intestinal microbiota homeostasis by secreting immunomodulatory agents [57]. Our study found isolate 10 in the control and RA group. Isolate 10 was not identified in all markers. Previous studies showed the presence of other bacteria that could cause inflammation,

namely *Enterobacter cloacae*. *E. cloacae* is one of the LPS-producing gram-negative bacteria [58]. A high LPS number stimulates the inflammatory response by macrophages, which weakens the intestinal epithelial barrier triggering chronic inflammation in both rats and humans [59]. The number of pathogenic bacteria that is not offset by probiotic bacteria exacerbates damage to the intestinal epithelial barrier [60]. The loss of the *Lactobacillus* bacteria group in RA patients is thought to be related to competition with pathogenic bacteria. Previous studies had shown that supplementation with vegetarian foods enriched with *L. plantarum* or *L. casei* could improve health and reduce the level of inflammation in RA patients [61,62]. Therefore, it can be said that different *Lactobacillus* species have different effects in RA patients. It is not yet known with certainty whether RA disease is initiated by the presence of specific pathogenic bacteria [63].

Isolate 11 was the only bacteria found specifically in the RA group, which was not amplified using the primer set used in this study. Isolate 11 is not supposed to be included in the bacterial family *Bacteroides*, *Clostridium*, *Bifidobacterium*, *Enterococcus*, or *Lactobacillus*. *Bifidobacterium*, *Eubacterium rectale*, and *Clostridium coccoides* bacterial groups were reported to decrease in RA patients [64]. Moreover, the *Bacteroides* in the RA group also decreased [65]. Several studies also revealed the presence of other bacteria associated with RA morbidity, including *Mycoplasma fermentans* [66], *E. coli* [67], and *Proteus mirabilis* [68], so that further research is needed to determine the family of bacterial isolate 11.

CONCLUSION

This study found that *Enterococcus* was the bacterial group found in abundance in the control (Non-RA) and RA patients in Malang. The abundance of *Enterococcus* in RA patients was higher than in the control patients. The bacterial group in control patients was dominated by the *Lactobacillus* bacteria, which was not found in the RA patients. The diversity of *Lactobacillus* species can have positive (symbiotic) effects that inhibit the presence of *Enteroccocus* bacteria in RA patients. Further analysis is required to determine the bacterial group of isolate 11 in the RA patients.

ACKNOWLEDGEMENT

This study was supported by the Institute of Research and Community Service (LPPM) Brawijaya University No: 696. 101/UN10.C10/PN /2019. We thank the Biosains institute of Brawijaya University and Microbiology Laboratory of Brawijaya University for providing laboratory equipment and facilities.

REFERENCES

[1] Maeda, Y., K. Takeda. 2017. Role of gut microbiota in rheumatoid arthritis. *J. Clin. Med.* 6(60). 1-7.

[2] RISKESDAS. 2013. Hasil Utama Riskesdas 2013. Available at: www.depkes.go.id.

[3] RISKESDAS. 2018. Hasil Utama Riskesdas 2018. Available at: www.depkes.go.id.

[4] Ciccia, F., A. Ferrante, G. Guggino, G. Triolo. 2016. The role of the gastrointestinal tract in the pathogenesis of rheumatic diseases. *Best Pract. Res. Clin. Rheumatol.* 30. 889–900.

[5] Panebianco, C., A. Andriulli, V. Pazienza. 2018. Pharmacomicrobiomics: Exploiting the drug-microbiota interactions in anticancer therapies. *J. Microbiome.* 6(1). 92.

[6] Asquith, M., D. Elewaut, P. Lin, J.T. Rosenbaum. 2014. The role of the gut and microbes in the pathogenesis of spondyloarthritis. *Best Pract. Res. Clin. Rheumatol.* 28. 687–702.

[7] Venuturupalli, S. 2017. Immune mechanisms and novel target in Rheumatoid arthritis. *Immunol. Allergy Clin. North Am.* 37(2):301-313.

[8] Rosestein, E.D., R.A. Greenwald, L.J. Kushner, G. Weissmann. 2004. Hyphothesis: the humoral timmune respone to oral bacteria provides a stimulus for the development of rheumatoid arthritis. *J. Inflamm.* 28(6). 311-318.

[9] Rinninella, E., P. Raoul, M. Cintoni, F. Franceschi, G. Migggiano. 2019. The 4-H of Biomarkers in arthritis: a lot of help, occasional harm, some hype, increasing hope. *J. Rheumatol.* 46(7). 758-763.

[10] Anderson, J., L. Caplan, J. Yazdany, M.L. Robbins, T. Neogi, K. Michaud, K. G. Saag, J.R. O'del, S. Kazi. 2012. Rheumatoid arthritis disease activity measures: American collage of rheumatology recommendations for use in clinical practice. *J. Arthritis Care Res.* 65(5). 640-647.

[11] Maslowski, K.M., A.T. Vieira, A. Ng, J. Kranich, F. Sierro, D. Yu, *et al.* 2009. Regulation of inflammatory responses by

gut microbiota and chemoattractant receptor GPR43. *J. Nature*. 461. (7268). 1282-6.

[12] Rogier, R., M.I. Koenders, S. Abdollahi-Roodsaz. 2015. Toll-like receptor mediated modulation of T cell response by commensal intestinal microbiota as a trigger for autoimmune arthritis. *J. Immunol.* 1-9.

[13] Stecher, B., W.D. Hardt. 2011. Mechanisms controlling pathogen colonization of the gut. *Curr. Opin. Microbiol.* 14. 82–91.

[14] Diamanti, A. P., M.M. Rosado, R. D'Amelio. 2018. Infectious agents and inflammation: The role of microbiota in autoimmune arthritis. *J. Front. Microbiol*. 8 (2696). 1-9.

[15] Rodriguez, J.P.L., R.E.M. Martines, C.A. Mendoza, N.P. Marin, G.J. Seymour. 2010. Rheumatoid arthritis and the role of oral bacteria. *J. Oral Microbiol.* 2(5784). 1-9.

[16] Zhang, X., D. Zhang, H. Jia, Q. Feng, D. Wang, D. Liang, *et al.* 2015. The oral and gut microbiomes are perturbed in rheumatoid arthritis and partly normalized after treatment. *Nat. Med*. 21(8). 895–905.

[17] Matysik, S., C.I.L. Roy, G. Liebisch, S.P. Claus. 2016. Metabolomics of fecal samples: a practical consideration. *Trend in Food Science and Technology.* 57. 244-255.

[18] Usami, M., M. Miyoshi, Y. Kanbara, M. Aoyama, H. Sakaki, K. Shuno, K. Hirata, M. Takahashi, K. Ueno, Y. Hamada, S. Tabata, T. Asahara, K. Nomoto. 2013. Analysis of fecal microbiota, organic acids and plasma lipids in hepatic cancer patients with or without liver cirrhosis. *J. Clin. Nutr.* 32. 444-451.

[19] Guinness, P., B. Walpole. 2015. Environmental systems and societies for the IB diploma coursebook. Cambridge University Press. USA.

[20] Shaheen, H., D. M. Harper, S.M. Khan, Z. Ullah. 2011. Species diversity, community structure and distribution patterns in westen Himalayan alpine pastures of Kashmir, Pakistan. *Mt Res. Dev.* 31(2). 153-159.

[21] Fatchiyah., E.L. Arumingtyas, S. Widyarti, S. Rahayu. 2011. Biologi molekuler prinsip dasar analisis. Erlangga. Jakarta

[22] Yusuf. F., S. Ilyas, H.A.R. Damanik, Fatchiyah. 2016. Microbiota composition, HSP70 and Caspase-3 expression as marker for colorectal cancer patients in Aceh, Indonesia. *The Indonesian Journal of Internal Medicine*. 48. (4). 289–299.

[23] Vanhoutte T., G. Huys, E.D. Brandt, J. Swings. 2004. Temporal stability analysis of the microbiota in human feses by denaturing gradient gel electrophoresis using universal and group-spesific 16S rRNA gene primers*. FEMS Microbiol. Ecol.* 48(3). 437-46.

[24] Maukonen J., J. Matto, R. Satokari, H. Soderlund, T. Mattila-Sandholm, M. Saarela. 2006. PCR DGGE and RTPCR SGGE show diversity and short-term temporal stability in the Clostridium cocoides-Eubacterium rectal group in the human intestinal microbiota. *FEMS Microbiol. Ecol.* 58. 517-28.

[25] Murphy, R., A.W. Stewart, I. Braithwaite, R. Beasley, R.J. Hancox, E.A. Mitchell. 2014. The ISAAC phase three study group: Antibiotic treatment during infancy and increased body mass index in boys: an international cross-sectional study. *Int. J. Obes. (Lond).* 38(8). 1115-1119.

[26] Round, J.L., S. K. Mazmanian. 2009. The gut microbiome shapes intestinal immune responses during helath and disease*. J. Nat. Rev. Immunol.* 9(5). 313-323.

[27] Conlon, M.A., A.R. Bird. 2015. The impat of diet and lifestyle on gut microbiota and human health. *Nutrients.* 7. 17-44.

[28] Singh, R.K., H.W. Chang, D. Yan, K.M. Lee, D. Ucmak, K. Wong, M. Aabrouk, B. Farahnik, M. Nkamura, T.H. Zhu, T. Bhutani, W. Liao. 2017. Influence of diet on the gut microbiome and implications for human health. *J. Transl. Med.* 15 (73).1-17.

[29] Cotillard, A., S.P. Kennedy, L.C. Kong, E. Prifti, N. Pons, E. Le Chatelier, *et al.* 2013. Dietary intervention impact on gut microbial gene richness. *Nature.* 500. 585-578.

[30] Dominika, S., N. Arjan, R.P. Karyan, K. Henryk. 2011. The study on the impact of Glycated pea protein on human intestinal bacteria. *Int. J. Food Microbiol.* 145. 267-72.

[31] David, L.S., C.F. Maurice, R.N. Carmody, D.B. Gootenberg, J.E. Button, B.E. Wolfe, *et al.* 2014. Diet rapidly and reproducibly alters the human gut microbiome. *Nature.* 505. 559-63.

[32] Clarke, S.F., E.F. Murphy, O. O'Sullivan, A.J. Lucey, M. Humpreys, A. Hogan, *et al.* 2014. Exercise and associated dietary extremes

ISSN. 2087-2852
E-ISSN. 2338-1655

impact on gut microbial diversity. *J. Gut.* 63. 1913-1920.

[33] Jubair, W.K., J.D. Hendrickson, E.L. Severs, H.M. Schulz, S.I.D. Adhikari, J.D. Pagan, *et al.* 2018. Modulation of inflammatory arthritis in mice by gut microbiota through mucosal inflammation and autoantibody generation. *J. Arthritis Rheumatol*. 70(8). 1220-1233.

[34] Xiao, M., X. Fu, Y. Ni, J. Chen, S. Jian, Wang, L. Li, G. Du. 2018. Protective effects of Paederia scandens extract on rheumatoid arthritis mouse model by modulating gut microbiota. *J. Ethnopharmacol*. 226. 97–104.

[35] Liu, X., B. Zeng, J. Zhang, W. Li, F. Mou, H. Wang, Q. Zou, B. Zhong, L. Wu, H. Wei, Y. Fang. 2016. Role of the gut microbiome in modulating arthritis progression in mice. *J. Sci. Rep*. 6. 30594.

[36] Mankia, K., P. Emery. 2015. Is localized autoimmunity the trigger for rheumatoid arthritis? Unravelling new targets for prevention*. J. Discov. Med*. 20. 129–135.

[37] Artis, D. 2008. Epithelial-cell recognition of commensal bacteria and maintenance of immune homeostasis in *the gut. Nat. Rev. Immunol.* 8. 411–420.

[38] Williams A., T. Hussell, C. Lloyd. 2012. Immunology: mucosal and body surface defences. WileyBlackwell. Chichester, West Sussex ; Hoboken, NJ.

[39] Tjärnlund A. 2005. Does IgA play a role in protection against pulmonary tuberculosis?. Stockholm University. Sweden.

[40] Hatakka, K., J. Martio, M. Korpela, M. Herranen, T. Poussa, T. Laasanen, M. Saxelin, H. Vapaatalo, E. Moilanen, R. Korpela. 2003. Effects of probiotic therapy on the activity and activation of mild rheumatoid arthritis–a pilot study. *Scand. J. Rheumatol.* 32. 211–215.

[41] Mayer A.K., A.H. Dalpke. 2007. Regulation of local immunity by airway epithelial cells. *Archivum Immunologi at Therapiae Experimentalis.* 55. 6. 353–62.

[42] Scher, J.U., S.B. Abramson. 2011. The microbiome and rheumatoid arthritis*. Nat. Rev. Rheumatol.* 7. 569–578.

[43] McIlnnes, L.B., G. Schett. 2011. The pathogenesis of rheumatoid arthritis*. N Engl. J. Med.* 365. 23. 1-15.

[44] Lourido, L., F.J. Blanco, C. Ruiz-Romero. 2017. Defining the proteomic landscape of rheumatoid arthritis: progress and prospective clinical applications*. Expert Rev. Proteomics.* 14. 431–444.

[45] Holers, V.M. 2013. Autoimmunity to citrullinated proteins and the initiation of rheumatoid arthritis. *Curr. Opin. Immunol.* 25. 728–735.

[46] Lee, N., W.U. Kim. 2017. Microbiota in T-cell homeostasis and inflammatory diseases. *Exp. Mol. Med.* 49(340). 1-10.

[47] Morris, E.K., T. Caruso, F. Buscot, M. Fischer, C. Hancock, T.S. Maier, T. Meiners, C. Muller, E. Obermainer, D. Prati. 2014. Choosing and using diversity indices: insights for ecological applications from the german biodiversity exploratories. *J. Ecol. Evol.* 4(18). 3514-3524.

[48] Flint, H.J., K.P. Scott, P. Louis, S.H. Duncan. 2012. The role of the gut microbiota in nutrition and health. *Nat. Rev. Gastroenterol. Hepatol.* 9. 577–589.

[49] Pien, B.C., P. Sundaram, N. Raoof, S.F. Costa, S. Mirrett, C.W. Woods, L.B. Reller, M.P. Weinstei. 2010. The clinical and prognostic importance of positive blood culturesin adults*. Am. J. Med*. 123. 819–828.

[50] McBride, S.J., A. Upton, S.A. Roberts. 2010. Clinical characteristics and outcomes ofpatients with vancomycin-susceptible *Enterococcus faecalis* and *Enterococcus faecium bacteraemia* – a five-year retrospective review. *Eur. J. Clin. Microbiol. Infect. Dis.* 29. 107–114.

[51] Billington, E.O., S.H. Phang, D.B. Gregson, J.D.D. Pitout, T. Ross, D.L. Church, K.B. Laupland, M.D. Parkins. 2014. Incidence, risk factors, and outcomes for *Enterococcus* spp. Stream infections: a population-based study. *Int. J. Infect. Dis*. 26. 76-82.

[52] Becker J., K.L. Winthrop. 2010. Update on rheumatic manifestations of infectious diseases. *Curr. Opin. Rheumatol.* 22. 72–77.

[53] Liu, X., Q. Zou, B. Zeng, Y. Fang, H. Wei. 2013. Analysis of fecal Lactobacillus community structure in patients with early rheumatoid arthritis. *J. Curr. Microbiol.* 67. 170–176.

[54] Van de Wiele T., J.T. van Praet., M. Marzorati., M.B. Drennan, D. Elewaut. 2016. How the microbiota shapes rheumatic diseases. *Nat. Rev. Rheumatol*. 12. 398–411.

[55] Abdollahi-Roodsaz S., L.A.B. Joosten, M.I. Koenders, I. Devesa, M.F. Roelofs, T. Radstake, *et al.* 2008. Stimulation of TLR2

ISSN. 2087-2852
E-ISSN. 2338-1655

and TLR4 differentially skews the balance of T cells in a mouse model of arthritis*. J. Clin. Invest.* 118(1). 205–216.

[56] M.V.P. Leão, R.C. Cassia, S.S.F. Dos Santos, C.R.G.E. Silva, A.O.C. Jorge. 2011. Influence of consumption of probiotics on presence of *Enterobacteria* in the oral cavity. *Braz. Oral Res*. 25(5). 401-406.

[57] Mortha, A., A. Chudnovskiy, D. Hashimoto, M. Bogunovic, S.P. Spenver, Y. Belkaid, M. Merad. 2014. Microbiota dependent crosstalk between macrophages and ILC3 promotes intestinal homeostatis. *Science.* 343. 1249-288.

[58] Moreira A.P., T.F. Texeira, A.B. Ferreira, C. PeluzioMdo, C. AlfenasRde. 2012. Influence of a high-fat diet on gut microbiota, intestinal permeability and metabolic endotoxaemia*. Br. J. Nutr.* 108. 801–809.

[59] Lim, S.M., J.J. Jeong, K.H. Woo, M.J. Han, D.H. Kim. 2015. Lactobacillus sakei OK67 ameliorates high-fat diet-induced blood glucose intolerance and obesity in mice by inhibiting gut microbiota lipopolysaccharide production and inducing colon tight junction protein expression. *Nutr. Res*. 36. 337–348.

[60] Guarner, F., A.G. Khan, J. Garisch, R. Eliakim, A. Gangl, A. Thomson, *et al.* 2012. World gastroenterology organisation global guidelines: probiotics and prebiotics. *J. Clin. Gastroenterol.* 46. 468–481.

[61] Pineda, M.A., M.A. McGrath, P.C. Smith, L. AlRiyami, J. Rzepecka., J.A. Gracie, W. Harnett, M.M. Harnett. 2012. The parasitic helminth product ES-62 suppresses pathogenesis in collagen-induced arthritis by targeting the interleukin- 17–producing cellular network at multiple sites. *Arthritis and Rheum.* 64(10). 3168-3178.

[62] Alipour, B., A. Homayouni-Rad, E. Vaghef-Mehrabany, S.K. Sharif, L. Vaghef Mehrabany, M. Asghari-Jafarabadi, M.R. Nakhjavani, J.M. Nia. 2014. Effects of *Lactobacillus casei* supplementation on disease activity and inflammatory cytokines in rheumatoid arthritis patients: a randomized double-blind clinical trial. *Int. J. Rheum. Dis.* 17. 519–527.

[63] Scher, J.U., V. Joshua, A. Artacho, S.A. Roodsaz, J. Ocknger, S. Kullberg, *et al.* 2016. The lung microbiota in early rheumatoid arthritis and autoimmunity*. J. Microbiome*. 4(60). 1-10.

[64] Seksik, P., L. Rigottier-Gois, G. Gramet, M. Sutren, P. Pochart, P. Marteau, R. Jian, J. Doré. 2003. Alterations of the dominant faecal bacterial groups in patients with Crohn's disease of the colon. *J. Gut.* 52(2). 237–242.

[65] Maeda, Y., T. Kurakawa, E. Umemoto, D. Motooka, Y. Ito, K. Gotoh, *et al.* 2016. Dysbiosis contributes to arthritis development via activation of autoreactive T cells in the intestine. *J. Arthritis Rhematol.* 68. 2646–2661.

[66] Sato, N., T. Oizumi, M. Kinbara, T. Sato, H. Funayama, S. Sato, K. Matsuda, H. Takada, S. Sugawara, Y. Endo. 2010. Promotion of arthritis and allergy in mice by aminoglycoglycerophospholipid, a membrane antigen specific to Mycoplasma fermentans*. FEMS Immunol. Med. Microbiol.* 59. 33–41.

[67] Newkirk, M.M., A. Zbar, M. Baron, A.R. Manges. 2010. Distinct bacterial colonization patterns of Escherichia coli subtypes associate with rheumatoid factor status in early inflammatory arthritis. *J. Rheumatol.* 49. 1311–1316.

[68] Ebringer, A., T. Rashid, C. Wilson. 2010. Rheumatoid arthritis, Proteus, anti-CCP antibodies and Karl Popper. *J. Autoimmun. Rev.* 9. 216–223.

ISSN. 2087-2852
E-ISSN. 2338-1655

Bitter Melon (*Momordica charantia* L.) and Star fruit (*Averrhoa bilimbi* L.) on Proinflammatory Cytokines Produced by Hyperglycemic Mice Model

Bella Pradina Novinda Wardani, Sri Rahayu, Muhaimin Rifa'i*

Department of Biology, Faculty of Mathematics and Natural Sciences, University of Brawijaya, Malang, Indonesia

Abstract

Hyperglycemia is a condition of excessive blood glucose in blood plasma caused by damage to the pancreatic beta-cell structure that causes impaired insulin secretion. This study aimed to investigate the combination of Bitter Melon and Star Fruit ethanol extract (SBME) on pro-inflammatory cytokines production in hyperglycemic albino mice models. This study was treated in 25 female albino mice weighing 25-30 and 9 weeks old. STZ was given in a dose of 145 mg.kg^{-1} BW intraperitoneally. Hyperglycemic mice were given orally with SBME ethanol extract at doses 10, 40, and 160 mg.kg^{-1} BW for two weeks. After treatment, pro-inflammatory molecules were analyzed by flow cytometry from the splenic cell. This study showed that SBME treatment can reduce the production of pro-inflammatory cytokines especially IL-1b, but increases IL-6 in hyperglycemic mice. After treatment with SBME at a dose of 40, the IL-1b pro-inflammation molecule decreased significantly (p>0,05). It reached a normal physiological level, but the dose has not been able to reduce the IL-6 pro-inflammation molecule significantly. The conclusion of this study was Bitter Melon and Star Fruit ethanol extract (SBME) with a treatment of 40 mg.kg^{-1} BW can suppress IL-1b pro-inflammatory cytokines in hyperglycemic mice models, but has not been able to reduce the expression of IL-6 pro-inflammatory cytokines. Suggesting this medicinal herb might be a useful strategy for future therapeutic interventions in degenerative diseases or diseases involving cell activation, but a study of doses is needed.

Keywords: *Averrhoa bilimbi* L., Hyperglycemia, Inflammation, *Momordica charantia* L.

INTRODUCTION

Hyperglycemia is a state of the body with high blood glucose levels. The hyperglycemic condition can trigger the appearance of various damages to the body's systems. The condition of hyperglycemia can occur due to several factors such as over nutrition, lack of exercise, stress, free radicals, increased ROS in the body, oxidative stress, and suffering from diabetes. Hyperglycemia is a typical criterion for people with diabetes, whether caused by decreased insulin secretion (Type 1 Diabetes/DMT1) or insulin resistance (Type 2 Diabetes/DMT2). Hyperglycemia, if left unchecked, can cause chronic diabetes to cause death [1].

Hyperglycemia is related to physiological conditions of the body, and one of them is due to immune system disorders. Hyperglycemia can affect the immune system because of increasing levels of pro-inflammatory cytokines IL-1b and IL-6 in monocyte cells. IL-1b and IL-6 are the central pro-inflammatory cytokines produced by macrophages [2]. Increased levels of IL-1b and IL-6 are related to NF-κB activation. NF-κB is an essential regulator of gene expression in pro-inflammatory cytokines [3].

* Correspondence address:
Muhaimin Rifa'i
Email : rifa123@ub.ac.id
Address : Dept. Biology, University of Brawijaya, Veteran Malang, 65145

People with diabetes need therapies throughout their lives to reduce symptoms, prevent disease progression, and prevent the development of complications [4]. Various treatments, such as insulin therapy and diet, have been carried out. One alternative that can be used is herbal medicine. Many traditional medicinal plants have been proven to be used as antidiabetic, such as bitter melon and starfruit.

Bitter melon (*Momordica charantia* L.) was known to have antidiabetic activity [5,6]. Bitter melon contains several active compounds such as saponins, flavonoids, polyphenols, vitamin C, charantin, vicine, and polypeptide-p, which are considered as the main hypoglycemic compounds of bitter melon fruit [6]. Pare fruit contains an active compound that resembles a sulfonylurea (an antidiabetic drug), called momordicin, which can stimulate the β cells of the pancreas to produce insulin [5].

Reactive Oxygen Species (ROS) will increase in the individual suffering from hyperglycemia and lead to oxidative stress [7]. However, an exogenous antioxidant from Starfruit (*Averrhoa bilimbi* L.) can overcome oxidative stress. Antioxidants can be obtained from Starfruit because of the content of active compounds such as flavonoids, saponins, and vitamin C [8]. That compounds are one of the natural ingredients that have antioxidant activity that can reduce inflammation. Therefore, this study was conducted to determine the effect of Bitter

melon and star fruit extract on the pro-inflammation cytokine such as IL-1b and IL-6 in hyperglycemic Balb/c mice.

MATERIAL AND METHOD

STZ Induction

The study was conducted using 25 female albino Balb/C mice aged nine weeks with a weight of 25 g. The treatment consisted of five treatment groups and was repeated five times. Before treatment, the mice were acclimatized for ten days in the pathogen-free facility provided by the Biology Department, Brawijaya University. Mice were maintenance in 12h dark/light with food and water added *ad libitum*. Hyperglycemia was induced by STZ in doses of 145 $mg.kg^{-1}$ BW intraperitoneally. The blood glucose level was tested using the Easy Touch glucometer strip. Mice were considered to have hyperglycemia when the fasting blood glucose level (FBG) > 200 $mg.dL^{-1}$.

Oral Administration of SBME

The simplicia of Bitter melon and starfruit was obtained from Materia Medica (Batu, East Java). The extraction of bitter melon and star fruit simplicia with ethanol was processed using the maceration method with ethanol as a solvent. Soaking was done with 1 L of ethanol and stirred, then filtered after maceration for 1 x 24 hours, and replaced with a new ethanol solvent and repeated thrice. The maceration solution was evaporated on a rotary evaporator. The frozen filtrate was further evaporated in freeze-drying and administered in the hyperglycemia mouse model.

Table 1. Treatment group

Group	Treatment
Normal (C-)	healthy mice
Hyperglycemia (C+)	mice induced by STZ
Treatment 1 (P1)	mice induced by STZ and given an SBME dose of 10 $mg.kg^{-1}$ BW
Treatment 2 (P2)	mice induced by STZ and given an SBME dose of 40 $mg.kg^{-1}$ BW
Treatment 3 (P3)	mice induced by STZ and given an SBME dose of 160 $mg.kg^{-1}$ BW

SBME was given orally with different doses (10, 40, or 160 $mg.kg^{-1}$ BW) in hyperglycemic mice models once a day for two weeks. The female balb/c mice were divided into five different groups following the oral administration of SBME. The five groups are as follows (Table 1). The design of this study was approved by the ethics commission number 1109-KEP-UB.

Spleen Cells Isolation

On the last day of treatment, mice were sacrificed, then the spleen was collected and washed in 2 mL PBS solution in a sterile petri dish. The spleen was crushed and homogenates were centrifugated at 1500 rpm at 10°C for 5 min. The supernatant was removed and the pellet resuspended with 1 mL sterile PBS.

Flow Cytometry Analysis

To analyze the SBME against pro-inflammatory cytokines, flow cytometry analysis was performed. Flow cytometric analysis was performed by FACS CaliburTM (BD-Biosciences, San Jose, CA). Intracellular cytokine staining was performed by a Cytoperm/Cytofix kit (BD-Biosciences Pharmingen) according to the manufacturer protocol and modified by Rifa'i [9]. Total of 200 µL isolated cells were taken and placed on microtubes and centrifugated at 2500 rpm for 5 minutes with 4°C temperature. Afterward, the supernatant was separated and added with 40 µL of antibody staining, then incubated for 15-20 minutes in the icebox (in the dark condition). The cells were then combined with 300 µL of PBS sterile and placed into flow cytometry for analysis.

Data Analysis

The data were analyzed using one-way ANOVA with significance level $p < 0.05$ using SPSS to determine the relationship between variables. It then continued with a Tukey test to find the most involving variable.

RESULT AND DISCUSSION

SBME Inhibits IL-Ib Expression in CD4 Cells

The administration of Bitter melon and starfruit (SBME) showed significant results. The relative number of $CD4^{+}IL\text{-}1b^{+}$ decreased compared to hyperglycemia positive control. This study tested three groups of different doses of SBME and compared them to negative controls and hyperglycemia positive control. The result showed a decrease in inflammation of IL-1b produced by CD4 in healthy mice was 7.55%. After being injected by STZ, the number of inflammations of IL-1b produced by CD4 increased became 10.01% and this value is significant with healthy mice ($p<0.05$) (Fig. 1).

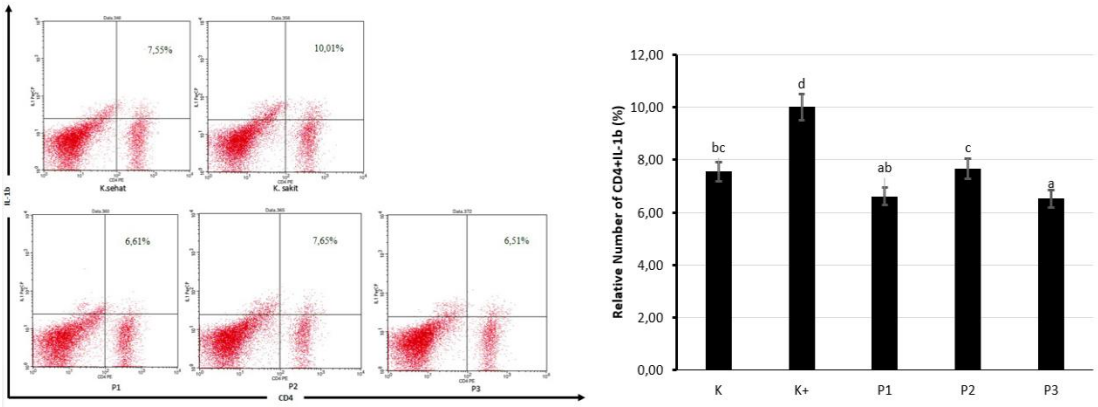

Figure 1. Production profile of IL-1b cytokine by CD4 T cells total percentage. SBME suppressed IL-1b expression in CD4 cells.

(**K**: a healthy group, K+ is a positive control induced with 145mg.kg^{-1} body weight STZ, **P1**: treatment 1 with STZ injection and 10 mg.kg^{-1} SBME, **P2**: treatment 2 with STZ injection and 40 mg.kg^{-1} SBME, **P3**: treatment3 with STZ injection and 160 mg.kg^{-1} SBME).

The administration of SBME in P1, P2, and P3 groups decreased the inflammation number significantly ($p<0.05$). The result showed that the inflammation number of IL-1b produced by CD4 T cells for P1 became 6.61%, P2 became 7.65%, and P3 became 6.51% compared to hyperglycemic positive, which 10.01%. This result showed that IL-1b produced by CD4 T cells seems important in susceptibility and progression of hyperglycemia. P3 became 6.51% compared to hyperglycemic positive, which 10.01%. This result showed that IL-1b produced by CD4 T cells seems important in susceptibility and progression of hyperglycemia.

The administration of SBME in P2 with doses 40 mg.kg^{-1} BW was significantly decreasing the production of IL-1b pro-inflammatory cytokine by CD4 T cells. This treatment has a more significant effect on the number of CD4 T cells that produce IL-1b compared to a dose of 10 mg.kg^{-1} BW and 160 mg.kg^{-1} BW. SBME with specific doses can be used to reduce inflammation in patients with hyperglycemia because it can reduce the relative number of macrophage cells that produce IL-1b pro-inflammatory cytokines. IL-1b is a type of pro-inflammatory cytokine that plays a role in mediating chronic inflammation and is produced mainly by macrophages and CD4+ T cells, whose actions are mediated by the activation of kappa B (NF-κB) nuclear factors [10,11,12].

SBME can reduce IL-1b production by CD4+ T cells under conditions of hyperglycemia because SBME contains a bioactive compound that beneficial to the body. SBME contains flavonoid which has anti-inflammatory activity. One of these activities is owned by a derivative of flavonoid composition consisting of isoliquiritigenin. This compound can release NF-kB by inhibiting the release of inhibitors and inhibiting the transcription factor NFAT. It can reduce the regulation of the inflammatory response and inhibit Th17 differentiation [13]. Furthermore, the previous study also reported that flavonoids act as insulin mimetic or insulin secretagogues by influencing pleiotropic, which can prevent and overcome insulin resistance in hyperglycemic [14].

SBME Inhibits IL-6 Expression in B220 Cells

Flow cytometry analysis and statistical analysis showed that IL-6 pro-inflammatory cytokine expressing B cells (B220+IL-6+) increased in hyperglycemic mice model. The result showed that the relative number of B220+IL-6+ in hyperglycemic mice reached 8.79%, while in normal mice, it was about 7.33%. The relative number of IL-6 between healthy and hyperglycemic mice showed significant result ($p <0.05$) (Fig. 2).

The administration of SBME against hyperglycemia on the Balb/c mice showed no significant result. The relative number of B220+ IL-6+ increased compared to DM positive control. This research tested three groups of different doses of SBME and compared them to negative control and hyperglycemia positive control. We found that the relative number of B220+ IL-6+ at P1, P2, and P3 difference on both decrease and increase result after given SBME orally. A significant increase observed on P3 ($p<0.05$) compared to hyperglycemic positive control was 9.55%. While on P1 and P2, a not significant ($P>0.05$) increase and decrease observed and compared to the hyperglycemic positive control, was 8.44% and 8.79%. (Fig. 2).

ISSN. 2087-2852
E-ISSN. 2338-1655

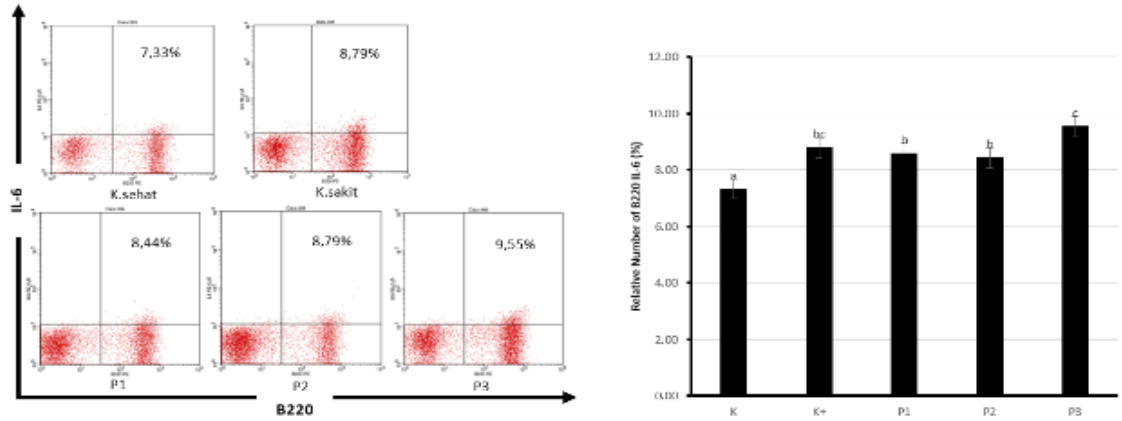

Figure 2. Production profile of IL-6 cytokine by B220 cells total percentage. (**K**: a healthy group, K+ is a positive control induced with 145mg.kg^{-1} body weight STZ, **P1**: treatment 1 with STZ injection and 10 mg.kg^{-1} SBME, **P2**: treatment 2 with STZ injection and 40 mg.kg^{-1} SBME, **P3**: treatment 3 with STZ injection and 160 mg.kg^{-1} SBME).

Based on the result shown by flow cytometry analysis, the conclusion is, SBME did not give a specific result to reduce the relative number of B220+ IL-6+. The administration of SBME at a dose of 10 mg.kg^{-1} BW, 40 mg.kg^{-1} BW, and 160 mg.kg^{-1} BW has not been able to reduce the number of IL-6 cytokines explored by lymphocyte B cells. The dosage also provides the amount of IL-6 pro-inflammatory cytokines. The given SBME cannot be used to reduce inflammation in patients with hyperglycemia.

Increased IL-6 cytokine production by B220 lymphocyte cells was due to an increase in B lymphocyte cell activity in producing IL-6 cytokines, which increases the increase in hyperglycemia, which can cause inflammation [15]. Besides, increasing the relative number of B220 cells in hyperglycemia mice injected with STZ will form free radicals in the body that cause oxidative reactions in various organs of the body and cause inflammation. The resulting inflammation will activate activation of the transcription factor Nf-kB, which is a transcription factor that increases the production of inflammatory cytokines and results in the proliferation and differentiation of CD40 cells (B220) through the application of cytokine regulations [16].

The increase in the relative number of IL-6 cells by B220 cells during SBME processing is due to the activation of the trans-signaling pathway to produce IL-6 pro-inflammatory cytokines [17]. Besides, the composition of flavonoids and momordicine in SBME also has an important role. Mammon compounds can help activate and activate B cell proliferation. Flavonoid compounds can also act as Mitogen-Activated Protein Kinase (MAPK), which can fight B cell proliferation [18]. This MAPK activation can help the phosphorylation of transcription factor proteins such as Nf-κB and activating it as a transcription [16], thus increasing the inflammatory effect. So, based on the results of this study, it can be known about the content of SBME compounds, which are immune stimulants, which can trigger the activation of Nf-kB thus increasing pro-inflammatory cytokines in hyperglycemia.

CONCLUSION

In this study, Bitter melon combined with star fruit (SBME) gave varying results as an anti-inflammatory depending on the therapeutic dose. This result happened because the dose used reduces the production of IL-1b cytokines, not with IL-6 cytokines. Thus because the dose used here was low. SBME can be only used to cure inflammation in hyperglycemia, but with further research doses. SBME activity with the right dose was able to reduce the relative number of pro-inflammatory cytokines such as IL-1B and IL-6 produced by T lymphocytes or B lymphocytes.

REFERENCES

[1] Yan, L.J. 2014. Pathogenesis of chronic hyperglycemia: from reductive stress to oxidative stress. *J. Diabetes Res.* 137919. 1-11.

[2] Fernandez-Rene J., M. Vayreda, C. Richart, C. Gutierrez, M. Broch, J. Vendrell, W. Ricart. 2001. Circulating interleukin-6 levels, blood pressure and insulin resistance in apparently healthy man and women. *J. Clin. Endocrinol. Metab*. 86. 1154-1159.

[3] Lorenzo. O., B. Picatoste, S. Ares-Carrasco, E. Ramírez, J. Egido, J. Tuñón. 2011.

Potential role of nuclear factor κB in diabetic cardiomyopathy. *Mediators Inflamm.* 1-9.

[4] Khairunnisa, E.N., H.S. Sastramihardja, S. Bhekti. 2014. Efek infusa belimbing wuluh (*Averrhoa bilimbi*) dalam menurunkan kadar glukosa darah puasa dan 2 jam post prandial mencit model diabet. *Prosiding Pendidikan Dokter*. 358-364.

[5] Nagy, M., M.A. Bastawy, N. Abdel-Hamid 2012. Effects of *Momordica charantia* on streptozotocin-induced diabetes in rats: role of insulin, oxidative stress and nitric oxide'. *Int. J. Health Sci*. 2(2). 8-13.

[6] Joseph, B., D. Jini. 2013. Antidiabetic effects of *Momordica charantia* (bitter melon) and its medicinal potency'. *Asian Pac. J. Trop. Dis.* 3(2). 93-102.

[7] Hidayati, D., A. Faizah, E.N. Prasetyo, N. Jadid, N. Abdulgani. 2018. Antioxidant capacity of snakehead fish extract (*Channa striata*) at different shelf life and temperatures. *IOP Conference Series: Journal of Physics: Conference Series 1028.* DOI: 10.1088/17426596/1028/1/012021.

[8] Susanti, E.Y., A. Candra, C. Nissa. 2017. Pengaruh pemberian sari belimbing wuluh (*Averrhoa bilimbi. L*) terhadap kadar glukosa darah puasa wanita dewasa. *Journal of Nutrition and Health*. 5(2). 102-115.

[9] Rifa'i, M., N. Widodo. 2014. Significance of propolis administration for homeostasis of CD4+CD25+ T immunoregulatory cells controlling hyperglycemia. *Springer Plus.* 3. 526.

[10] Numasaki, M., J. Fukushi, M. Ono, S.K. Narula, P.J. Zavodny, T. Kudo, … M.T. Lotze. 2003. Interleukin-17 promotes angiogenesis and tumor growth. *Blood.* 101(7). 2620–2627.

[11] Liang, Y., Y. Zhou, P. Shen. 2004. NF-κB and its regulation on the immune system. *Chinese Society of Immunology*. 1(5). 343–350.

[12] Tak, P.P., G.S. Firestein. 2014. NF-κB: A key role in inflammatory diseases. *J. Clin. Invest*. 107(1). 7-11.

[13] Martinez, G., M.R. Mijares, J.B De Sanctis. 2019. Effect of flavonoids and its derivatives on immune cell responses. *Recent Pat. Inflamm. Allergy Drug Disc.* 13(2). 84-104

[14] Gupta, R., M. Mathur, V.K. Bajaj, P. Katariya, S. Yadav, R. Kamal, R.S. Gupta. 2011. Evaluation of the antidiabetic and antioxidant activity of *Moringa oleifera* in experimental diabetes. *J. Diabetes.* 4. 164-171.

[15] Defuria, J., A.C. Belkina, M.J. Bogdan, J.S. Cappione, J.D. Carr, Y.R. Nersesova, D. Markham, K.J. Strissel, A.A., B.S. Nikolajczyk. 2013. B cells promote inflammation in obesity and type 2 diabetes through regulation of T-cell function and an inflammatory cytokine profile. *Prot. Natl. Acad Sci. USA*. 110(13). 5133-5138

[16] Craxton, A., G. Shu, J.D. Graves, J. Saklatvala, E.G. Krebs, E.A. Clark. 1998. P38 MAPK is required for CD-4induced gene expression and proliferation in B lymphocyte. *J. Immunol*. 161. 3225-3230.

[17] Scheller, J., A. Chalaris, D. Schmidt-Arras, S. Rose-John. 2013. The Pro- and Anti-Inflammatory Properties of the Cytokine Interleukin-6. *Biochimicaet Biophysica Acta*.1 81(5). 878-888.

[18] Middleton, E.Jr., C. Kandaswami, T.C. Theoharides. 2000. The effects of plant flavonoids on mammalian cells: implications for inflammation, heart disease, and cancer. *J. Pharmacol*. 52(4). 673-751.

ISSN. 2087-2852
E-ISSN. 2338-1655

Characterization of Probiotics Isolated from Intestine of Mackerel Fish (*Rastrelliger* sp.) from Lembata Regency of East Nusa Tenggara

Helena Daten[1*], Tri Ardyati[1,2], Yoga Dwi Jatmiko[1,2]

[1]Master Program of Biology, Faculty of Mathematics and Natural Sciences, Universitas Brawijaya, Malang
[2]Department of Biology, Faculty of Mathematics and Natural Sciences, Universitas Brawijaya, Malang

Abstract

The research aimed to isolate, characterize, and analyze the ability of lactic acid bacteria (LAB) potential as probiotics to produce hydrolase enzyme. The LAB was isolated using MRS agar by the spread plate method. The LAB characterization includes antimicrobial activity, tolerance to low pH, bile salt, salinity, autoaggregation properties, and ability to produce hydrolytic enzymes. The isolate which has the highest ability to inhibit *Aeromonas hydrophila* is KBP 3.3, while the isolate which inhibits the highest *Streptococcus agalactiae* is KBP 1.1.1. The KBP 3.3 and KBP 1.1.1 were able to survive at pH 1 for 24 hours with a survival rate of 93.6% and 98.3%. The KBP 3.3 and KBP 1.1.1 are tolerant to 7.5% bile salt concentrations for 24 hours of 99.46% and 99.11%. The KBP 3.3 is tolerant to 0.5 % salinity for 24 hours with the highest survival rate of 113.38%, while KBP 1.1.1 is 94%. The KBP 3.3 and 1.1.1 have autoaggregation properties of 92.18% and 87.84%. The KBP 3.3 produced the highest lipase enzyme, while KBP 1.1.1 produced the protease enzyme.

Keywords: hydrolytic enzyme, lactic acid bacteria, mackerel, probiotic

INTRODUCTION

Lembata Regency is located in East Nusa Tenggara Province; one of the largest producers of marine fish in Indonesia. Fish with high economic value and widely caught in Lembata Regency are mackerel (*Rastrelliger* sp.). Mackerel is a type of fish that live in shallow sea waters and low salt salinity [1]. Mackerel production in Lembata Regency until the end of 2016 was 209.27 tons [2]. The number of mackerel catches increased until 2016 by 53.23% [3]. Mackerel is nutritious because it contains protein, omega 3, vitamin B12, vitamin D, vitamin B2, vitamin B6, phosphorus, iodine, and high selenium. Catch fish supplies such as mackerel cannot supply the increasing public demand due to natural factors such as rainfall and wind. One alternative to meet community demand for fish is aquaculture [4].

Intensive aquaculture causes the fish to experience stress, which lowers its immune system. It is a cause of increased susceptibility to disease [5,6]. Examples of infectious diseases are hemorrhagic and septicemia caused by the bacterial pathogen *Aeromonas hydrophila* [7] and *Streptococcus agalactiae* [8]. Symptoms of the disease are loss of appetite, red discoloration of the anus and base of the fins, eyes, gills, internal organs, and hemorrhagic muscles. Pathogenic bacterial infections are usually prevented by administering antibiotics, chemotherapy, and vaccines. Specifically for antibiotic therapy, if it is carried out intensively, it will result in the emergence of microbes that are resistant to these antibiotics [9,10]. One solution to solve this problem is the application of environmentally friendly and sustainable cultivation using probiotics [7].

Probiotics are beneficial microbes that can improve the health of their host and it can be used as a pathogenic biocontrol agent in aquaculture. Previous research obtained probiotics as biocontrol agents to be applied to aquaculture. *Paenibacillus ehimensis* NPUST1 isolated from tilapia ponds that have the ability to inhibit pathogens *Aeromonas hydrophila* and *Streptococcus iniae* [7], and *Rummeliibacillus stabekisii* can inhibit the growth of *Streptococcus agalactiae* [10]. Moreover, the consortium of *Saccharomyces cerevisiae, Aspergillus oryzae,* and *Bacillus subtilis* can also improve the immune system of tilapia and inhibit pathogens *Aeromonas hydrophila* and *Streptococcus iniae* [11]. Probiotics from mackerel intestines from the Indonesian sea have also been reported, namely *Lactobacillus plantarum, Leuconostoc mesenteroides* [14], and *Bacillus megaterium* (QM B1551 strain, NBRC15308 strain, IAM 13418 strain, and ATCC strain 14581) [13]. Probiotics from mackerel intestines, especially from Indonesia, are still less explored. Therefore, the research was aimed to isolate, characterize the LAB potential as probiotics, and analyze the ability of probiotics to produce hydrolase enzyme.

* Correspondence address:
Helena Daten
Email : helenadaten061095@gmail.com
Address : Dept. Biology, University of Brawijaya, Veteran Malang, 65145

ISSN. 2087-2852
E-ISSN. 2338-1655

MATERIAL AND METHOD

Sample Collection and Pathogenic Bacterial Strains Used

Mackerel was obtained from a fish auction place, Lewoleba Impres Market, Lembata Regency. Morphometry of 10 fishes included weight and length of mackerel. The mackerel was then brought under cold conditions to the Microbiology Laboratory, Faculty of Mathematics and Natural Sciences, Brawijaya University. Furthermore, the pathogen used was *Aeromonas hydrophila* obtained from the Fish Disease Laboratory, Faculty of Fisheries and Marine Sciences, Brawijaya University. Meanwhile, *Streptococcus agalactiae* was obtained from the Research Center for Freshwater Aquaculture Fisheries, Sempur, Bogor, West Java.

Isolation and Characterization of LAB

The length of the mackerel that has been used as a sample ranges from 18-19 cm. The weight of the fish is 76.5-77.2 g. Mackerel intestine contents were removed using tweezers in sterile conditions. The fish intestine of 25 g was blended using a blender in 100 mL of NaCl 0.85%. The obtained suspension was serially diluted from 10^{-1}-10^{-6} dilutions. Lactic acid bacteria were isolated by the spread plate method in MRS agar containing 1% $CaCO_3$ and incubated at 37°C for 48 hours. Lactic acid bacteria that grow are characterized by the formation of clear zones around the colony. Lactic acid bacteria were purified by the spread plate method. After that, Gram stain and catalase test were carried out to ensure that the isolates obtained were LAB [14].

Screening of Antimicrobial Activity

The antimicrobial activity test method used the well diffusion method as described by Speranza [15]. The number of cells of each lactic acid bacteria and pathogen is 10^7 CFU.mL^{-1}. Lactic acid bacteria were cultured in MRS broth media, while *Aeromonas hydrophila* and *Streptococcus agalactiae* were cultured in Trypticase Soy Broth (TSB) media [7,16]. Pathogen isolates of 0.1 mL were spread on Trypticase Soy Agar (TSA) media. After that, 800 µL of each lactic acid bacteria was put into a well with a diameter of 5 mm, then incubated at 37°C for 48 hours. Clear zone diameters were measured and the inhibition index was calculated with formula 1 [17].

$$\text{Inhibitory index} = \frac{\text{clear zone diameter - well diameter}}{\text{well diameter}} \quad \ldots\ldots\ldots\ldots 1)$$

In-vitro Tests for Probiotic Properties: Tolerance to low pH, Bile salt, and Salinity

The pH variations used were pH 1, 3, and 5, while the concentration of bile salts used were 2.5%, 5%, and 7.5% [14]. The salinity variation used were 0.5%, 3%, and 6.5% [18]. Lactic acid bacteria that have antimicrobial activity and were used for further tests are KBP 3.3, KBP 4.3, KBP 4.2.1, and KBP 1.1.1. Lactic acid bacteria were each added as much as 10% with a cell density of 10^7 CFU.mL^{-1} into the MRS broth as measured by pH, bile salts, and salinity. Then, incubated at 37°C for 24 hours and sampling at 0, 4, and 24 hours to determine the number of cells using a hemocytometer [19]. The survival rate of lactic acid bacteria was calculated using formula 2 [20]. The N1 is the final cell amount and N0 is the initial cell amount.

$$\text{Survival rate (\%)} = \frac{\text{Log N1}}{\text{Log N0}} \text{ X 100} \quad \ldots\ldots\ldots\ldots 2)$$

Auto-Aggregation Property

Lactic acid bacteria culture with 10^7 CFU.mL^{-1} cells was centrifuged at 6000 rpm, at room temperature for 10 minutes. The pellet was suspended in a saline buffer (0.85% NaCl) to 15 mL. The suspension was measured optical density (OD) at a wavelength of 600 nm. After that, the suspension was left for 60 minutes at room temperature, then the suspension was re-centrifuged at 3000 rpm for 2 minutes and the supernatant was measured again at the same wavelength. The percentage of auto-aggregation was calculated using formula 3 [21].

$$\text{\% Auto-aggregation} = \frac{(\text{OD0} - \text{OD60})}{\text{OD0}} \text{ X 100} \quad \ldots\ldots\ldots 3)$$

Enzymatic Activity

Hydrolase enzyme activities tested were protease, amylase, lipase, and cellulase enzymes. This test was used the paper disc diffusion method. Protease enzyme activity was tested using skim milk media and amylase test using agar strach [21]. Lipase test was used lipolytic agar [22] and cellulase test was used carboxymethyl cellulose (CMC) agar [23]. After that, incubation at 37 °C for 48 hours and clear zone was formed and also the hydrolysis index was calculated using formula 4 [22].

$$\text{Indeks hidrolisis} = \frac{\text{Diameter of clearzone}}{\text{Diameter of disc}} \quad \ldots\ldots\ldots\ldots (4)$$

ISSN. 2087-2852
E-ISSN. 2338-1655

RESULT AND DISCUSSION

The number of lactic acid bacteria obtained was eleven isolates. All of the LAB isolates were negative catalase and Gram-positive. The LAB cells are basil (KBP 1.1.1, KBP 3.3, KBP 2.1, and KBP 1.1.2.1) with cell sizes of 2-3 µm, and cocci (KBP 3.1, KBP 3.2, KBP 4.3, KBP 6.2, KBP 4.2, KBP 2.3, and KBP 4.2.1) sizes of ± 1 µm. The number of isolated lactic acid bacterial cells was 7 x 10^6 CFU.g^{-1}. The number of LAB cells in the intestines of marine fish is usually constant during the capture and storage period of 10^6-10^7 CFU.g^{-1}. The fish intestine is a potential source of probiotics because LAB cell viability remains stable, compared to probiotics isolated from gills and fish skins. The amount of LAB that commonly lives in the intestines of mackerel is 2x10^6 CFU.g^{-1} [24]. The LABs are not dominant in the normal intestinal microbiota of fish, at variance with homeotherms, but some strains can colonize the intestine [25].

The LAB is found and symbiotic throughout the gastrointestinal tract, including the stomach and the intestines [26]. The population level of lactic acid bacteria associated with the intestine is affected by nutritional and environmental factors like chromic oxide, stress, and salinity [27]. Although some lactic acid bacteria strains can colonize the intestine of the host, living acid bacteria from food or feed preparations, are in most cases, lost from the intestine within a few days after the intake has stopped [24]. The fish intestine is prebiotic for supplementation of materials that can support the growth of LAB in the intestinal tract of hosts, while beneficial bacteria, a bacterial group of lactic acid bacteria (LAB), has elicited most interest due to their ability to release various beneficial compounds such as free fatty acids (FFA), digestive enzymes, and antimicrobial compounds [28].

Antimicrobial activity

Probiotics can inhibit pathogens by providing nutrients and enzymes to increase host growth, enhance the immune response by stimulating the immune system, and not causing environmental pollution [8]. Probiotics have inhibitory activity if the inhibitory index values range of 2.2-4.4 (moderate-very strong category) [29]. Therefore, the results show that KBP 1.1.1, KBP 3.3, KBP 4.3, and KBP 4.2.1 are the isolates that have inhibitory activity against *Aeromonas hydrophila*. The isolate with the highest inhibitory index value was the KBP 3.3 isolate of 7.16 ($p < 0.05$). Other isolates that have high inhibitory ability are KBP 4.2.1, KBP 4.3, and KBP 1.1.1, with an inhibitory index value of 4.5, 4.1, and 2.3, respectively (Fig. 1).

Inhibitory activity by LAB against pathogens is carried out using the metabolites it produces. Probiotics *Bacillus licheniformis* KADR5 and *Bacillus pumilus* KADR6 are able to inhibit *Aeromonas hydrophila* ATCC 49140 (inhibitory index > 1.6) due to the activity of lysozyme enzymes by damaging the cell wall of pathogenic bacteria [30]. In addition, several probiotics have inhibitory activity against *Aeromonas hydrophila* Ah01, such as *Lactococcus lactis* Q-8, *L. lactis* Q-9, and *L. lactis* Z-2 [29]. This inhibitory activity is due to lactic acid compounds, which suppress lipopolysaccharide (LPS) production and damage the Gram-negative bacterial membrane [31].

Another pathogen that causes disease in fish is *Streptococcus agalactiae*. Inhibitory activity occurs if probiotics have inhibitory index values in the moderate-strong category (1 to 2.6) [9]. The results showed that KBP 1.1.1 and KBP 4.2.1 inhibit pathogens with inhibitory index values of 3.24 and 2.89, respectively (Fig. 2).

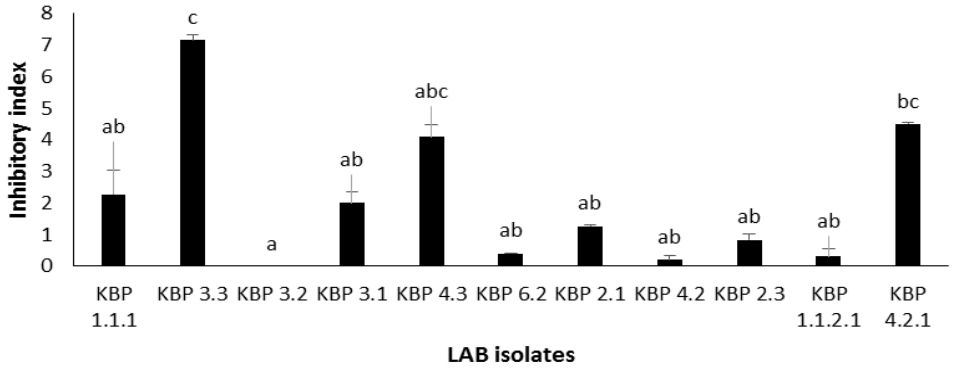

Figure 1. Antimicrobial activity of lactic acid bacteria against *Aeromonas hydrophila*

ISSN. 2087-2852
E-ISSN. 2338-1655

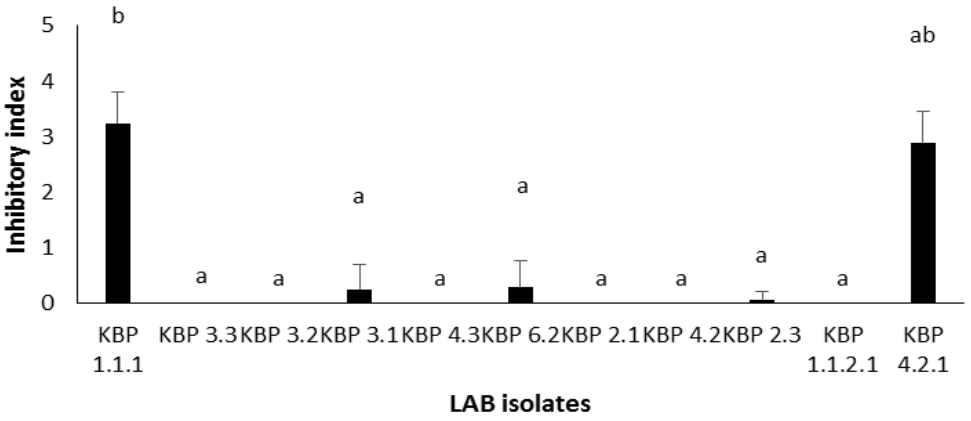

Figure 2. Antimicrobial activity of lactic acid bacteria against *Streptococcus agalactiae*

Bacteriocin type nisin A and organic acids produced by *Lactococcus lactis* subsp. lactis CRL 1655 is inhibiting the pathogen *Streptococcus agalactiae* [32]. Probiotics such as *Bacillus cereus* NY5 and *Bacillus subtilis* also have the ability to inhibit the pathogen *Streptococcus agalactiae* due to increased lyzc gene expression to produce the enzyme lysozyme [8]. Previous studies showed that the c-type lysozymes were effective in lysing both Gram-negative and Gram-positive strains. The host could recognize the bacterial challenges, generate acute stress, and enhance body immunity by secreting specific proteins such as lysozymes [33]. Moreover, some lactic acid bacteria produce bacteriocin which inhibits *Streptococcus agalactiae*, with an inhibitory index of 0.6-1.8, namely *Enterococcus faecium* BNM58 and *Weissella cibaria* BNM69 [34]. In this study, KBP 4.2.1 isolate is a potential isolate that has the ability to inhibit pathogens *Aeromonas hydrophila* and *Streptococcus agalactiae*.

Low pH Tolerance

One of the probiotic criteria is tolerance of the fish's gastrointestinal conditions [35]. The stomach pH value of tilapia ranges about 1.5 – 5.8 [14,36,37]. The intestinal pH value of tilapia ranges about 6.9 – 7.0 [14,37]. Therefore, based on the results, tolerant lactic acid bacteria isolate of gastric pH (1, 3, and 5) are KBP 3.3 and KBP 1.1.1. The survival rate of the two isolates at pH 1 was significantly different from the other two isolates for 24 hours. The survival rate of KBP 3.3 at pH 1 decreased insignificantly after incubation at 4-24 hours, from 94.7% to 93%, while the survival rate of KBP 1.1.1 increased from 95.98% to 98.3% (Fig. 3).

The isolate of KBP 3.3 had the highest survival rate at 4-24 hours, 100.86% to 98.89%. The isolate of KBP 4.2.1 had a lower survival rate than the other three isolates at 4-24 hours, 35% to 34%. The survival rate at pH 5 did not show a significant difference (Fig. 3). Previous studies have shown that *Lactococcus lactis* CLFP 101, *Lactobacillus plantarum* CLFP 238, and *Lactobacillus fermentum* CLFP 242 were tolerant to pH 3 and 5, while at pH 1, no isolates survived [38]. Moreover, the LAB that tolerate at pH 1 are *Lactococcus lactis* (strains 8HT, 9HT, 11HT and 33HT) and *Enterococcus faecalis* 14HT [39]. Other bacteria are *Leuconostoc mesenteroides* [40] and *Pediococcus pentosaceus* tolerance to pH 3 and 5 with a survival rate of 75% [41]. Therefore, KBP 3.3 and KBP 1.1.1 have a higher tolerance at pH 1, 3, and 5 compared to previous studies.

Bile Tolerance

Tilapia and freshwater fish generally have concentrations of bile salts ranging from 1-10% [14,36]. Therefore, the results showed that KBP 3.3 and KBP 1.1.1 isolates were tolerant of the concentration of bile salt 2.5-7.5%. The survival rate of the two isolates at 4-24 was above 97%. However, KBP 3.3 isolate was one of the isolates that showed an increase in cell number during oxgal exposure of 2.5% (Fig. 4).

Along with the increase in bile salts, the survival rate of KBP 3.3 and KBP 1.1.1 did not decrease. The results of previous studies indicate that the more increased the concentration of bile salts, the value of survival rate decreases. With variations in bile salt concentrations of 2.5, 5.0, 7.5, and 10% it was reported that the survival rate of *Lactococcus lactis* CLFP 101, *Lactobacillus plantarum* CLFP 238, and *Lactobacillus fermentum* CLFP 242 was 100% [38]. Moreover, *Lactococcus lactis* (strains 8HT, 9HT, 11HT and 33HT) and *Enterococcus faecalis* 14HT also tolerance at 10% bile salt concentrations [39].

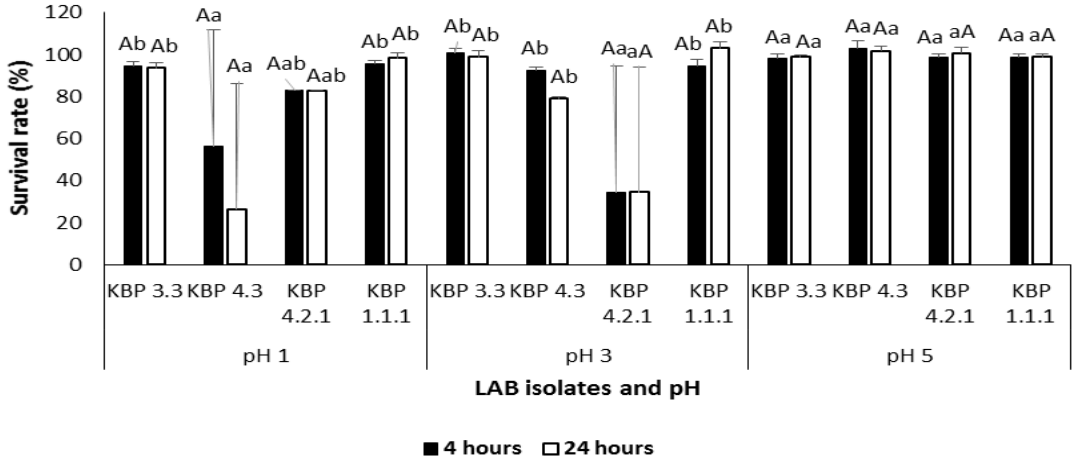

Figure 3. Lactic acid bacteria tolerance at pH 1, 3, and 5

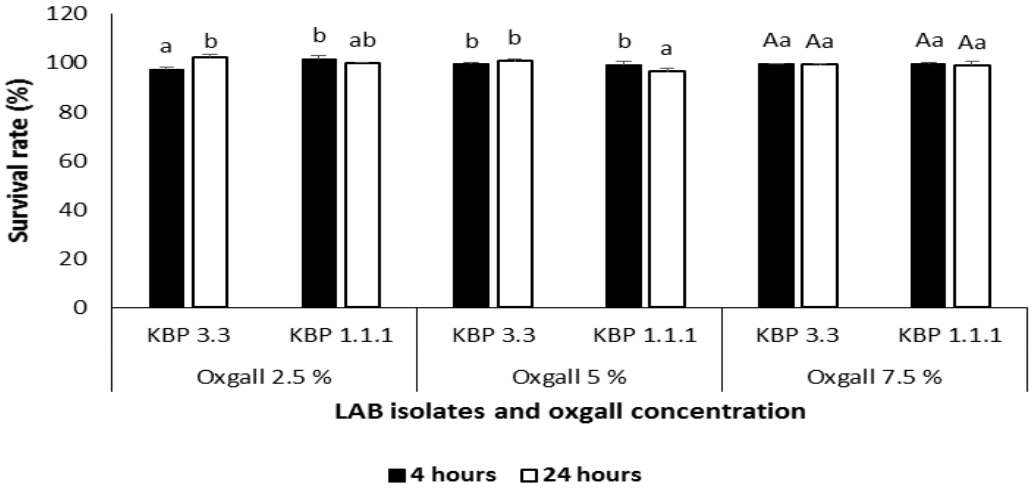

Figure 4. Lactic acid bacteria tolerance to bile salt concentration

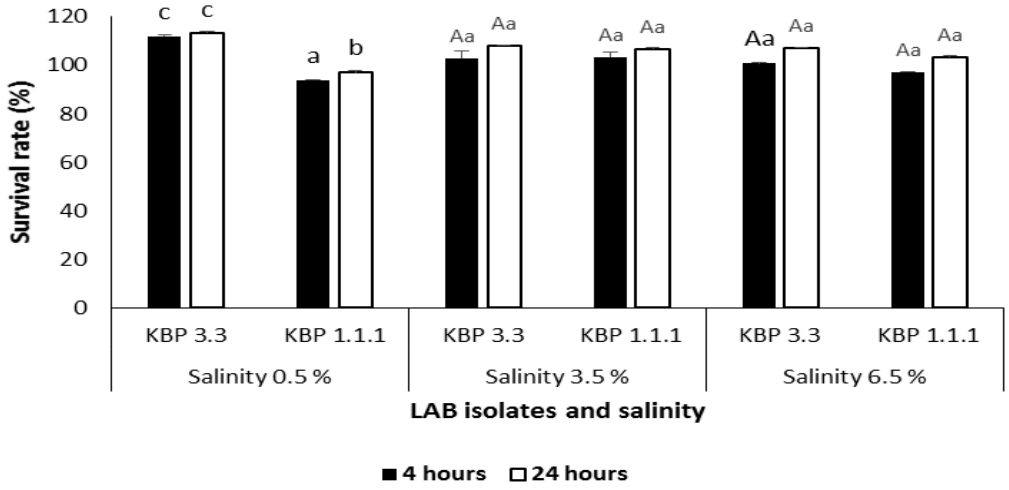

Figure 5. Tolerance of lactic acid bacteria to salinity

ISSN. 2087-2852
E-ISSN. 2338-1655

Salinity Tolerance

Lactic acid bacteria can be found in some seawater fish that live in tropical seas. The population of lactic acid bacteria in the aquatic environment is influenced by the temperature and salinity of freshwater [42]. Seawater salinity concentrations in Lembata regency ranged from 33.86-34.85 PSU, while water temperatures ranged from 3.5-30.01°C [43,44,45]. Moreover, freshwater salinity, in general, is 0.5-6.5% [20]. Therefore, lactic acid bacteria with probiotic potency must tolerance the host environment.

The results showed that KBP 3.3 and KBP 1.1.1 isolates were tolerant of freshwater salinity. The survival rate of KBP 3.3 and KBP 1.1.1 are above 100%. It shows that the LAB can maintain the number at 24 hours in the range of salinity 0.5-6.5% (Fig. 5). The salinity affects the ability of probiotics. It is supported by previous research that *Lactobacillus* is more commonly found in freshwater fish [46], while the *Streptococcus* species is more found in marine fish [47]. If *Lactobacillus* species are applied to marine fish, the numbers will decrease, while the number of *Streptococcus* species does not change [42]. Lactic acid bacteria have the ability to tolerate environmental conditions because of their ability to produce lizosim enzymes. Lizosim plays a role in inhibiting pathogenic microbes and surviving in environmental stressful conditions such as pH, low salinity, and temperature [48-51].

Auto-aggregation Assays

One of the probiotic criteria is to have the ability to colonize in the host intestine [52]. The ability of autoaggregation of probiotics is excellent if the value of autoaggregation is above 30-60% [53]. The results showed that KBP 3.3 and KBP 1.1.1 have the potency to colonize in the host intestine. It is supported by the autoaggregation values of the two isolates above 50%. However, the autoaggregation value of KBP 3.3 was higher (92.18%) compared to KBP 1.1.1 (87.84 %).

The autoaggregation property depends on bacterial strains, so it varies greatly among the same bacterial species [54,55]. The good of autoaggregation property is not only seen from the results of the in vitro test but is supported by the in vivo test because many factors influence these characteristics, such as the host, defense mechanisms, native microbes in the intestine, and peristalsis [54]. Some LAB reported to have the ability to colonize are *Enterococcus faecium* strain CGMCC1.2136 (9.05%) [56], *Lactococcus cremoris* SMF110 (40.3%), *Lactococcus cremoris* SMM69 (20.1%), *Lactobacillus curvatus* BCS35 (17.9%), *Enterococcus faecium* SMF110 (40.3%), *Lactococcus cremoris* SMM69 (20.1%) [57], *Lactobacillus plantarum* (11.5%), *Lactobacillus fermentum* (14.2%), and *Lactococcus lactis* (17.2%) [38].

Enzymatice Activity

Lactic acid bacteria with probiotics potency work optimally if producing hydrolase enzymes [58]. Carnivorous and omnivorous freshwater fish need probiotics that have the activity of the enzyme hydrolase (protease, lipase, amylase, and cellulase) to help the digestive process of fish [59]. The results indicate that KBP 3.3 and KBP 1.1.1 isolates have the activity of the enzyme hydrolase, except for the amylase enzyme. The isolate of KBP 3.3 had the highest lipase enzyme activity (hydrolysis index of 2.96), while KBP 1.1.1 had the highest protease enzyme activity of 3.28 (Fig. 6).

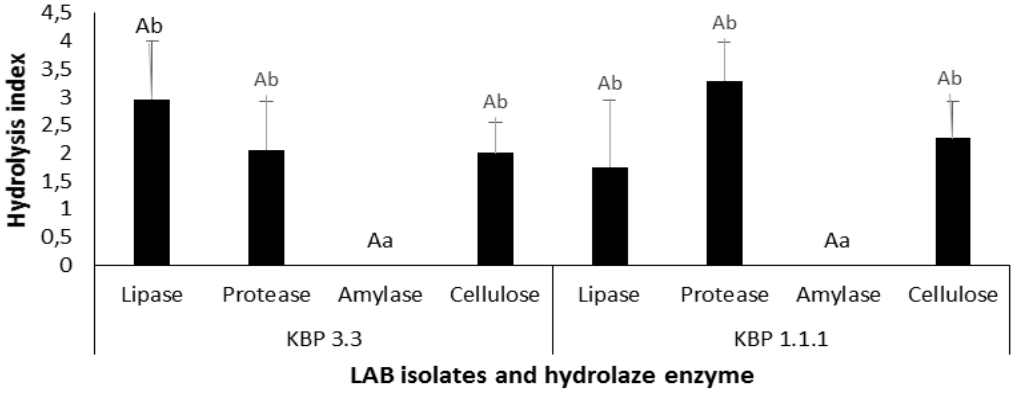

Figure 6. Hydrolase enzyme activity produced by lactic acid bacteria

ISSN. 2087-2852
E-ISSN. 2338-1655

Lactic acid bacteria generally have the activity of the hydrolase enzyme. It is supported by previous studies, namely *Enterococcus faecium* [60], *Lactobacillus curvatu*s and *Leuconostoc mesenteroides* produce the enzyme protase, lipase, and amylase [61], *Lactococcus lactis* and *Enterococcus faecalis* produce enzymes protease and amylase [39], while C*arnobacterium* sp. produced cellulase enzymes [62]. This study together with others, confirmed that enzyme production varied according to bacterial species and food habits [63,64].

CONCLUSION

Lactic acid bacteria were successfully isolated from the intestines of mackerel as much as eleven isolates. The isolates of KBP 3.3 and KBP 4.3 are isolates that have the ability to inhibit *Aeromonas hydrophila*, KBP 1.1.1 have the ability to inhibit *Streptococcus agalactiae*, while KBP 4.2.1 have the ability to inhibit the two pathogens. The isolates of KBP 3.3 and KBP 1.1.1 tolerant to low pH, high bile salt concentrations, and low water salinity. Both of these isolates also have the ability to produce the enzymes protease, lipase, and cellulase.

REFERENCES

[1] Kongseng, S., R. Phoonsawat, A. Swatdipong. 2020. Individual assignment and mixed-stock analysis of short mackerel (*Rastrelliger brachysoma*) in the Inner and Eastern Gulf of Thailand. *Fish. Res*. 221. 105-372.

[2] Statistic Center of East Nusa Tenggara. 2018. Mackerel production based on Regency/City in East Nusa Tenggara Province 2015-2016. Available at: https://ntt.bps.go.id/dynamictable/2018/02/09/611/produksi-ikan-kembung-menurut-kabupaten-kota-di-provinsi-nusa-tenggara-timur-2015-2016.html.

[3] Ministry of Marine and Fisheries. 2018. Business potential and investment opportunities for marine and fisheries in the Province of East Nusa Tenggara. Directorate General of Strengthening Competitiveness of Marine and Fisheries Products. 1-63.

[4] Nurdin, S., M. A. Mustapha, T. Lihan, M. Zainuddin. 2017. Applicability of remote sensing oceanographic data in the detection of potential fishing grounds of *Rastrelliger kanagurta* in the archipelagic waters of Spermonde, Indonesia. *Fish. Res*. 196. 1–12.

[5] Cerezuela, R., F.A. Guardiola, P. Gonzalez, J. Meseguer, M.A. Esteban. 2012. Effects of dietary *Bacillus subtilis, Tetraselmis chuii*, and *Phaeodactylum tricornutum*, singularly or in combination, on the immune response and disease resistance of sea bream (*Sparus aurata* L.). *Fish Shellfish Immunol*. 9(33). 342.

[6] Aly, S. M., Y.A. Ahmed, A.A.G. Aziz, M.F. Mohamed. 2008. Studies on *Bacillus subtilis* and *Lactobacillus acidophilus*, as potential probiotics, on the immune response and resistance of Tilapia nilotica (*Oreochromis niloticus*) to challenge infections. *Fish Shellfish Immunol*. 25(1-2). 128-136.

[7] Chen, S.W., C.H. Liu, S.Y. Hu. 2019. Dietary administration of probiotic *Paenibacillus ehimensis* NPUST1 with bacteriocin-like activity improves growth performance and immunity against *Aeromonas hydrophila* and *Streptococcus iniae* in Nile tilapia (*Oreochromis niloticus*). *Fish Shellfish Immunol*. 84. 695–703.

[8] Xia, Y., M. Wang, F. Gao, M. Lu, G. Chen. 2020. Effects of dietary probiotic supplementation on the growth, gut health and disease resistance of juvenile Nile tilapia (*Oreochromis niloticus*). *Animal Nutrition*. 6(1). 69-79.

[9] Gobi, N., B. Vaseeharan, J.C. Chen, R. Rekha, S. Vijayakumar, M. Anjugam. 2018. Dietary supplementation of probiotic *Bacillus licheniformis* Dahb1 improves growth performance, mucus and serum immune parameters, antioxidant enzyme activity as well as resistance against *Aeromonas hydrophila* in tilapia *Oreochromis mossambicus*. *Fish Shellfish Immunol*. 74. 501–508.

[10] Tan, H.Y., S. Chen, S. Hu. 2019. Improvements in the growth performance, immunity, disease resistance, and gut microbiota by the probiotic *Rummeliibacillus stabekisii* in Nile tilapia (*Oreochromis niloticus*). *Fish Shellfish Immunol*. 92. 265–275.

[11] Iwashita, M.K.P., I.B. Nakandakare, J.S. Terhune. 2015. Dietary supplementation with *Bacillus subtilis*, *Saccharomyces cerevisiae* and *Aspergillus oryzae* enhance immunity and disease resistance against *Aeromonas hydrophila* and *Streptococcus*

iniae infection in juvenile tilapia *Oreochromis niloticus*. *Fish Shellfish Immunol*. 43(1). 60–66.

[12] Kanno, T., T. Kuda, C. An, H. Takahashi, B. Kimura. 2012. Radical scavenging capacities of saba-narezushi, Japanese fermented chub mackerel, and its lactic acid bacteria. *LWT - Food Sci. Technol.* 47(1). 25–30.

[13] Ismail, Y.S., Febriani, C. Yulvizar, R. Ramadhani. 2019. Identification of the bacterium isolate from Mackerel Fish *(Rastrelliger* sp.) using 16S rRNA Gene. *IOP Conference Series: Earth and Environmental Science*. 293. 12-43.

[14] Kavitha, M, M. Raja, P. Perumal. 2018. Evaluation of probiotic potential of *Bacillus* spp. isolated from the digestive tract of freshwater fish Labeo calbasu. *Aquac. Rep*. 11. 59–69.

[15] Speranza, B., A. Racioppo, L. Beneduce. 2017. Autochthonous lactic acid bacteria with probiotic aptitudes as starter cultures for fish-based products. *Food Microbiol*. 65. 244–253.

[16] Zhang, L., C. Wang, H. Liu, P. Fu. 2019. The important role of phagocytosis and interleukins for nile tilapia (*Oreochromis niloticus*) to defense infection of *Aeromonas hydrophila* based on transcriptome analysis. *Fish Shellfish Immunol*. 92. 54–63.

[17] Wahyuni, D.S., M.B. Sudarwanti, P. Lisdiyanti. 2014. Screening of antibacterial activities of actinomycetes isolates from Indonesia. *Glob. Vet*. 13(2). 266-272.

[18] Raj, N.S., T.R. Swaminathan, A. Dharmaratnam, S.A. Raja, D. Ramraj, K.K. Lal. 2019. *Aeromonas veronii* caused bilateral exophthalmia and mass mortality in cultured Nile tilapia, *Oreochromis niloticus* (L.) in India. *Aquaculture*. 512. 734278.

[19] Asaduzzaman, M., M. Ohya, H. Kumura. 2020. Searching for high ZnPP-forming edible bacteria to improve the color of fermented meat products without nitrite/nitrate. *Meat Sci*. 165. 108-109.

[20] Rajoka, M.Sh.R, H.F. Hayat, S. Sarwar, H.M. Mehwish, F. Ahmad, N. Hussain, *et al*. 2018. Isolation and evaluation of probiotic potential of lactic acid bacteria isolated from poultry intestine. *Microbiology*. 87(1). 116–126.

[21] Padmavathi, T., R. Bhargavi, P.R. Priyanka, N.R. Niranjan, P.V. Pavitra. 2018. Screening of potential probiotic lactic acid bacteria and production of amylase and its partial purification. *J. Gen. Eng. Biotechnol*. 16(5). 357-362.

[22] Niken, C.B., Suharjono. 2015. Uji kualitatif dan kuantitatif isolat bakteri lipolitik dari limbah cair pabrik pengolahan ikan Kecamatan Muncar, Banyuwangi. *Jurnal Tropika*. 3(3). 151-155.

[23] Habbale, D., R. Bhargavi, T.V. Ramachandra. 2019. Saccharification of macroalgal polysaccharides through prioritized cellulase producing bacteria. *Heliyon*. 5. 13-72.

[24] Svanevik, C.M., B.T. Lunestad. 2011. Characterisation of the microbiota of Atlantic mackerel (*Scomber scombrus*). *Int. J. Food Microbiol.* 151. 164–170.

[25] Gänzle, M.G. Lactic metabolism revisited: metabolism of lactic acid bacteria in food fermentations and food spoilage. *Curr. Opin. Food Sci*. 2. 106–117.

[26] Parada, J.L., C.R. Caron, A.B.P. Medeiros, C.R. Soccol. 2007. Bacteriocins from Lactic Acid Bacteria: Purification, Properties and use as Biopreservatives. *Braz. Arch. Biol. Technol*. 50. 521-542.

[27] Françoise, L. 2010. Occurrence and role of lactic acid bacteria in seafood products. *Food Microbiol.* 27. 698–709.

[28] Bairagi A., K.S. Ghosh, S.K. Sen, A.K. Ray. 2002. Enzyme producing bacterial flora isolated from fish digestive tracts. *Aquac. Int.* 10(2). 109–121.

[29] Feng, J., X. Chang, Y. Zhang, X. Yan, J. Zhang, G. Nie. 2019. Effects of Lactococcus lactis from *Cyprinus carpio* L. as probiotics on growth performance, innate immune response and disease resistance against *Aeromonas hydrophila*. *Fish Shellfish Immunol*. 93. 73–81.

[30] Ramesh, D., A. Vinothkanna, A.K. Rai, V.S. Vignesh. Isolation of potential probiotic *Bacillus* spp. and assessment of their subcellular components to induce immune responses in Labeo rohita against *Aeromonas hydrophila*. *Fish Shellfish Immunol*. 45. 268-276.

[31] Alakomi, H.L., E. Skyttä, M. Saarela, T. Mattila-Sandholm, K. Latva-Kala, I.M. Helander. 2000. Lactic acid permeabilizes gram-negative bacteria by disrupting the

ISSN. 2087-2852
E-ISSN. 2338-1655

outer membrane, Application. *Environ. Microbiol*. 66. 2000-2001.

[32] Espeche, M.C., M.C. Otero, F. Sesma, M. Nader, M.E. Fatima. 2009. Screening of surface properties and antagonistic substances production by lactic acid bacteria isolated from the mammary gland of healthy and mastitic cows. *Vet. Microbiol*. 135(3-4). 346-357.

[33] Gao, F.Y., L. Qu, S.G. Yu, X. Ye, Y.Y. Tian, L.L. Zhang. 2012. Identification and expression analysis of three c-type lysozymes in *Oreochromis aureus*. *Fish Shellfish Immunol*. 32 (5). 779-488.

[34] Muñoz-Atienza, E., B. Gómez-Sala, C. Araújo, C. Herranz, L.M. Cintas. 2013. Antimicrobial activity, antibiotic susceptibility and virulence factors of Lactic Acid Bacteria of aquatic origin intended for use as probiotics in aquaculture. *BMC Microbiol*. 13(1). 1-22.

[35] Guo, X., D.D. Chen, K.S. Peng, Z.W. Cui, X.J. Zhang, S. Li. 2016. Identification and characterization of *Bacillus subtilis*, from grass carp (*Ctenopharynodon idellus*) for use as probiotic additives in aquatic feed. *Fish Shellfish Immunol*. 52. 74–84.

[36] Pinpimai, K., C. Rodkhum, N. Chansue, T. Katagiri., M. Maita, N. Pirarat. 2015. The study on the candidate probiotic properties of encapsulated yeast, *Saccharomyces cerevisiae* JCM 7255, in Nile Tilapia (*Oreochromis niloticus*). *Res. Vet. Sci.* 102. 103-111.

[37] Zidni, I., E. Afrianto, I. Mahdiana, H. Herawati. 2017. Laju pengosongan lambung ikan mas (*Cyprinus carpio*) dan ikan nila (*Oreochoromis niloticus*). *Jurnal Perikanan dan Kelautan*. 9(2). 147-151.

[38] Balcázar, J.L., D. Vendrell, I. de Blas, I. Ruiz-Zarzuela, J.L. Muzquiz, O. Girones. 2008. Characterization of probiotic properties of lactic acid bacteria isolated from intestinal microbiota of fish. *Aquaculture*. 278. 188–191.

[39] Reda, R.M., K.M. Selim., H.M. El-Sayed, M.A. El-Hady. 2018. In vitro selection and identification of potential probiotics isolated from the gastrointestinal tract of Nile tilapia, *Oreochromis niloticus*. *Probiotics Antimicro*. 10. 692–703.

[40] Allameh, S.K., H. Daud, F.M. Yusoff, C.R. Saad, A. Ideris. 2012. Isolation, identification and characterization of *Leuconostoc mesenteroides* as a new probiotic from intestine of snakehead fish (*Channa striatus*). *Afr. J. Biotechnol*. 11(16). 3810-3816.

[41] Jaafar, R.S., F.N. Al-Knany, B.A. Mahdi, A.M. R. Al-Taee. 2019. Study the Probiotic Properties of *Pediococcus pentosaceus* Isolated from Fish Ponds in Basra City, South of Iraq. *J. Pure Appl. Microbiol.* 13(4). 2343-2351.

[42] Al Bulushi, I.M., S.E. Poole, R. Barlow, H.C. Deeth, G.A. Dykes. 2010. Speciation of Gram-positive bacteria in fresh and ambient-stored sub-tropical marine fish. *Int. J. Food Microbiol*. 138(1-2). 32-38.

[43] Stanis, S. 2005. Pengelolaan sumberdaya pesisir dan laut melalui pemberdayaan kearifan lokal di kabupaten Lembata propinsi Nusa Tenggara Timur. Master Thesis. Graduate School, Diponegoro University. Semarang.

[44] Slamet, A. 2019. Analisis massa air di perairan utara pulau Lembata, Nusa Tenggara Timur. Master Thesis. Department of Marine Science and Technology, Faculty of Fisheries and Marine Sciences, Bogor Agricultural University.

[45] Tubalawony, S., E. Kusmanto, Muhadjirin. 2012. Suhu dan salinitas permukaan merupakan indikator upwelling sebagai respon terhadap angin muson tenggara di perairan bagian utara laut Sawu. *Ilmu Kelautan*. 17(4). 226-239.

[46] Bucio, A., R. Hartemink, J. W. Schrama, J. Verreth, F.M. Rombouts. 2006. Presence of lactobacilli in the intestinal content of freshwater fish from a river and from a farm with a recirculation system. *Food Microbiol*. 23(5). 476-482.

[47] Baeck, G.W., J.H. Kim, D.K. Gomez, S.C. Park. 2006. Isolation and characterization of *Streptococcus* sp. from diseased flounder (*Paralichthys olivaceus*) in Jeju Island. *J. Vet. Sci*. 7(1). 53-58.

[48] Dong, H.B., Y.Q. Su, Y. Mao. 2014. Dietary supplementation with *Bacillus* can improve the growth and survival of the kuruma shrimp *Marsupenaeus japonicus* in high temperature environments. *Aquac. Int*. 22. 607–617.

[49] Liu, K.F., C.H. Chiu, Y.L. Shiu, Y.W. Cheng, C.H. Liu. 2010. Effects of the probiotic, *Bacillus subtilis* E20, on the survival, development, stress tolerance, and immune status of white shrimp, *Litopenaeus*

ISSN. 2087-2852
E-ISSN. 2338-1655

vannamei larvae. *Fish Shellfish Immunol*. 28. 837–844.

[50] Lin, Y.C., C.M. Tayag, C.L. Huang, W.C. Tsui, J.C. Chen. 2010. White shrimp *Litopenaeus vannamei* that had received the hot-water extract of *Spirulina platensis* showed earlier recovery in immunity and up-regulation of gene expressions after pH stress. *Fish Shellfish Immunol*. 29. 1092–1098.

[51] Soonthornchai, W., W. Rungrassamee, N. Karoonuthaisiri, P. Jiravanichpaisal. 2010. Expression of immune-related genes in the digestive organ of shrimp, *Penaeus monodon*, after an oral infection by *Vibrio harveyi*. *Dev. Comp. Immunol*. 34. 19–28.

[52] Kos, B., J. Suskovic, S. Vukovic, M. Simpraga, J. Frece, S.M. Matosic. 2003. Adhesion and aggregation ability of probiotic strain *Lactobacillus acidophilus* M92. *J. Appl. Microbiol.* 94. 981-987.

[53] Fernandez-Pacheco, P., M. Arévalo-Villena, A. Bevilacqua, M.R. Corbo, A. Briones Pérez. 2018. Probiotic characteristics in *Saccharomyces cerevisiae* strains: Properties for application in food industries. *LWT Food Sci. Technol*. 97. 332-340.

[54] Caggia, C., M. De Angelis, I. Pitino, A. Pino, C. Randazzo. 2015. Probiotic features of *Lactobacillus* strains isolated from Ragusano and Pecorino Siciliano cheeses. *Food Microbiol*. 50. 109-117.

[55] Das, P., S. Khowala, S. Biswas. 2016. In vitro probiotic characterization of *Lactobacillus* casei isolated from marine samples. *LWT - Food Sci. Technol*. 73. 383-390.

[56] Tarkhani, R., A. Imani, S.H. Hoseinifar, O. Ashayerizadeh, K.S. Moghanlou, R. Manaffar, H.V. Doan, M. Reverter. 2019. Comparative study of host-associated and commercial probiotic effects on serum and mucosal immune parameters, intestinal microbiota, digestive enzymes activity and growth performance of roach (*Rutilus rutilus caspicus*) fingerlings. *Fish Shellfish Immunol*. 19. 1-35.

[57] Munoz-Atienza, E., C. Araújo, S. Magadan, P.E. Hernandez. 2014. In vitro and in vivo evaluation of lactic acid bacteria of aquatic origin as probiotics for turbot (*Scophthalmus maximus* L.) farming. *Fish Shellfish Immunol*. 41. 570-580.

[58] Pundir R.K., S. Rana, N. Kashyap, A. Kaur. 2013. Probiotic potential of lactic acid bacteria isolated from food samples: an in vitro study. *J. Appl. Pharmaceut. Sci*. 3(3). 85-93.

[59] Agung, L.A., Widanarni, M. Yuhana. 2015. Application of micro-encapsulated probiotic *Bacillus* NP5 and prebiotic mannan oligosaccharide (MOS) to prevent *streptococcosis* on tilapia *Oreochromis niloticus*. *Res. J. Microbiol*. 10(12). 571-581.

[60] Shin, H.J., H.J. Choi, D.W. Kim, C.S. Ahn, Y.G. Lee, Y.K. Jeong. 2012. Probiotic potential of *Pediococcus pentosaceus* BCNU 9070. *J. Life Sci*. 22. 1194-1200.

[61] Askarian, F., A. Kousha, W. Salma, E. RingØ. 2011. The effect of lactic acid bacteria administration on growth, digestive enzyme activity and gut microbiota in Persian sturgeon (*Acipenser persicus*) and beluga (*Huso huso*) fry. *Aquac. Nutr*. 17(5). 488-497.

[62] Askarian, F., Z. Zhou, R.E. Olsen, S. Sperstad, E. Ringø. 2012. Culturable autochthonous gut bacteria in Atlantic salmon (*Salmo salar* L.) fed diets with or without chitin. *Aquaculture.* 326. 1-8.

[63] Saha, S., R.N. Roy, S.K. Sen, A.K. Ray. 2006. Characterization of cellulose producing bacteria from the digestive tract of tilapia, *Oreochromis mossambica* (Peters) and grass carp, *Ctenopharyngodon idella* (Valenciennes). *Aquac. Res*. 37(4). 380–388.

[64] Ambas, I., N. Buller, R. Fotedar. 2015. Isolation and screening of probiotic candidates from marron, Cherax cainii, gastrointestinal tract (GIT) and commercial probiotic products for the use in marron culture. *J. Fish Dis*. 38(5). 467–476.

ISSN. 2087-2852
E-ISSN. 2338-1655

Virtual Prediction of Phenolic and Glucosinolate Compounds with Keap1 Protein as Anti-aging by Stimulating Nrf2

Viona Faiqoh Hikmawati[1,2], Fajar Mustika Alam[1,2], Jihan Shavira Ainnayah[1,2], Fatchiyah Fatchiyah[1,2,*]

[1]Department of Biology, Faculty of Mathematics and Natural Sciences, University of Brawijaya, Malang, Indonesia
[2]Research Center for Smart Molecules of Natural Genetic Resources (SMONAGENES), University of Brawijaya, Malang, Indonesia

Abstract

Aging is caused by an imbalance between antioxidants and ROS. Nuclear Factor Erythroid 2-related factor 2 (Nrf2) is a transcription factor that regulates antioxidant genes. Under normal conditions, Nrf2 will bind keap1 and cause degradation of Nrf2. Nrf2 activation can be stimulated by secondary metabolites, such as glucosinolate (glucoraphanin and sulforaphane) and phenolic (kaempferol and quercetin) groups found in broccoli (*Brassica oleracea*). The purposes of this study were to analyze the interaction of the four compounds with Keap1 through molecular docking, to identify interactions that inhibit Keap1, and also to know the bioactivity scores, drug-likeness, and bioactivity prediction of each compound. The Nrf2-Keap1 protein (ID: 2FLU) structure was retrieved from the protein database, whereas the quercetin (CID: 5280343); kaempferol (CID: 5280863), sulforaphane (CID: 5350), and glucoraphanin (CID: 656556) were obtained from the PubChem Database. Molecular docking was done with HEX 8.0. The docking results were visualized with Discovery Studio 2020. Drug-likeness and bioactivity scores of the compounds were identified using mollinspiration. Prediction of bioactivity was carried out with PASS Online. The results showed that the binding energy of quercetin with Keap1 was -268.72 kcal.mol^{-1}, and glucoraphanin with Keap1 was -318.01 kcal.mol^{-1}. We found that quercetin from the phenolic group and glucoraphanin from the glucosinolate group had a strong interaction with Keap1, indicated by the number of interactions occurred and the smaller energy needed. Hence both compounds could inhibit the interaction of Keap1-Nrf2. Consequently, Nrf2 could transcribe antioxidant genes. The interaction between Keap1 and quercetin may play a role related to ROS reduction activities, such as enhancing HMOXI expression. This study indicates that quercetin has more potential in drug development as peroxidase inhibitors.

Keyword: Aging, bioinformatic, glucoraphanin, keap1, quercetin

INTRODUCTION

Aging is a biological and multifactorial phenomenon characterized by a decrease in the physiological function of cells and tissues. One cause of aging is oxidative stress [1]. Oxidative stress is caused by an imbalance between antioxidants and free radicals in the body, such as Reactive Oxygen Species (ROS). ROS levels will increase along with age and can cause cell damage, as well as disrupt the stability and function of molecules, such as proteins, carbohydrates, and fats [2]. Therefore, the body is more susceptible to aging diseases, such as cardiovascular, neurodegenerative, cancer, and diabetes [1].

Nuclear Factor Erythroid 2-related factor 2 (Nrf2) is a transcription factor that regulates antioxidant enzymes. Nrf2 levels will diminish with age [3]. Under normal conditions, Nrf2 interacts with Kelch-like ECH-associated protein 1 (Keap1) to initiate interactions with Cullin3 (Cul3) and Rbx 1. As a result, the ubiquitin ligase3 complex is formed. Nrf2 in the ubiquitin ligase3 complex is the target of proteasome degradation. Hence, Nrf2 can not transcribe antioxidant enzymes [4].

Nrf2 activation can be stimulated by bioactive compounds or secondary metabolites plants [4]. Some secondary metabolites of plants, such as glucosinolate and phenolic compounds, are known to have antioxidant activity [5], anticancer, antibacterial, and anti-inflammation [6]. Broccoli (*Brassica oleracea* L.) is a cruciferous edible green plant with high levels of glucosinolate (33%) and phenolic compounds (28%). The glucosinolate compounds found in broccoli are glucoraphanin and sulforaphane, while the most common phenolic compounds are kaempferol and quercetin [7]. Therefore, this study was conducted to find out the inhibition of Keap1-Nrf2 interaction by phenolic compounds (quercetin and kaempferol) and glucosinolate (sulforaphane and glucoraphanin) through *in silico* analysis. We would like to determine which compounds work better to stimulate the Nrf2 pathway. This study also supports existing *in vivo* and *in vitro* research about the stimulation of Nrf2 with flavonoid and glucosinolate compounds.

* Correspondence address:
Prof. Dra. Fatchiyah, M.Kes., Ph.D
Email : fatchiya@ub.ac.id
Address : Faculty of Mathematics and Natural Sciences, University of Brawijaya, Veteran Malang, 65145

MATERIAL AND METHOD

The 3D structure of the compounds was obtained from PubChem (https://pubchem.ncbi.mlm.nih.gov/). The compounds used included the flavonoid group, namely quercetin (CID: 5280343) and kaempferol (CID: 5280863), and the glucosinolate group, namely sulforaphane (CID: 5350) and glucoraphanin (CID: 656556). We obtained the structure of the Nrf2-Keap1 protein complex (ID: 2FLU) from rcsb.pdb.org. Ligands were prepared to minimize energy using Open Babel in PyRx 0.8 software. Water molecules removal was done using Discovery Studio 2020 [8].

Drug-likeness and Bioactivity Prediction

Drug-likeness is an evaluation of drug ability based on several physical-chemical and biological properties of each compound. The *drug-likeness* test was carried out using *Lipinski's Rule of Five*. The rules state that *druglike* molecules must have molecular weight (MW) <500, logp ≤ 5, the number of hydrogen bond acceptors ≤10, the number of hydrogen bond donors ≤5 and should not violate more than one rule [9].

The bioactivity score of the compound was obtained from https://www.molinspiration.com/. These compounds are expected to bind biological targets, such as GPCR ligands, Protease Inhibitors, Enzyme Inhibitors, and kinase inhibitors [9]. The prediction of drug-likeness and bioactivity scores of each compound were performed with https://www.molinspiration.com/ [9].

Biological Activity Prediction Using PASS Online

Biological activities were displayed using the PASS Online server. The biological activity spectrum of each compound showed specific toxicity and pharmacological effects. The compound's activity spectrum was calculated through two parameters, namely Pa (probable activity) and Pi (probable inactivity). Pa and Pi values range from 0-1 and Pa + Pi <1 [10].

Molecular Docking and Visualization

Molecular docking was done using HEX 8.0. The docking results were visualized using Discovery Studio 2020 [8].

RESULT AND DISCUSSION

Evaluation of Drug-likeness

Evaluation of the drug-likeness from four bioactive compounds was based on Lipinski's five rules. These five rules consist of Log P (partition coefficient), molecular weight, the number of hydrogen donors and receptor bonds, and the polar surface area. Based on the physicochemical characterization of the tabulated compounds (Table 1), the four bioactive compounds had molecular weight below 500, which indicated that they are easily transported, diffused, and absorbed compared with heavy molecules [11]. The four bioactive compounds had a log P value below 5, which indicated that they had a high permeability to cell [11].

Sulforaphane, quercetin, and kaempferol possessed bioactive scores in acceptable ranges, such as the number of hydrogen bond acceptors below 10 and the number of hydrogen bond donors below 5. Meanwhile, glucoraphanin had 11 hydrogen bond acceptors, which did not meet the requirements of Lipinski Rules, leading to the reduction in the ability of a molecule to permeate a membrane bilayer [12]. In general, an orally active drug has no more than one violation of the Lipinski Rules. In this study, all four bioactive compounds can be considered as a drug in humans, since the overall score of the compounds is in acceptable ranges.

Bioactivity Score

Biological targets for drugs, such as enzymes, ion channels, and receptors, are targets for drug activity. Bioactivity scores of drugs are calculated based on different parameters such as binding to G protein-coupled receptor ligands (GPCR), nuclear receptor ligands, ion channels, kinase inhibition, protease inhibition, and enzyme inhibition activity [9]. All of these parameters indicated the probability of a molecule to be active, leading to the maximum production of the physiological action [10]. A compound with a bioactivity score of more than 0.00 is most likely to possess considerable biological activities. A compound is moderately active if it has a bioactivity score between -5.0 and 0.0, and inactive if it is less than -5.0 [11].

The bioactivity scores of the four bioactive compounds are tabulated in Table 2. Quercetin and kaempferol had high bioactivity scores as kinase inhibitors, nuclear receptor ligands, and enzyme inhibitors. Sulforaphane had a high bioactivity score on the inhibitor of the enzyme, while glucoraphanin had a high bioactivity score on the enzyme inhibitor, GPCR ligands, protease inhibitors, and nuclear receptor ligands.

ISSN. 2087-2852
E-ISSN. 2338-1655

Table 1. Physicochemical characteristics of four bioactive compounds

Compound	Molecular Weight (MW)	Donor atom H	Receptor atom H	Log p	Lipinski's Violation
Quercetin	302.24	5	7	1.68	0
Kaempferol	286.64	4	6	2.17	0
Sulforaphane	177.29	0	2	1.15	0
Glucoraphanin	436.51	4	11	-4.94	1

Table 2. Bioactivity scores of four bioactive compounds

Compound	GPCR Ligand	Kinase Inhibitor	Nuclear Receptor Ligand	Protease Inhibitor	Enzyme Inhibitor
Quercetin	-0.06	0.28	0.36	-0.25	0.28
Kaempferol	-0.10	0.21	0.32	-0.27	0.26
Sulforaphane	-0.35	-1.98	-0.84	-0.72	0.44
Glucoraphanin	0.39	-0.34	0.10	0.21	0.62

Bioactivity Prediction

The bioactivity prediction of all compounds is shown in Table 3. Only activities with Pa > Pi is considered as possible for a particular compound. If Pa > 0.7, the probability of experimental pharmacological action is high, and if 0.5 < Pa < 0.7, probability of experimental pharmacological action is less [9]. Using PASS Online server, selected bioactive constituents were analyzed to evaluate the possible biological activity. Based on the PASS prediction result, sulforaphane was found to have antioxidant activity from the Glutathione S-Transferase Substrate (GST) pathway and CYP2E1 inhibitor. Glutathione S-Transferase Substrate (GST) is a phase II detoxification enzyme that results from the expression of cryoprotective genes induced by Nrf2. GST plays a role in the secondary detoxification of Reactive Oxygen Species (ROS), so DNA damage can be avoided, and cells stay alive [9-10].

Sulforaphane also had inhibitory activity against CYP2E1. CYP2E1 (Cytochrome P450) is a CYP isoform that has a role in the production of ROS. The presence of CYP2E1 in the brain can trigger lipid peroxidation and apoptosis, thereby increase blood permeability to the brain, and can cause brain cell damage. CYP2E1 inhibitor activity in this compound can certainly delay aging by preventing the occurrence of chronic diseases associated with aging, such as neurodegenerative diseases [13].

PASS prediction result showed that the flavonoid compounds group (kaempferol and quercetin) had the activity as HMOXI expression enhancer and peroxidase inhibitor. HMOXI expression enhancer is an antioxidant enzyme secreted to respond to oxidative stress. Activation of this enzyme is regulated by the transcription factor Nrf2. Therefore, if Nrf2 stimulation is increased coupled with the presence of kaempferol and quercetin compounds, which have HMOXI expression enhancer activity, the expression of antioxidant enzymes can elevate, leading to the reduction of the ROS accumulation in the body [14]. One of the peroxidase inhibitors is through the enzyme Glutathione peroxidase 2, which plays a role in catalyzing the reduction reaction of hydrogen peroxide. Glutathione peroxidase is regulated by Nrf-2, which is a transcription factor for the gene product, antioxidant [15]. All these activities from three compounds were related to Nrf2 induction.

Table 3. Bioactivity prediction of four bioactive compounds

Compound	Activity	Pa value	Pi value
Sulforaphane	Glutathione S-Transferase Substrate (GST)	0.936	0.002
	CYP2E1 inhibitor	0.703	0.004
Kaempferol	HMOXI expression enhancer	0.945	0.002
	Peroxidase inhibitor	0.956	0.001
Quercetin	HMOXI expression enhancer	0.957	0.002
	Peroxidase inhibitor	0.962	0.001

ISSN. 2087-2852
E-ISSN. 2338-1655

Docking Analysis

The Kelch-Neh2 complex structure was obtained from Protein Data Bank with ID 2FLU. In the Kelch-Neh2 complex, the Nrf2 protein is in the P chain, and the Keap1 protein is in the X chain [16]. The Neh2 domain in Nrf2 with the ETGE and DLG regions is the Kelch-binding region of Keap1 with strong bonds [17]. The Kelch-domain consists of DGR (Double glycine region) and CTR (C¬-terminal region). This domain is the binding site of Neh2 in Nrf2. The Kelch-domain starts with amino acid residues 327-611 (Fig. 1). Based on previous studies, the essential active site is found in serin and arginine residues in the Kelch-domain [17-18].

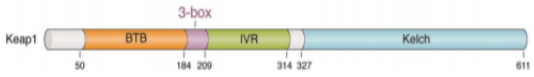

Figure 1. Domain architecture of Keap1[23]

Quercetin is a flavonoid compound that has antioxidant activity. Five hydrogen bonds occurred between quercetin and amino acid residues Val 465, Val 369, Val 463, Ile416, and Ala607 in the Keap1-quercetin complex. Four hydrophobic interactions were also established between quercetin and amino acid residues Ala607, Ala366, and Cys368 (Fig.2). The energy affinity from the docking results between Keap1 and quercetin was -268.72 kcal.mol^{-1} (Table 4). The interaction of Keap1 and quercetin showed that the ligand did not bind to the active side. However, the bonds that occurred between them were still in the Kelch domain, which contributed to the binding of Nrf2. Therefore, quercetin can stimulate Nrf2 expression. In another previous study, quercetin increased the expression of Nrf by *in vivo* [20]. Another *in vitro* study demonstrated that quercetin could activate Nrf2 [21]. The enhancement of Nrf2 expression is important because it is required for binding to ARE (Antioxidant Responses Element), which mediates the transcription of Nrf2-regulated genes with the products of antioxidant and detoxifying enzymes [3].

The conformation with the lowest energy is the conformation with the strongest binding. Binding energy itself is the sum of the intermolecular forces upon the receptor-ligand complex [22].

Table 4. Comparison of energy values and bond types of 4 compounds

	Ligand	Energy (kcal.mol^{-1})	Name	Distance (Å)	Category
Glucosinolate	Glucoraphanin	-318.01	X:ARG326:HH21 - :LIG1:O	2.83488	Hydrogen Bond
			X:VAL420:HN - :LIG1:O	1.7772	Hydrogen Bond
			X:VAL467:HN - :LIG1:O	3.07319	Hydrogen Bond
			:LIG1:H - X:VAL561:O	2.91043	Hydrogen Bond
			X:GLY419:CA - :LIG1:O	2.82909	Hydrogen Bond
			:LIG1:H - X:THR560:OG1	2.51532	Hydrogen Bond
			:LIG1:H - X:VAL561:O	2.84092	Hydrogen Bond
			X:CYS368 - :LIG1	4.85342	Hydrophobic
			X:ALA607 - :LIG1	4.51101	Hydrophobic
	Sulforaphane	-179.66	X:VAL369:HN - :LIG1:O	2.32618	Hydrogen Bond
			X:GLY419:HN - :LIG1:S	2.55596	Hydrogen Bond
			:LIG1:S - X:TYR426:O	3.41717	Hydrogen Bond
			:LIG1:H - X:VAL418:O	2.56679	Hydrogen Bond
Phenolic	Kaempferol	-251.54	X:VAL467:HN - :LIG1:O	2.66797	Hydrogen Bond
			:LIG1:H - :LIG1:O	2.21303	Hydrogen Bond
			:LIG1:H - X:VAL420:O	2.72538	Hydrogen Bond
			:LIG1:H - X:VAL604:O	2.88415	Hydrogen Bond
			X:ALA366:CA - :LIG1:O	2.86789	Hydrogen Bond
			:LIG1 - X:ALA366	3.9726	Hydrophobic
	Quercetin	-268.72	X:VAL465:HN - :LIG1:O	2.3514	Hydrogen Bond
			:LIG1:H - :LIG1:O	2.2166	Hydrogen Bond
			:LIG1:H - X:VAL369:O	2.45654	Hydrogen Bond
			:LIG1:H - X:ILE416:O	2.89961	Hydrogen Bond
			:LIG1:H - X:VAL463:O	2.8104	Hydrogen Bond
			X:ALA607:CA - :LIG1:O	3.21145	Hydrogen Bond
			:LIG1 - X:ALA607	4.66263	Hydrophobic
			:LIG1 - X:CYS368	4.90849	Hydrophobic
			:LIG1 - X:ALA607	4.03925	Hydrophobic
			:LIG1 - X:ALA366	4.97704	Hydrophobic

ISSN. 2087-2852
E-ISSN. 2338-1655

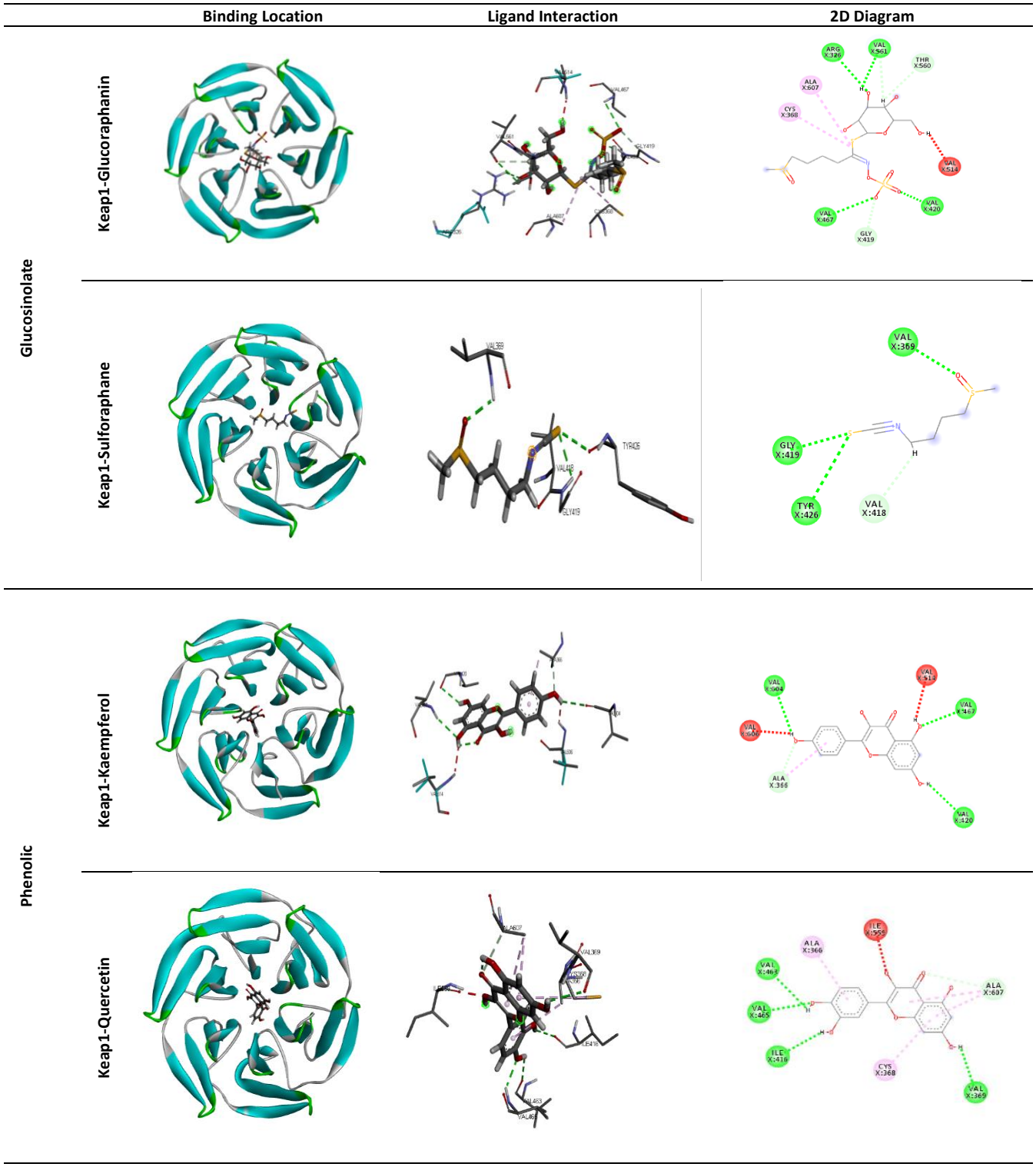

Figure 2. The 3D and 2D structures of molecular docking between Keap1 and glucosinolate group (glucoraphanin and sulforaphane) and or phenolic compounds (kaempferol and quercetin). The binding location of each complex is shown in the left column. The ligand-binding interactions between the ligand and amino acids of Keap1 are shown in the middle column. The 2D interaction between Keap1 and each ligand is shown in the right column.

In previous studies, sulforaphane was able to activate Nrf2 by changing the conformation of Keap1. This conformation involves modifying nucleophilic groups in proteins, including cysteine thiols. Conformation changes of Keap1 may stimulate Nrf2 to transcribe antioxidant genes in the nucleus [16]. The docking results between Keap1 and sulforaphane showed that the ligand did not bind to the active site of the Kelch-domain. There were four interactions of hydrogen bonds in sulforaphane with residues of Gly418, Val419, Val369, and Tyr426 in the Kelch domain (Fig. 2). The interaction between Keap1 and sulforaphane compounds had an energy of -179.66 kcal.mol^{-1} (Table 4).

The most abundant glucosinolate in broccoli is a derivative of methionine 4-methyl-sulfinyl butyl glucosinolate (glucoraphanin), which produces isothiocyanate sulforaphane [24]. This compound can induce Nrf2, a transcription factor that regulates the expression of phase 2 detoxification and antioxidant genes [25]. The docking results between Keap1 and glucoraphanin showed that the ligand did not bind to the active site of the Kelch domain. Seven hydrogen bonds occurred between glucoraphanin with amino acid residues Arg326, Gly419, Val420, Val467, Thr560, Val561. Two hydrophobic interactions were established between glucoraphanin with Cys368 and Ala607 of Keap1 (Fig. 2). The hydrogen bonds help to optimize the hydrophobic interactions and may increase the binding affinity complex [26]. These hydrophobic interactions also help in stabilizing the biochemical environment of the target [27]. The energy affinity from the docking results between Keap1 and glucoraphanin was -318.01 kcal.mol^{-1} (Table 4). This number of energy states the intermolecular forces upon the receptor-ligand complex [22].

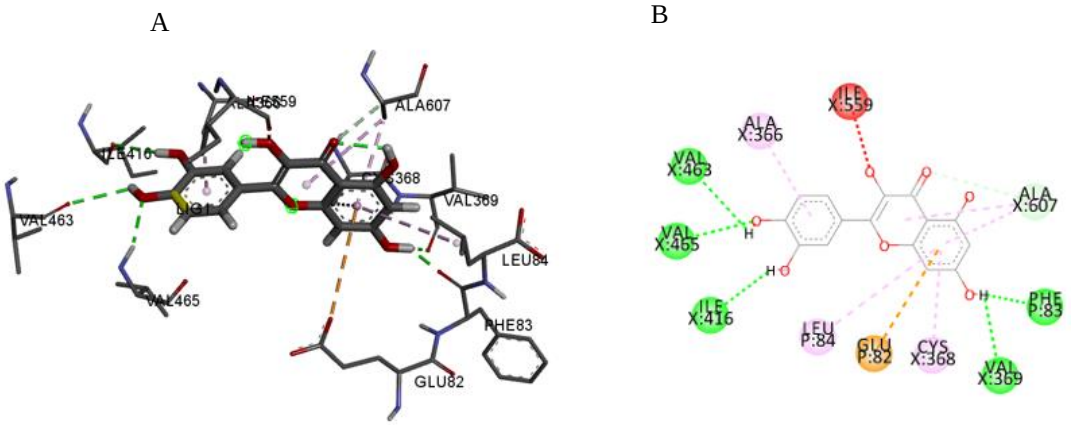

Figure 3. Docking result of Keap1-quercetin complex to Nrf2 A. Ligand-binding Interaction, B. 2D Interaction

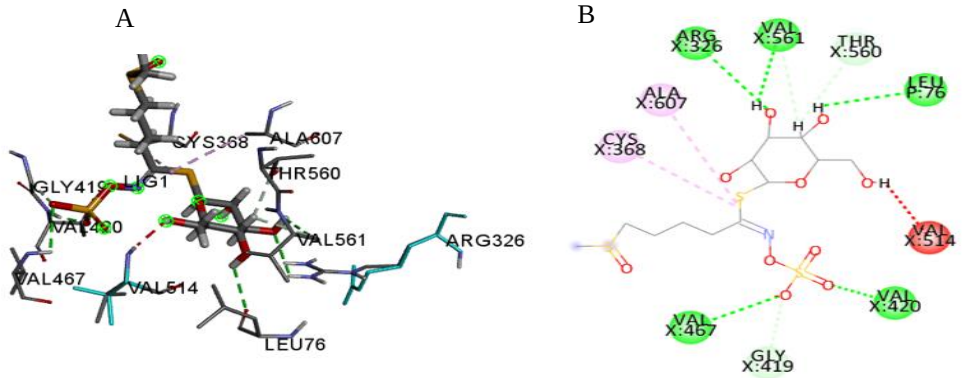

Figure 4. Docking result of Keap1-glucoraphanin complex to Nrf2. A. Ligand-binding Interaction, B. 2D Interaction

ISSN. 2087-2852
E-ISSN. 2338-1655

Quercetin and glucoraphanin bound to the Kelch domain, which functioned as the Nrf2 binding region. Both compounds had strong interaction and could easily bind to Keap1, proven by more amount of interactions and smaller binding energy than other compounds [28]. The strong interaction indicates a stronger impact on Nrf2 to prevent being sequestered by Keap1. Therefore, degradation of Nrf2 by proteasome can be prevented. Consequently, Nrf2 will be free, then it can enter the nucleus to form heterodimers with small MAF proteins [4]. The heterodimer complex is recognized by ARE, leading to the induction of antioxidant gene expression [15]. It shows that quercetin and glucoraphanin can change the stability of the Nrf2-Keap1 interaction.

The combination of Keap1 and quercetin in the form of ligand complex could disturb the Nrf2 binding on the Kelch domain of Keap1 (Fig.3). As a result, the Nrf2 binding site to Keap1 changed into Val 463, Val 465, ILE 416, Val 369, and ALA 607 which were different from the residue amino acid in keap1-Nrf2. The same thing also happens in a result docking of complex keap1-glucoraphanin to Nrf2 (Fig. 4). This complex disturbs Nrf2 binding on the Kelch domain of keap, so that, binding site to Keap 1 changed into Val326, Val561, Ala607, Cys368, Val467, and Val420, which were distinct from residue amino acid in Keap1-Nrf2. Keap1-Nrf2 has a binding site in serin and arginine residue amino acid.

Hydrogen bonds are known to increase the binding affinity of ligand interactions. Besides, hydrogen bonds strongly contribute to the transportation, adsorption, distribution, and metabolism of a molecule [29]. The combination of hydrophobic bonds with hydrogen bonds can optimize binding affinity. In addition, the presence of hydrophobic bonds can increase the biological activity of the drug [22].

CONCLUSION

Quercetin and glucoraphanin are the strongest compounds to activate Nrf2 by inhibiting Keap1, followed by kaempferol and sulforaphane. Both of these compounds had low binding energy, more hydrogen bonds, and high hydrophobic interactions. Quercetin has a higher potential in drug development than glucoraphanin based on its biological activity as a peroxidase inhibitor.

ABBREVIATION

Nrf-2	Nuclear Factor Erythroid 2-related factor
Keap1	Kelch ECH-associating protein1
GST	Glutathione S-Transferase Substrate
Pa	probable activity
Pi	probable inactivity
DGR	Double glycine region
CTR	C¬-terminal region
Val	Valin
Ile	Isolysin
Ala	Alanine
Cyst	Cysteine
Arg	Arginine
Gly	Glycine
Tyr	Tyrosine
ARE	Antioxidant Responses Element

ACKNOWLEDGEMENT

We send our regards to our research group for helping us to finish this research. Thanks a lot to Hazna Noor Meidinna for English proofreading assistance. We would like to thank the laboratory assistants for their guidance and feedback on our project.

REFERENCES

[1] De Almeida, A.J.P.O., T.P. Ribeiro, I.A. De Medeiros. 2017. Aging: Molecular pathways and implications on the cardiovascular system. *Oxid. Med. Cell. Longev*. doi: 10.1155/2017/7941563.

[2] Zhong, H., C. Hong, Z. Han, S.J. Hwang, B. Kim, Z. Xu, J. Lee, K.H. Kim, M.H. Jin, C. Zou. 2019. Erjingwan Extracts Exert Antiaging Effects of Skin through Activating Nrf2 and Inhibiting NF- B, *Evidence-based Complement. Altern. Med*. doi: 10.1155/2019/5976749.

[3] Silva-Palacios, A., M. Ostolga-Chavarría, C. Zazueta, M. Königsberg, 2018. Nrf2: Molecular and epigenetic regulation during aging. *Ageing Res. Rev.* 47. 31–40. doi: 10.1016/j.arr.2018.06.003.

[4] Bellezza, I., I. Giambanco, A. Minelli, R. Donato. 2018. Nrf2-Keap1 signaling in oxidative and reductive stress. *Biochim. Biophys. Acta - Mol. Cell Res.* 1865(5). 721-733. doi: 10.1016/j.bbamcr.2018.02. 010.

[5] James, D., S. Devaraj, P. Bellur, S. Lakkanna, J. Vicini, S. Boddupalli. 2012. Novel concepts of broccoli sulforaphane and disease: Induction of phase II antioxidant and detoxification enzymes by enhanced-glucoraphanin broccoli. *Nutr. Rev.* 70(11). 654–665. doi: 10.1111/j.1753-4887.2012.00532.x.

[6] Wang, J., X. Fang, L. Ge, F. Cao, L. Zhao, Z.

Wang, W. Xiao 2018. Antitumor, antioxidant and anti-inflammatory activities of kaempferol and its corresponding glycosides and the enzymatic preparation of kaempferol. *PLoS One*. 13(5). 1–12. doi: 10.1371/journal.pone.0197563.

[7] Vanduchova, A., P. Anzenbacher, E. Anzenbacherova. 2019. Isothiocyanate from Broccoli, Sulforaphane, and Its Properties. *J. Med. Food*. 22(2). 121–126. doi: 10.1089/jmf.2018.0024.

[8] Adam, M., L. Chaubah, B. W. Bontes, N. A. Mulachelah. 2019. Molecular docking of polycyclic aromatic hydrocarbons as potentially carcinogenic molecules through binding with aryl hydrocarbon receptor. *JSMARTech*. 1(1). 1–4.

[9] Hussain, S. M., M. S. Hussain, A. Ahmed, N. Arif. 2016. Characterization of isolated bioactive phytoconstituents from Flacourtia indica as potential phytopharmaceuticals - An in silico perspective. *J. Pharmacogn. Phytochem.* 5(6). 323–331

[10] Malik A., S. Afaq, B. El Gamal, M. Abd Ellatif, W.N. Hassan, A. Dera, R. Noor, M. Tarique. 2019. Molecular docking and pharmacokinetic evaluation of natural compounds as targeted inhibitors against Crz1 protein in *Rhizoctonia solani*. *Bioinformation*. 15(4). 277–286. doi: 10.6026/97320630015277.

[11] Khan, T., S. Dixit, R. Ahmad, S. Raza, I. Azad, S. Joshi, A.R. Khan. 2017. Molecular docking, PASS analysis, bioactivity score prediction, synthesis, characterization and biological activity evaluation of a functionalized 2-butanone thiosemicarbazone ligand and its complexes. *J. Chem. Biol.* 10(3). 91–104. doi: 10.1007/s12154-017-0167-y.

[12] Pollastri, M.P. 2010. Overview on the rule of five. *Curr. Protoc. Pharmacol.* 49. 1–8. doi: 10.1002/0471141755.ph0912s49.

[13] Jin, M., A. Ande, A. Kumar, S. Kumar. 2013. Regulation of cytochrome P450 2e1 expression by ethanol: Role of oxidative stress-mediated pkc/jnk/sp1 pathway. *Cell Death Dis.* 4(3). 1–10. doi: 10.1038/cddis.2013.78.

[14] Reichard, J.F., G.T. Motz, A. Puga. 2007. Heme oxygenase-1 induction by NRF2 requires inactivation of the transcriptional repressor BACH1. *Nucleic Acids Res.* 35(21). 7074–7086. doi: 10.1093/nar/gkm638.

[15] Lo, S.C., X. Li, M. T. Henzl, L.J. Beamer, M. Hannink. 2006. Structure of the Keap1:Nrf2 interface provides mechanistic insight into Nrf2 signaling. *EMBO J.* 25(15). 3605-3617.doi: 10.1038/sj.emboj.7601243

[16] Zhuang, C., Z. Wu, C. Xing, Z. Miao. 2017. Small molecules inhibiting Keap1-Nrf2 protein-protein interactions: a novel approach to activate Nrf2 function. *Medchemcomm*. 8(2). 286–294. doi: 10.1039/c6md00500d.

[17] Dinkova-Kostova, A.T., W.D. Holtzclaw, R.N. Cole, K. Itoh, N. Wakabayashi, Y. Katoh, M. Yamamoto, P. Talalay. 2002. Direct evidence that sulfhydryl groups of Keap1 are the sensors regulating induction of phase 2 enzymes that protect against carcinogens and oxidants. *Proc. Natl. Acad. Sci. U. S. A.* 99(18). 11908–11913. doi: 10.1073/pnas.172398899.

[18] Itoh, K., N. Wakabayashi, Y. Katoh, T. Ishii, T. O'Connor, M. Yamamoto. 2003. Keap1 regulates both cytoplasmic-nuclear shuttling and degradation of Nrf2 in response to electrophiles. *Genes to Cells*. 8(4). 379–391. doi: 10.1046/j.1365-2443. 2003.00640.x.

[19] Xu, D., M.J. Hu, Y.Q. Wang, Y.L. Cui. Antioxidant activities of quercetin and its complexes for medicinal application. *Molecules*. 24.(6). doi: 10.3390/molecules 24061123.

[20] Domitrovic, O., R. Jakovac, H. Vasiljev, M. Vladimir-Knezevic, S. Cvijanovic, D. Tadic, Z. Romic, Z. Rahelic. 2012. No Title Differential hepatoprotective mechanisms of rutin and quercetin in CCl(4)-intoxicated BALB/cN mice. *Acta Pharmacol*. 33. 1260–1270.

[21] G. C. Weng, C.J.; Chen, M.J.; Yeh, C.T.; Ye, . 2011. Hepatoprotection of quercetin against oxidative stress by induction of metallothionein expression through activating MAPK and PI3K pathways and enhancing Nrf2 DNA-binding activity. *Biotechnol*. 28. 767–777.

[22] Fitria, L., M.H. Widyananda, S.P. Sakti. 2019. Analysis of allopurinol, cucurbitacin b, morindine, and piperine as xanthine oxidase inhibitor by molecular docking. *JSMARTech*. 1(1). 6–11.

[23] Canning, P., F.J. Sorrell, A.N. Bullock. 2015. Structural basis of Keap1 interactions with

Nrf2. *Free Radic. Biol. Med.* 88(Part B). 101–107. doi: 10.1016/j.freeradbiomed. 2015.05.034.

[24] Lin, H.L., H. Zhang, C. Medower, P.F. Hollenberg, W.W. Johnson. 2011. Inactivation of cytochrome P450 (P450) 3A4 but not P450 3A5 by OSI-930, a thiophene-containing anticancer drug. *Drug Metab. Dispos.* 39(2). 345–350. doi: 10.1124/dmd.110.034074.

[25] Goncalves, S., R. Anabela. 2017. Inhibitory properties of phenolic compounds against enzymes linked with human diseases. Londong: INTECH Open.

[26] Panigrahi, S. 2008. Strong and week hydrogen bonds in protein-ligand complexes of kinases: a comparative study. *Amino Acids*. 34. 617–633.

[27] Varma, A.K., R. Patil, S. Das, A. Stanley, L. Yadav, A. Sudhakar. 2010. Optimized hydrophobic interactions and hydrogen bonding at the target-ligand interface leads the pathways of Drug-Designing. *PLoS One*. 5(8). doi: 10.1371/journal.pone. 0012029.

[28] Elokely, K.M., R.J. Doerksen. 2013. Docking challenge: Protein sampling and molecular docking performance. *J. Chem. Inf. Model.* 53(8). 1934–1945. doi: 10.1021/ci400040d.

[29] Williams, J.E., M. Ladbury. 2005. Hydrogen Bonds in Protein-Ligand Complexes. Methods and Principles in Medicinal Chemistry. John Willey and Publisher. USA.

Effect of Water Clover (*Marsilea crenata*) Ethanol Extracts on Follicle and Oocyte Diameter of Goat: In Vitro Study

Siska Nanda Widhaningrum[1], Septiawan Putranto[1], Sri Rahayu[2*], Gatot Ciptadi[3]

[1]Master Program of Biology, Faculty of Mathematics and Natural Sciences, University of Brawijaya, Malang, Indonesia
[2]Department of Biology, Faculty of Mathematics and Natural Sciences, University of Brawijaya, Malang, Indonesia
[3]Faculty of Animal Husbandry, University of Brawijaya, Malang, Indonesia

Abstract

Water clover (*Marsilea crenata*) is one of the herbal plants that has been using in alternative medicine. It possesses pharmacologically active compounds like flavonoid, which has cellular activities such as antioxidant and estrogenic activity. This study aimed to evaluate the impact of water clover ethanol extract (WCE) at different concentrations on the growth of follicles and oocytes based on follicles and oocytes diameter, respectively, after six days of culture. This experimental study used 24 isolated antral follicles (2.5-3.2 mm), which were randomly divided into four groups including control (without supplemented WCE) and experimental groups that supplemented with different concentrations of WCE (21.6, 43.2, and 86.4 µg ml^{-1}) in culture medium for six days culture. The diameter of follicles was measured on days 0, 3, and 6. Additionally, oocytes diameter was also measured on day 6. The results indicate that the mean diameter of antral follicles and oocyte diameter of WCE 43.2 µg ml^{-1} was significantly increase compared to the other groups (P≤0.05). According to our results, WCE exerts its effect on the growth of the antral follicle and oocyte based on follicles and oocytes diameter respectively in a dose-dependent manner after six days of the antral follicle cultured.

Keywords: antral follicle, flavonoid, *in vitro*, oocyte, water clover.

INTRODUCTION

Reproduction is a critical biological process and very important in all living systems to maintain species survival [1]. The ovarian follicle is the structural and functional unit of the female reproductive system, which plays a role in folliculogenesis [2]. Folliculogenesis is the physiological process that involves a complex interaction among endocrine, paracrine, and autocrine factors for activation, growth, and maturation of the ovarian follicles. So, it influences steroidogenesis, angiogenesis, oocyte maturation, as well as follicular atresia [3].

During folliculogenesis, *reactive oxygen species* (ROS) will be generated as a result of cellular metabolism. Cell living under aerobic need oxygen, so ROS such as *superoxide anion radical* ($O2^-$), *hydroxyl radical* (OH^-), and *hydrogen peroxide* (H_2O_2) will be generated from oxygen [4]. Also, *superoxide anion radical* ($O2^-$) reacts with *nitric oxide* (NO-) to form *peroxynitrite* ($ONOO^-$), so it will form *reactive nitrogen species* (RNS) [5]. The increase of ROS and RNS levels react with cellular lipids, protein, and nucleic acid, so that lead to significant damage of cell structure and thereby cause oxidative stress (OS). Several studies indicate that OS is involved in the initiation of apoptosis in antral follicles, so that affect of folliculogenesis and steroidogenesis [6]. However, the role of endogen antioxidants such as *superoxide dismutase* (SOD), *glutathione peroxidase*, and *catalase* reduced the increase of free radical and maintain the proper redox state of cells as the signalling molecules in normal physiological processes [5].

Folliculogenesis includes the growth and maturation of follicle which provides the microenvironment necessary for oocyte growth and development, so it will produce matured oocyte (metaphase II) [7]. The growth of follicles is characterized by increasing in follicular diameter due to an increase in oocytes diameter, the number of granulosa cells layer, and formation of the antrum (accumulation of follicular fluid) [8]. Oocyte quality can be determined by the oocyte growth based on oocyte diameter [9].

Water clover (*Marsilea crenata*) is one of the herbal plants that has been using in alternative medicine for osteoporosis, infection of the urinary tract, and inflammation of the esophagus [10]. It is caused by the phytochemical content of flavonoids in WCE, which have cellular activities such as antioxidant, anti-inflammatory, anti- tumor, anti-osteoporosis, and estrogenic [11]. The previous study explained that the

*Correspondence address:
Sri Rahayu
Email : yayuksrirahayu8@gmail.com
Address : Dept. Biology, University of Brawijaya, Veteran Malang, Malang 65145

presence of flavonoids as an antioxidant in semen extender can improve the quality of semen from the effects of freezing [12]. Besides, isoflavone, the subclass of flavonoid also exerts estrogenic activity that plays an important role in folliculogenesis [13]. Therefore, the present study aimed to evaluate the impact of water clover ethanol extract (WCE) at the different concentrations on the growth of follicles and oocytes based on the follicles and oocytes diameter respectively, after the six days of the antral follicle cultured.

MATERIAL AND METHOD

Extraction of *Marcilea crenata*

The leaves of WCE were collected in Surabaya, East Java, Indonesia. Leaves were washed thoroughly with water then dried in the greenhouse at room temperature (25°C) during 4-5 days. The dried leaves were ground into powder [14] then extracted with ethanol 70% through the maceration method with modification [15]. Ethanol extraction of phenolic compounds in WCE was carried out at the Biochemistry Laboratory, Faculty of Mathematics and Natural Sciences, Brawijaya University. The next step was freeze-dried for 24 hours to get the extracts in the form of pasta.

Isolated Antral Follicles and IVGC

This study used the antral follicle of Etawah Crossbred (PE) to analyze the effect of WCE on folliculogenesis. Goat ovaries were collected from slaughterhouse Malang City, East Java, Indonesia. The ovaries were washed with sterile 0.9% physiological saline and then were transported to the laboratory in a container kept at 37°C in sterile 0.9% physiological saline supplemented with antibiotics, which consist of 0.01 g streptomycin and 0.006 g penicillin (Meiji, Japan). After arrived at the laboratory, some fat tissues were removed from ovaries and washed again in sterile 0.9% physiological saline [16].

The antral follicles with diameter size of 2.5-3.2 mm (n=24) were isolated with the slicing technique and cultured for 6 days in 300 µL of culture medium in each well. The culture medium containing TCM-199 medium supplemented with 10% heat-activated Fetal Bovine Serum (FBS), 1% antibiotic Pen-Strep, 0.1 $IU.mL^{-1}$ FSH, 1 $IU.mL^{-1}$ HCG, 4% *polyvinyl-pyrrolidone*, then covered under sterilized paraffin oil and incubation at 37°C in 5% CO_2 [17]. WCE were added in the treated groups at 21.6, 43.2, and 86.4 $\mu g.mL^{-1}$. And then, half of the culture medium (approximately 150 µL) was replaced every day, except the culture medium of the third day that was completely replaced.

Morphological Evaluation of Follicular Growth

Evaluation of the growth of antral follicles morphology was checked by stereo-microscope (SMZ 645 Nikon, Tokyo, Japan) that have been approved with a camera at x20 magnification and observed on days 0, 3, and 6. And then measured of follicular diameter were carried out *by Image raster software* [18].

Evaluation of Oocyte Quality

Evaluation of oocyte quality used oocyte diameter was carried out on the sixth day of culture. The oocytes in selected antral follicles were isolated with the slicing technique and then measured of oocyte diameter by an inverted microscope at x10 magnification [8].

Statistical Analysis

The data were presented in mean values and Standard Error (SE). The data were analyzed by one-way ANOVA using SPSS 16 for windows. If the result of ANOVA Test shows significantly different ($P \leq 0.05$) and followed by Posthoc Test using Duncan with a confident level of 95% ($\alpha=0.05$).

RESULT AND DISCUSSION

Effect of WCE on the diameter of cultured isolated antral follicles

One of the purposes of this study was to evaluate the impact of different concentrations of WCE on the growth of isolated cultured antral follicles for six days. The mean diameter in the sixth day cultured of the isolated cultured antral follicles, which were treated by WCE 43.2 $\mu g.mL^{-1}$ was significantly increase compared to the other groups (Table 1, Fig. 1).

During folliculogenesis, the increasing of follicular diameter occurred due to the influence of gonadotropins, such as FSH promotes proliferation and differentiation of granulosa cell through cAMP-PKA and PI3K-AKT pathway [19]. Thus, the follicle able to form an antrum (follicular fluids were produced by the granulosa cell), and the follicular diameter will increase. In addition, 17β-estradiol through sex steroidogenesis also promotes proliferation and differentiation of granulosa cells in the presence of FSH stimulation [20]. The differentiation of granulosa cells can be divided into 2 groups, such as cumulus cells surrounding the oocyte to promote maturation oocyte and mural granulosa

ISSN. 2087-2852
E-ISSN. 2338-1655

cell to produce sex steroid. So, the increase in the number of granulosa cells, oocyte diameter, and antrum formation cause the increase of follicular diameter [8].

Tabel 1. The average follicles diameter during *in vitro* culture

Groups	Diameter of Follicles (µm)		
	Day-0	Day-3	Day-6
Control	2927.30 ± 160.29	3105.06 ± 241.44*	3023.75 ± 120.77
D21.6 µg.ml^{-1}	2889.77 ± 184.05	2770.85 ± 260.75	2879.03 ± 205.02
D43.2 µg.ml^{-1}	2873.25 ± 82.83	3106.83 ± 210.63*	3462.75 ± 341.26*
D86.4 µg.ml^{-1}	2838.10 ± 214.68	2781.14 ± 300.51	2879.77 ± 245.14

Notes: symbol (*) indicate a significant difference between treatment ($p<0.05$).

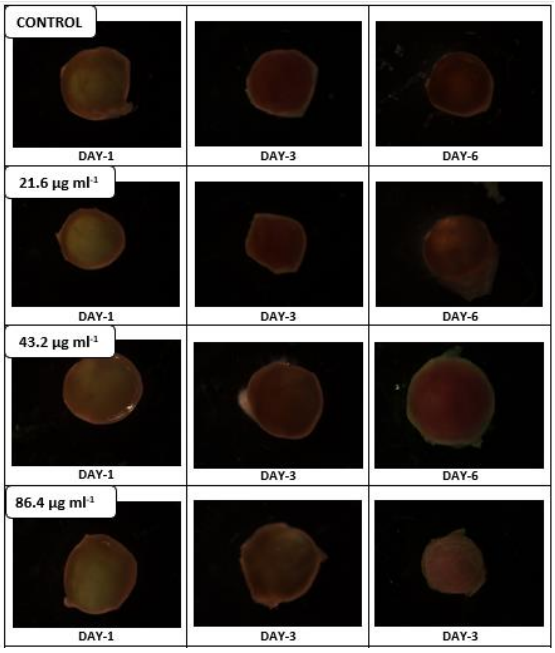

Figure 1. Isolated antral follicles in vitro culture in different treatments: the control group (first row), this experimental group supplemented with 21.6, 43.2, and 86.4 µg.mL^{-1} (second, third, and fourth row respectively) on day 0, day 3, and day 6. Images were observed by the stereo microscope that has been approved with a camera at x20 magnification

The increased follicular diameter after WCE treatment may occurred by antioxidant activity in WCE with binding to free radicals through the phenolic hydroxyl structure of flavonoid [21]. So, it can inhibit cell damage due to the increase of free radicals and can maintain the level of intracellular homeostasis between prooxidant and antioxidant [5]. In addition, flavonoids also regulate the activity of the antioxidant enzyme to inhibit cell damage and followed by apoptosis [22]. In addition, OS causes a decrease in follicular diameter, which can initiate apoptosis in antral follicles and affect follicular development and steroidogenesis [5]. Overproduction of ROS can impact the IVC of antral follicles because they act as the second messenger and induce the opening of a non-specific pore in the inner mitochondria membrane. Thus, it releases cytochrome C and is followed by caspase activation to induce apoptosis and loss of follicular function [23].

The growth of the antral follicle also occurred due to the presence of phytoestrogens in WCE that produce estrogenic activity/agonist. So, there was a bind between phytoestrogen and estrogen receptor, such as ERα and ERβ in cytoplasm or nucleus through genomic and non-genomic action with lower binding compared to endogenous estrogen 17β-estradiol [24]. This complex yields estrogenic activity functioned as transcription factors that initiate the transcription activity of a gene [19-21]. This complex also yields a rapid cellular response, such as MAPK/ERK, PI3K/AKT, cAMP/PKA, PKC, tyrosine kinase pathway, which is also be used to increase transcription activity [25].

According to Rosales-Tores [20], the presence of estrogenic activity may increase the response of granulosa cells to FSH stimulation. It enables the increasing proliferation and differentiation activity by expressing several genes that play important role in the folliculogenesis of antral follicles, such as FSH (FSHR), luteinizing hormone receptor (LHR), aromatase (CYP19a1), cytochrome P450 (CYP11a1), 17α-hydroxylase P450c17), 3β-hydroxysteroid dehydrogenase (3β-HSD).

Whereas, the decreasing of follicular diameter occurred due to the phytoestrogens at certain dosage enable to yield antiestrogenic activity/antagonist, so they unable to promote proliferation and differentiation in follicle development of antral follicle. Based on the previous study, phytoestrogens at high doses inhibit the activity of cytochrome p450 (CYP11a1), which can convert cholesterol into pregnenolone, thus affect estrogen production [26]. Genistein, one of the phytoestrogens also alters the level of precursor hormones of estrogen, such as estrone, testoserone, DHEA, progresterone, and enables cause follicle atresia

ISSN. 2087-2852
E-ISSN. 2338-1655

that followed by reduction of oocyte maturation. Besides, genistein also significantly increases the expression of the cell cycle inhibitor (*cyclin-dependent kinase inhibitor 1a/cdkn1a*), thus it can inhibit proliferation of granulosa cells [27].

Effect of WCE on the diameter of oocytes

The presence of WCE in the culture medium enables to increase oocyte maturation characterized by an increase of oocyte diameter at WCE 43.2 µg.mL^{-1} compared to the other groups (Fig. 2 and 3). The increasing oocyte diameter may occur due to antioxidant activity in WCE. So, it can suppress free radical activity in oocytes. However, overproduction of ROS exceeds physiological limit, so it can induce destabilization of *maturation promoting factor* (MPF), decrease survival factor, and stimulate apoptosis in oocyte through mitochondria [28].

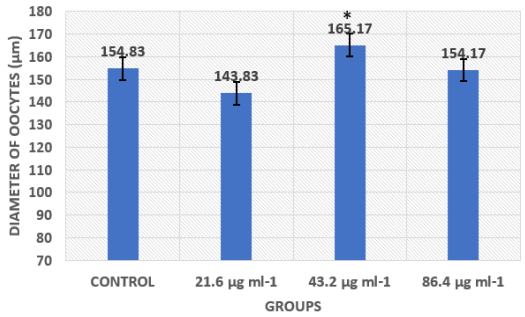

Figure 2. The average diameter of oocytes after antral follicle culture in different treatments. Symbol (*) indicate a significant difference between treatment ($p<0.05$).

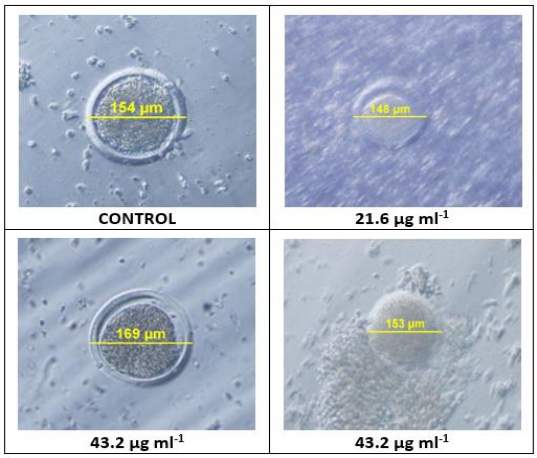

Figure 3. The diameter of oocytes after antral follicle culture in different treatments.

The decreasing of oocyte diameter occurred due to the phytoestrogens at high doses enable to inhibit the kinase activity of *cyclin-dependent kinase* 2 (cdk2)/*cell division cycle* 2 (cdc2) [29]. Thus, induce G2/M arrest in mammalian cell and maintain in meiotic arrested condition and followed by the inhibition of meiotic maturation [30].

The increasing of oocyte diameter related to the increasing of follicle diameter at WCE 43.2 µg.mL^{-1} (Fig. 1). It indicates the relationship between follicular diameter and oocyte maturation level characterized by the increasing of oocyte diameter [31]. It happened because there is an acquisition of competence development of oocyte that initiated by interaction between granulosa cells and oocyte through gap junction, su/ch as transfer of small molecules (cAMP, cGMP, RNA, and metabolite) so the oocyte able to regulate oocyte meiotic maturation and reach the final development competence stage [32].

CONCLUSION

According to our result, WCE exerts its effect on the growth of antral follicle and oocyte based on follicles and oocytes diameter, respectively in a dose-dependent manner after the sixth day in vitro culture of the antral follicle.

ACKNOWLEDGEMENT

The authors thank the Central Laboratory of Biological Sciences'staff for assistance in conducted research and S. Rahayu, G. Ciptadi for support and facilitate this project.

REFERENCES

[1] Evans, T.J. 2015. Handbook of toxicology of chemical warfare agents: reproductive toxicity and endocrine disruption of potential chemical warfare agents. Elsevier.

[2] Jones, A.S.K., A. Shikanov. 2019. Follicle development as an orchestrated signaling network in a 3D Organoid. *J. Biol Eng*. 13(2). doi: 10.1186/s13036-018-0134-3.

[3] Ricardo, J.D.F., L.D.L. Ferreira, J.V.S. Roberto, R.S. Rodrigues. 2018. Control of growth and development of prentral follicle: Insights from *In Vitro* culture. *Anim Reprod*. 15(1). 648-659.

[4] Sugino, N. 2005. Reactive Oxygen Specis in ovarian physiology. *Reprod. Med Biol*. 4. 31-44.

[5] Patrick, J.D., D.P. Sally, L. Ulrike. 2012. Roles of Reactive Oxygen Species and antioxidants in ovarian toxycity. *Biol. Reprod*. 86(2). 27-37.

[6] Francesca, C., C. Natascia, D. Danila, T. Simona. 2015. Influence of ROS on ovarian function. New Discoveries in Embriology.

INTECH open science open mind. doi: 10.5772/61003.

[7] Itoh, T., K. Masayuki, A. Hiroyuki, S. Yutaka, H. Hiroyoshi. 2002. Growth, antrum formation, and estradiol production of bovine preantral follicles cultured in a serum-free medium. *Biol. Reprod.* 67.1099-1105.

[8] Harris, A., S. Rahayu, G. Ciptadi. 2014. The morphological measurement of immature oocyte obtained from follicle different size in Indonesia local goat. *Int. J Biosci*. 4(4). 211-216.

[9] Sugimura, S., D. Richani, R.B. Gilchrist. 2018. Follicular guidance for oocyte developmental competence. *Proceedings of the 10th International Ruminant Reproduction Symposium (IRRS2018).*

[10] Hardoko, W.L. Gunawan, R. Handayani. 2019. Inhibition activities of water clover (*Marcilea crenata*) leaf extract on HMG-CoA reduktase enzyme. *FaST-Jurnal Sains dan Teknologi.* 3(1). 45-57.

[11] Titisari, N., A. Fauzi, A. Adyana, P. Trisunuwati. 2016. the effects of water clover (*Marcilea crenata*) extract against estrogen, progresteron and uterine histology on rat (*Rattus norvegicus*). *Int. J. PharmTech Res.* 9(6). 165-171.

[12] Wahyuningsih, S., G. Ciptadi, K. Pridiawati. 2019. The effect of water clover (*Marcilea crenata*) extract addition in egg yolk and skim milk extender on frozen goat semen quality. *IOP Conference Series: Earth and Environmental Sciences 387 012103*. ISTAP.

[13] Trisunuwati, Pratiwi. 2016. The role of leaf water clover (*Marsilea crenata*) sueeze towards estrogen blood level and uterine histology in rats (*Rattus norvegicus*). *Jurnal Ternak Tropika.* 17(2). 1-7.

[14] Sarker, S.D., Z. Latif, A.I. Gray. 2006. An overview of natural product isolation. Natural Product Isolation 2nd Ed. Humana Press Inc. Totowa. 1-26.

[15] Islam, M.S., I. Arihiro, S. Kiyotake, K.N. Hisashi 2017. Isolation and identification of two potential phytotoxic substances from the aquatic fern *Marsilea crenata*. *J. Plant Biol*. 60. 75-81.

[16] Ciptadi, G., M.N. Ihsan, S. Rahayu, D.H.K. Widjaya, M. Mudawamah. 2017. A feasibility study of prepubertal and over mature aged local goat in relation to result of *In Vitro* growth culture to obtain additional M-II oocyte resources. *AIP Conference Proceeding. The 8th International Conference on Global Resource Conservation* (ICGRC 2017).

[17] Ciptadi, G., S. Rahayu, A.I. Putri, H.N. Karima, A. Budiarto, P.F.P. Susiati, Mudawamah. 2019. Utilization of local goat ovary from slaughterhouse as a material source for in vitro culture, conservation and freezing of oocyte cells. *IOP Conf. Series: Earth and Enviromental Science 259*.

[18] Silva, G.M., R. Rossetto, R.N. Chaves, A.B.G. Duarte, V.R. Araújo, C. Feltrin, … J.R. Figueiredo, 2015. *In vitro* development of secondary follicles from pre-pubertal and adult goats cultured in two-dimensional or three-dimensional systems. *Zygote*. 23(4). 475–484.

[19] Shimada, M., Y. Yamashita. 2011. The key signaling cascades in granulosa cells during follicular development and ovulation process. *J. Mamm. Ova Res*. 28. 25-31.

[20] Rosales-Torres, A.M., A.G. Sánchez, C.G. Aguilar. 2012. Review [revisión] follicular development in domestic ruminants [desarrollo folicular en rumiantes domesticos]. *Trop. Subtrop.Agroecosystems.* 15(1). 147-160.

[21] Martinchik, A.N., V.V. Zubtsov, 2012. Phytoestrogen is properties of flax seed lignans. *Vopr Pitan*. 81. 61–66.

[22] Cui, J., Y. Shen, R. Li. 2013. Estrogen synthesis and signaling pathways during aging: from periphery to brain. *Trends Mol. Med.* 19(3). 197-209.

[23] Patel, S., J. Peretz, Y.X. Pan, W.G. Helferich, J.A. Flaws. 2016. Genistein exposure inhibits growth and alters steroidogenesis in adult mouse antral follicles. *Toxicol. Appl. Pharmacol*. 293. 53-62.

[24] Hashem, N.M., Y.A. Soltan. 2015. Impacts of phytoestrogens on livestock production: a review. *2nd International Conference on the Modern Approaches in Livestock's Production System*, *Egypt*.

[25] Hayashi, S., Y. Yamaguchi. 2008. Estrogen signaling pathway and hormonal therapy. *Breast Cancer*. 15. 256–261.

[26] Tiemann, U., F. Schneider, J. Vanselow, W. Tomek. 2007. *In vitro* exposure of porcine granulosa cells to the phytoestrogens genistein and daidzein: Effects on the biosynthesis of reproductive steroid

hormones. *Reprod Toxicol*. 24. 317-25. doi: 10.1016/j.reprotox.2007.07.008.

[27] Agarwal, A., S. Gupta, S. Sikka. 2006. The role of free radicals and antioxidants in reproduction. *Curr. Opin. Obstet. Gynecol*. 18(3). 325-332.

[28] Khazaei, M., A. Faranak. 2017. Reactive Oxygen Species generation and use of antioxidants during *In Vitro* maturation of oocytes. *Int. J. Fertil. Steril*. 11(2). 63-70.

[29] Dixon, R.A., D. Ferreira. 2002. Genistein. *Phytochemistry*. 60. 205–211.

[30] Yoshida, N., K. Mizuno. 2012. Effect of physiological levels of phytoestrogens on mouse oocyte maturation in vitro. *Cytotechnology*. 64. 241-24.

[31] Mardenli, O., H. Aryan, R. Abdulkarim, M. Al-Mezaid, L. Bogdan. 2017. Effects of follicle size and oocytes diameter on developmental competence and in vitro embryo production of Awassi sheep ewes oocytes. *Internasional Educational Applied Scientific Research Journal (IEASRJ)*. 2(9). 13-15.

[32] Li, H.J., M.L., Sutton-McDowall, X. Wang, S. Sugimura, J.G. Thompson, R.B. Gilchrist. 2016. Extending prematuration with cAMP modulators enhances the cumulus contribution to oocyte antioxidant defence and oocyte quality via gap junctions. *Hum. Reprod*. 31. 810-821.

ISSN. 2087-2852
E-ISSN. 2338-1655

Plant Growth Promoting Endophytic Bacteria of *Coffea canephora* and *Coffea arabica* L. in UB Forest

Esti Rizkiana Pratiwi[1*], Tri Ardyati[2], Suharjono Suharjono[2]

[1]Master Program of Biology, Department of Biology, Faculty of Mathematics and Natural Sciences, University of Brawijaya, Malang, Indonesia

[2]Department of Biology,Faculty of Mathematics and Natural Sciences, University of Brawijaya, Malang, Indonesia

Abstract

Plant Growth Promoting (PGP) Endophytic bacteria are used as an alternative biofertilizer to support soil health and plant productivity. This research aimed to isolate, analyze the potential, and identify the endophytic bacteria of Robusta and Arabica coffee plants as biofertilizer agents. Endophytic bacteria were isolated from the roots of coffee plants and tested for their potential to produce IAA, phosphate-solubilizing, and nitrogen fixation. Potential endophytic bacterial isolates were identified based on 16S rDNA sequence similarity. Total isolates from Robusta coffee consisting of ten IAA-producing bacteria, eight phosphate-solubilizing, and seven nitrogen fixation bacteria isolates. Total isolates from Arabica coffee roots were 12 isolates of IAA-producing bacteria, seven isolates of phosphate-solubilizing bacteria, and six isolates of nitrogen fixation bacteria. The highest potential of the isolate from Robusta roots was SS.E2 isolate to produce IAA 110.73 µg.mL^{-1}; SS.P3 isolate to dissolve phosphate 4.42 µg.mL^{-1}, and SS.N2 isolate to produce ammonium 3.15 µg.mL^{-1}. The highest potential of the isolate from Arabica roots was SW.E9 isolate to produce IAA up to 257.16 µg.mL^{-1}; SW.P5 isolate to dissolve phosphate up to 4,55 µg.mL^{-1}; and SW.N6 isolate to produce ammonium up to 1.16 µg.mL^{-1}. Isolates SS.E2, SW.E9, SS.P3, SW.P5, SS.N2, and SW.N6 were respectively identified as *Bacillus cereus* ATCC 14579, *Bacillus cereus* ATCC 14579, *Rahnella aquatilis* B35, *Kluyvera intermedia* TPY16, *Rahnella aquatilis* B35, and *Pseudomonas tolaasii* NCPPB 2192. Potential PGP isolates can be developed as biofertilizer agents for the coffee plant.

Keywords: Coffee, Endophytic bacteria, IAA, Nitrogen, Phosphate

INTRODUCTION

Coffee fruit is used as a popular beverage commodity for the global community. The value of the coffee sale price is determined by its quality. Organic coffee fruit and beverage products have a higher selling price than conventional coffee [1,2]. Robusta and Arabica coffee are agricultural commodities that commercially provide added value economically for the community and government [3].

UB Forest is a land for the conversion of forests into coffee plantations (Agroforestry). Forest land that converted to agricultural land causes a decrease in plant diversity and soil microbes [4]. Soil microbes play an important role in the cycle of elements that increase soil fertility and provide nutrients for plants [5-6]. Decreasing microbial diversity and soil fertility is a major factor in reducing the productivity of coffee plants.

Some species of bacteria have the potential to promote plant growth (Plant Growth Promoting/PGP). PGP microbes associate symbiosis that positively impacts plant health and growth, improves soil quality and nutrient cycles [7,8,9]. Endophytic bacteria associate and colonize plant tissues and play a role in spurring plant growth and development (PGP agents) [10].

Various PGP bacteria are being developed into biofertilizer products as an alternative to synthetic fertilizers. *Bacillus subtilis* endophytic cocoa beans increased the development of cocoa plants and as an antimicrobial pathogen [11]. *Bacillus subtilis* LK14 endophytic roots and stems of *Solanum lycopersicum* can produce IAA and increase root and stem biomass, as well as the amount of chlorophyll a and b [12]. *Agrobacterium tumafaciens* and *Azotobacter vinelandii* endophytic sweet potatoes produce IAA [13]. *Herbaspirillum* endophytic rice plants were able to fix nitrogen and produce IAA [14]. Endophytic bacteria from the leaves, fruits, stems, and roots of Arabica coffee plants are *Bacillus, Burkholderia, Clavibacter, Curtobacterium, Escherichia, Micrococcus, Pantoea, Pseudomonas, Serratia,* and *Stenotrophomonas* [15].

The diversity of endophytic bacteria from the roots of coffee plants are widely reported. However, the diversity and potential of endophytic bacteria in coffee plants as PGP agents, especially in UB Forest, have not been studied yet. This study aims to isolate, analyze the potential, and identify potential isolates of Robusta and Arabica coffee root endophytic bacteria from UB Forest as PGP agents.

* Correspondence address:
Esti Rizkiana Pratiwi
Email : rizkianaesti@gmail.com
Address : Dept. Biology, University of Brawijaya, Veteran Malang, 65145

MATERIAL AND METHOD

Coffee Plant Root Sampling

Root samples were taken from Arabica and Robusta coffee plants in UB Forest agroforestry land, Malang, East Java Province, Indonesia. UB Forest Agroforestry is located at 07.824545°SL and 112.578390°EL and 07.821705°SL and 112.577551°EL. Three samples were taken from each type of coffee plant. Each sample was a composite root of three plants. The root sample of each plant is the secondary roots with a healthy tip at a depth ±10 cm. Root samples were put in plastic bags and stored in isothermic boxes/cool boxes.

Isolation of Endophytic Bacteria in Coffee Plants

The endophytic bacterial roots of coffee plants were isolated according to the method of previous studies [15,16,17]. The root sample of the coffee plant is cut off 10 cm long, then washed with running water and rinsed with sterile distilled water. The roots are cut into pieces with a length of ± 2 cm and then sterilized by immersing the surface in Ethanol 70% for one minute, sodium hypochlorite 5.25% for 5 minutes, and Ethanol 70% half minutes and then washed three times in sterile distilled water for one each minute. A 10 gram sterile root sample plus 90 mL of sterile physiological saline solution (0.85% NaCl) is blended to homogeneous. The root sample suspension is made in a dilution series of up to 10^{-6}. Each 0.1 mL sample suspension was inoculated in a pour plate on Tryptic Soy Agar (TSA) media containing 1 $\mu g.mL^{-1}$ L-Tryptophan and then incubated at 28°C for 48 hours to obtain a culture of IAA-producing endophytic bacterial isolates [16-17].

Phosphate solubilizing endophytic bacteria were isolated by method of previous studies [19-20]. A root sample suspension of 0.1 mL was inoculated by pour plate on a Pikovskaya agar medium consisting of Glucose (5 $g.L^{-1}$); $Ca_3(PO_4)_2$ (2.5 $g.L^{-1}$); KCl (0.1 $g.L^{-1}$); $(NH4)_2SO_4$ (0.25 $g.L^{-1}$); NaCl (0.1 $g.L^{-1}$); $MgSO_4.7H_2O$ (0.025 $g.L^{-1}$); $MnSO_4.H_2O$ (0.25 $g.L^{-1}$); $FeSO_4.7H_2O$ (0.25 $g.L^{-1}$); yeast extract (0.25 $g.L^{-1}$) and agar (15 $g.L^{-1}$), then incubated at 28°C for 72 hours.

Nitrogen-fixing endophytic bacteria were also isolated [20]. A root sample suspension of 0.1 mL was inoculated on N-free media (without Bromothymol blue) consisting KH_2PO_4 (0.5 $g.L^{-1}$); $FeCl_3.6H_2O$ (0.015 $g.L^{-1}$); $MgSO_4.7H_2O$ (0.2 $g.L^{-1}$); NaCl (0.1 $g.L^{-1}$); DL-Malic Acid (5 $g.L^{-1}$); KOH (4.8 $g.L^{-1}$), yeast extract (0.05 $g.L^{-1}$) and agar (15 $g.L^{-1}$), then incubated at 28°C for 7 days. Each IAA-producing endophytic bacterial isolate, phosphate-solubilizing, and nitrogen fixation was purified by spread plate.

Bacterial Potency Assay for Producing IAA

Each endophytic bacterial isolate was tested for its potential in producing IAA hormones [16,20]. An oose loop full isolate culture was inoculated into 25 mL of Tryptic Soy Broth (TSB) media containing 2% of L-Tryptophan (1 $\mu g.mL^{-1}$) and incubated at 28°C for 48 hours. Each cell culture with OD 1,0 as much as 5 mL was inoculated into 50 mL of TSB media containing 2% of L-Tryptophan (1 $\mu g.mL^{-1}$) and then incubated at 28°C for 72 hours. Bacterial culture was taken 2 mL every 24 hours and then centrifuged at 10.000 rpm for 10 minutes. The 2 mL supernatant was added 4 mL of Salkowski reagent and incubated in a dark room for 30 minutes until it turned pink. The suspension was measured for absorbance at a wavelength of 535 nm, then the IAA concentration is calculated based on the IAA standard curve.

Bacterial Potency Assay for Phosphate Solubilizing

Each endophytic bacterial isolate was tested for its potential in dissolving phosphate [19,20]. An oose loop full isolate culture was inoculated into 25 mL liquid Pikovskaya media (pH 7) containing 0.5% Tricalcium Phosphate (TCP) and incubated at 28°C for 72 hours. Each isolate culture (OD 1,0) was inoculated as much as 5 mL into 50 mL liquid Pikovskaya media (pH 7) containing 0.5% TCP and incubated at 28°C for 72 hours. Bacterial culture was taken 2 mL every 24 hours and then centrifuged at 10.000 rpm for 20 minutes. Supernatant 1 mL was added with 10 mL Chloromolybdate reagent and 0.1 mL Chlorostannous acid. The suspension was added with sterile distilled water up to a volume of 50 mL then incubated for 10 minutes. The sample suspension was measured for absorbance at a wavelength of 690 nm and the concentration was calculated based on a standard phosphate curve.

Bacterial Potency Assay for Nitrogen Fixation

Each endophytic bacterial isolate was tested for potential fixation of nitrogen [20]. A 1 oose loop full isolate culture was inoculated into 25 mL liquid N-Free (without Bromothymol blue) media and incubated at 28°C for 7 days. Bacterial cultures (OD 0,6) of 5 mL were inoculated into 50 mL of liquid N-Free media and incubated at 28°C for 7 days. Bacterial culture was taken 2 mL every 2 days and then added 10 µL $ZnSO_4$ and 2.5 µL NaOH 2N were incubated for 30 minutes until the

ISSN. 2087-2852
E-ISSN. 2338-1655

culture became clear. The suspension is centrifuged at 10.000 rpm for 10 minutes. A 1 mL supernatant was added with 0.5 mL of Nessler's reagent and sterile distilled water up to 5 mL volume. The suspension is incubated for 30 minutes until it is yellow. The suspension was measured for absorbance at a wavelength of 425 nm and ammonium concentration was calculated based on the standard ammonium curve.

Identification of Potential Endophytic Bacteria Based on 16S rDNA Sequences

Potential endophytic bacterial isolates of PGP agents were isolated by chromosomal DNA according to the modification of the ZR Fungal/ Bacterial DNA MiniPrep Kit method. The 16S rDNA sequences were amplified using universal primers 27f (5 '-GAG AGT TTG CTG GCT ATC CAG-3') and 1492r (5 '-CTA CGG CTA TGT CCT TAC GA-3'). The 16S rDNA sequence was amplified with a PCR mix composition consisting of a 25 µL master mix, 5 µL DNA template (50 ng.mL^{-1}), each primer 2 µL (10 pmol), and Nuclease free water 16 µL. The PCR program for 16S rDNA amplification consisted of Pre-denaturation at 94°C (5 minutes) followed by 35 cycles including denaturation (94°C; 0.5 minutes), annealing (55°C; 0.5 minutes), extension (72°C; 1.5 minutes) and post-extension (72°C, 7 minutes) [20-21]. The 16S rDNA sequence was sequencing at First Base, Malaysia. The 16S rDNA was alignment sequence with the reference sequence, and the phylogeny tree was constructed based on the Maximum-Likelihood algorithm, with 1000 bootstraps using the MEGA 6.0 program [20,22,23].

RESULT AND DISCUSSION

IAA-producing Endophytic Bacteria

IAA-producing endophytic bacteria that were isolated from the roots of Robusta and Arabica Coffee plants were as many as 10 isolates and 12 isolates, respectively. Each endophytic bacterial isolate has a different potential ($p < 0.05$) in producing IAA hormones (Fig.1). Figure 1 shows SS.E2 isolates from endophytic roots Robusta coffee that producing IAA hormone with the highest concentration up to 110.73 µg.mL^{-1} at 72 hours incubation time ($p < 0.05$) among the endophytic bacterial isolates of Robusta Coffee plant roots. SW.E9 isolates from endophytic roots Arabica coffee were able to produce IAA hormone with the highest concentration up to 257.16 µg.mL^{-1} in 72 hours incubation time ($p < 0.05$) among the endophytic bacterial isolates of Arabica Coffee plant roots.

SS.E2 and SW.E9 isolates were able to produce higher IAA than *Bacillus aryabhattai* MBN3 endophytic *Vigna radiata* root, which produced IAA 92.03 µg.mL^{-1} [24]. The L-tryptophan compound as an IAA precursor that was added to the media can increase the production of IAA, and bacterial culture in the media will trigger auxin biosynthesis (IAA) [25]. The addition of L-tryptophan as much as 0.2 mg.mL^{-1} produced the highest IAA of 62.92 µg.mL^{-1} in SB28 isolates [18].

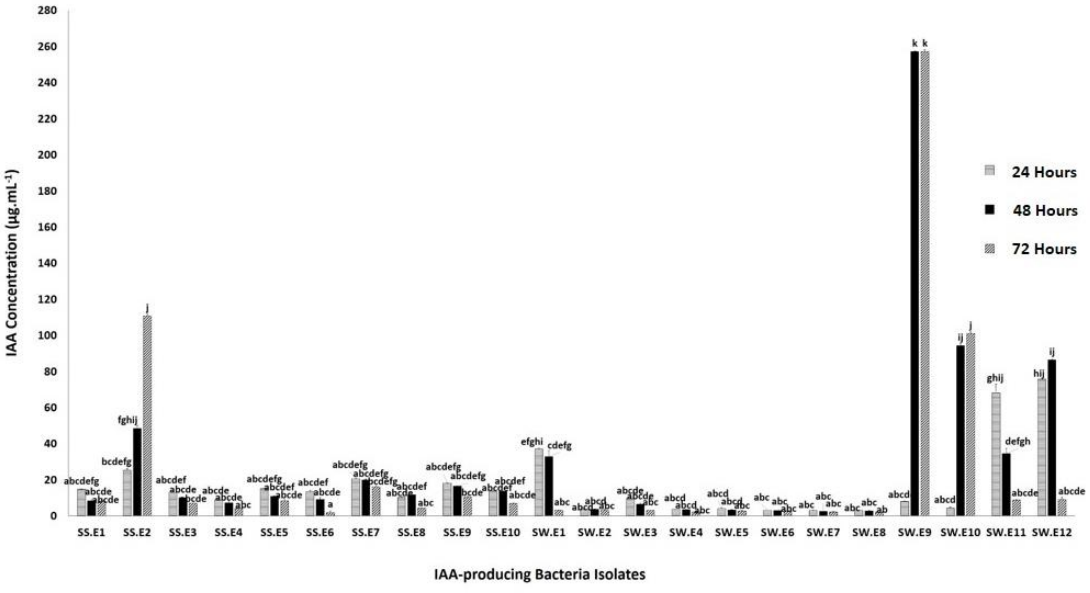

Figure 1. The concentration of IAA hormone produced by IAA-producing bacteria at various times incubation.
*Data were expressed as mean ± standard deviation of three replications using Two-Way ANOVA analysis at α = 0.05. The notation above of the different histograms states the difference in potential between isolates ($p < 0.05$).

ISSN. 2087-2852
E-ISSN. 2338-1655

Phosphate Solubilizing Endophytic Bacteria

Phosphate Solubilizing Endophytic Bacteria from roots of Robusta Coffee and Arabica Coffee plants were successfully isolated as many as 8 isolates and 7 isolates, respectively. Each isolate can dissolve different phosphates (Fig. 2). Figure 2 shows the isolates of SS.P3 from endophytic roots Robusta Coffee plants in 48 hours incubation time had the highest potential ($p<0.05$) to dissolving phosphate up to 4.42 $\mu g.mL^{-1}$. SW.P5 isolates from endophytic roots Arabica Coffee plant has the highest potential ($p<0.05$) dissolving phosphate with a concentration up to 4.55 $\mu g.mL^{-1}$ at 48 hours incubation time.

The concentration of SS.P3 and SW.P5 isolates were lower than EB14 isolates that can dissolve phosphate for 12.54 $\mu g.mL^{-1}$ with an incubation time of 48 hours [26]. In general, bacteria can dissolve phosphate because it produces organic acids, which reduce the pH of the media [27]. By using tricalcium phosphate (TCP) as a P source in the culture medium, produced the highest phosphate concentration reaching 764.7 $\mu g.mL^{-1}$ [28].

Nitrogen-Fixing Endophytic Bacteria

A total of 7 isolates and 6 isolates of nitrogen-fixing endophytic bacteria were found from the roots of Robusta Coffee and Arabica Coffee, respectively. Each isolate can produce different ammonium (Fig.3). Figure 3 shows that SS.N2 isolate from endophytic roots Robusta Coffee plants has the highest potential ($p <0.05$) producing ammonium up to 3.15 $\mu g.mL^{-1}$ at the incubation time of 3 days (72 hours). The highest ammonium concentration from endophytic roots Arabica Coffee plant is SW.N6 isolate that reached 1.16 $\mu g.mL^{-1}$ at 7 days incubation time ($p <0.05$). The potential of SS.N2 and SW.N6 isolates was almost the same as EB5 isolates in producing 1.6 $\mu g.mL^{-1}$ ammonium [26]. Molecular nitrogen is modified by endophytic bacteria to be converted into ammonium as a nutrient for the growth of host plants [29].

Potential Endophytic Bacterial Species of PGP Agents

PGP activity by isolates, which indicated the highest IAA production, was identified as *Bacillus cereus* ATCC 14579^T SS.E2 and SW.E9 isolate. The isolates that had the highest phosphate-solubilizing concentration was identified as *Rahnella aquatilis* B35 isolate SS.P3 and *Kluyvera intermedia* TPY16 isolate SW.P5. The highest ammonia production activity was performed by *Rahnella aquatilis* B35 isolate SS.N2 and *Pseudomonas tolaasii* NCPPB 2192 isolate SW.N6. The potential isolates have each different potency in their activity as PGP. Each plant has endophytic bacteria that capable of producing biological compounds or secondary metabolites obtained from the transfer host plant to endophytic bacteria [30].

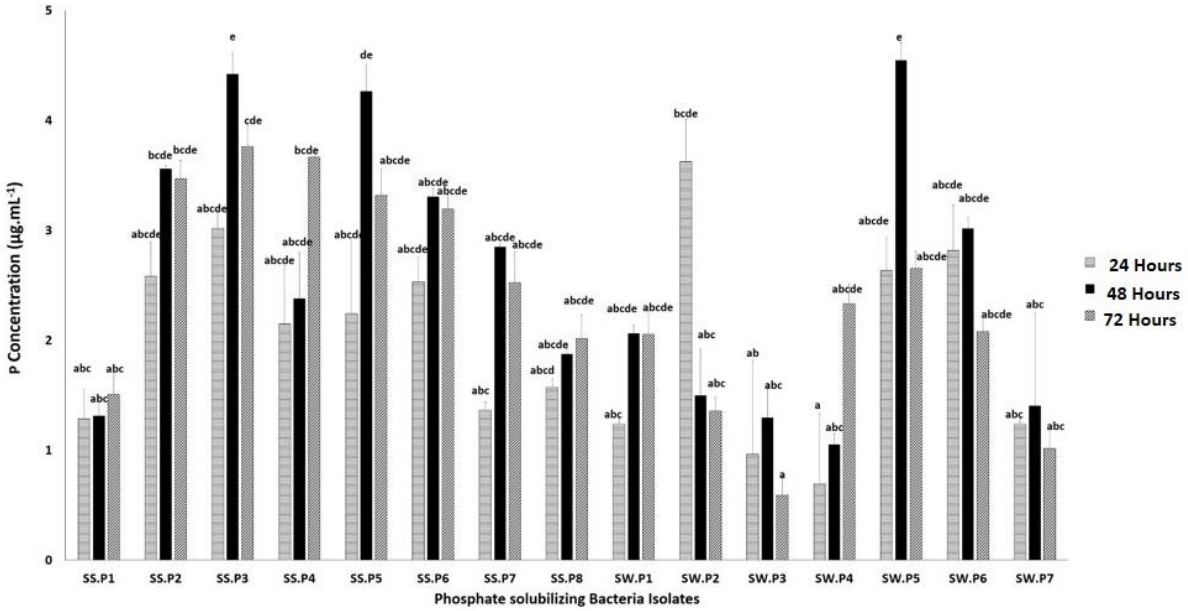

Figure 2. The concentration of Phosphate dissolved by Phosphate solubilizing bacteria at various times incubation.
*Data were expressed as mean ± standard deviation of three replications using Two-Way ANOVA analysis at α = 0.05. The notation above of the different histograms states the difference in potential between isolates ($p <0.05$).

ISSN. 2087-2852
E-ISSN. 2338-1655

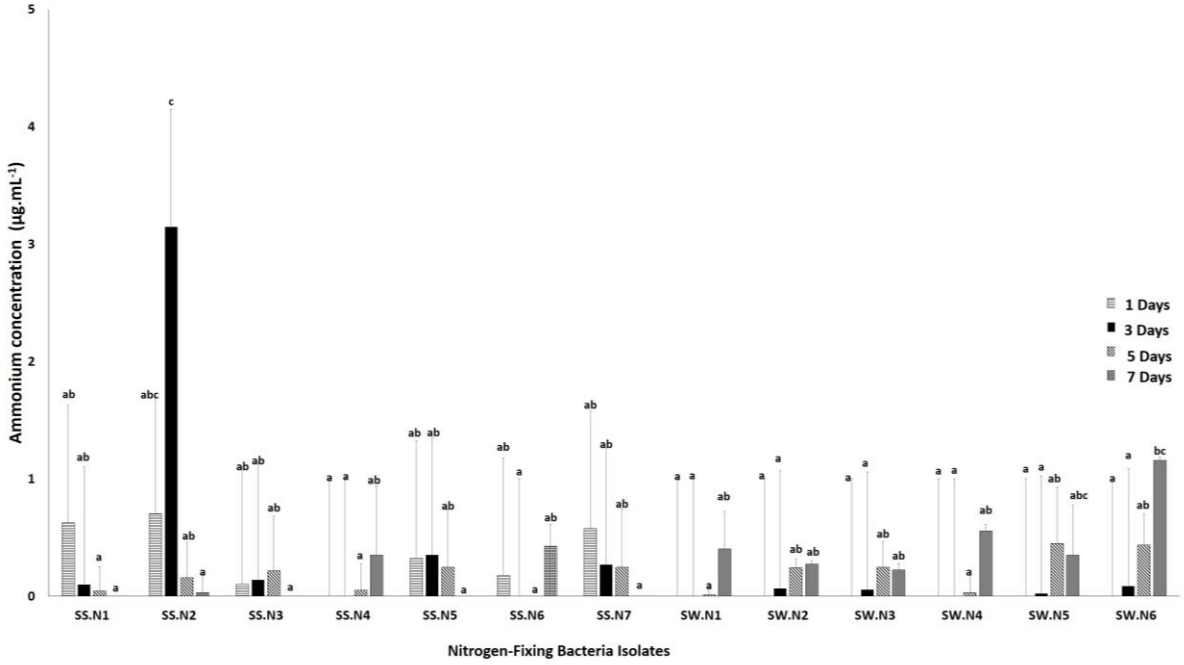

Figure 3. The concentration of Ammonium produced by Nitrogen-Fixing bacteria at various times incubation
*Data were expressed as mean ± standard deviation of three replications using Two-Way ANOVA analysis at α = 0.05. The notation above of the different histograms states the difference in potential between isolates (p <0.05).

Phylogenetic tree of Potential Bacteria Species Based on 16S rDNA

The phylogeny tree of selected IAA production isolates (SS.E2 and SW.E9) were constructed from 16s rDNA sequences and compared with reference strain sequences. As shown in figure 4a, isolates SS.E2 and SW.E9 are in the same cluster as *Bacillus cereus* ATCC 14579^T.

The SS.E2 and SW.E9 isolates have sequence similarity (99.9%) with *Bacillus cereus* ATCC 14579^T. The SS.P3 and SW.P5 isolates were identified as *Rahnella aquatilis* B35 and *Kluyvera intermedia* TPY16 with similarity values of 99.9%, respectively (Fig. 4b and 4c). The SS.N2 and SW.N6 isolate was identified as *Rahnella aquatilis* B35 and *Pseudomonas tolaasii* NCPPB 2192 with similarity values 99.9% and 99.0%, respectively (Fig. 4c and 4d).

The genus *Pseudomonas* and *Bacillus* are commonly found as endophytic bacteria. Plant growth promoting MQ23 and MQ23R endophytic bacteria were identified as *Bacillus cereus* ATCC 14579^T (100%), had the N_2 binding gene (*nifH* gene) and were able to produce siderophore, IAA, and antifungal activity [31]. *Bacillus cereus* ATCC 14579 and *Bacillus aerius* 24K strains are known for producing IAA and ACC-Deaminase activities, respectively [32]. Endophytic *Bacillus subtilis* strains had PGP activity such as phosphate solubilizing, IAA production, and biological nitrogen fixation, which can significantly increase the dried weight of the aerial part, the dried weight of the radicular system, the diameter of the stem, and the number of leaves in eucalyptus plants [33]. *Pseudomonas taiwanensis* and *Pseudomonas geniculata* strains have PGP activities such as ammonia production, HCN, IAA, siderophore, phosphate solubilizing, and ACC deaminase activity [34].

Rahnella sp. are positive reported the N2 binding gene (nifH gene) based on PCR amplified by *nifH* and *nifH-b1* primers [35]. *Rahnella aquatilis* from the soybean rhizosphere had phosphate solubilizing activities with the organic acid release that drop the pH of the culture medium [36]. The *Kluyvera* genus as a PGP agent has not been much explored and reported. However, the study found that *Kluyvera ascorbata* could be used to control *Plutella xylostella* (Lepidoptera: Plutellidae) [37].

ISSN. 2087-2852
E-ISSN. 2338-1655

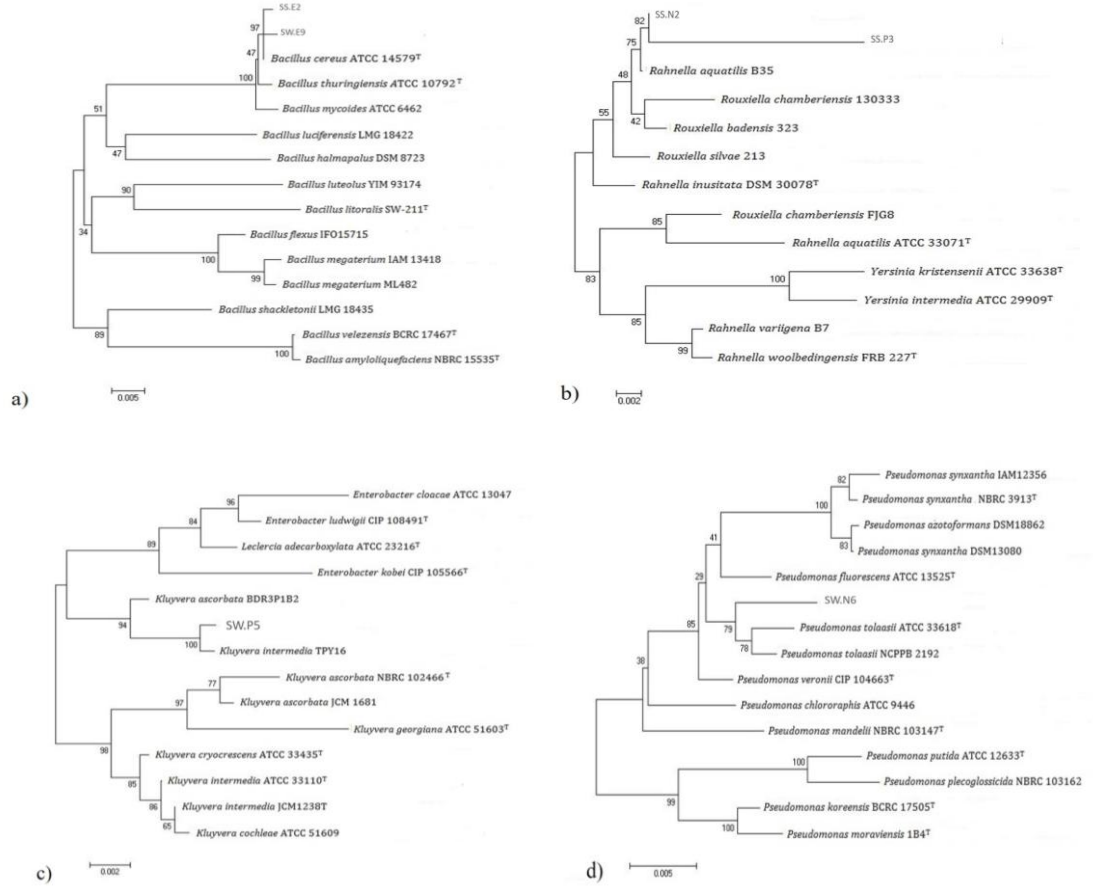

Figure 4. Phylogenetic Tree of Potential Bacteria as PGP using Maximum-Likelihood algorithm with 1000 of bootsraps, MEGA 6.0 program: a) SS.E2 & SW.E9 isolate, b) SS.P3 & SS.N2 isolate, c) SW.P5 isolate, d) SW.N6 isolate

CONCLUSIONS

Based on the results of the study, we concluded that isolates endophytic root Robusta coffe and Arabica coffe can be developed as PGP agents. SS.E2 and SW.E9 isolates produced the highest IAA were respectively identified as *Bacillus cereus* ATCC 14579 (99.9%). SS.P3 and SW.P5 isolates is the highest to dissolving phosphate that respectively identified as *Rahnella aquatilis* B35 (99.9%) and *Kluyvera intermedia* TPY16 (99.9%). Meanwhile, Isolates SS.N2 and SW.N6 is the highest to fixing nitrogen and respectively identified as *Rahnella aquatilis* B35 (99.9%), and *Pseudomonas tolaasii* NCPPB 2192 (99.0%).

ACKNOWLEDGEMENT

Kemenristekdikti (Indonesian Ministry of Research and Higher Education) for finances research through Thesis Grants. Microbiology Laboratory, Department of Biology, University of Brawijaya, for providing the facilities this research. Supervisor and colleagues for discussing consultation, supporting, and motivation in research.

REFERENCES

[1] Montavon, P., E., Duruz, G. Rumo, G. Pratz. 2003. Evolution of green coffee protein profiles with maturation and relationship to coffee cup quality. *J. Agric. Food Chem.* 51(8). 2328-2334.

[2] De Los Santos-Briones, C., S.M.T. Hernández Sotomayor. 2006. Coffee biotechnology. *Braz. J . Plant. Physiol*. 18(1). 217-227.

[3] Ayelign, A., K. Sabally. 2013. Determination of Chlorogenic Acids (CGA) in Coffee Beans using HPLC. *Am. J. Res. Commun*. 1(2). 78-91.

[4] Kusumawati, I.A, P. Cahyo. 2019. Dampak perubahan penggunaan lahan Di UB Forest terhadap karbon biomassa mikroba dan total populasi bakteri. *Jurnal Tanah dan Sumber Dya Lahan.* 6(1). 1165-1172.

[5] Joergensen, R.G., J. Wu, P.C. Brookes. 2010. Measuring soil microbial biomass using an

automated procedure. *Soil Biol. Biochem*. 43(5). 873–876.

[6] Guillaume, T., D. Maranguit, K. Murtilaksono, Y. Kuzyakov. 2016. Sensitivity and resistance of soil fertility indicators to land-use changes: New concept and examples from conversion of Indonesian rainforest to plantations. *Ecol. Indic*. 67. 49–57.

[7] Khan, A.L, M. Waqas, A.R. Khan, J. Hussain, S.M. Kang, S.A. Gilani. 2013. Fungal endophyte Penicillium janthinellum LK5 improves growth of ABA-deficient tomato under salinity. *World J. Microbiol. Biotechnol*. 29(11). 2133–2144.

[8] Karthik, C., M. Oves, R. Thangabalu, R. Sharm, S.B. Santhosh, A.P. Indra. 2016. Cellulosimicrobium funkei-like enhances the growth of Phaseolus vulgaris by modulating oxidative damage under Chromium (VI) toxicity. *J. Adv. Res*. 7(6). 839–850.

[9] Puri, A., K.P. Padda, C.P. Chanway. 2016. Seedling growth promotion and nitrogen fixation by a bacterial endophyte Paenibacillus polymyxa P2b–2R and its GFP derivative in corn in a long-term trial. *Symbiosis.* 69(2). 123–129.

[10] Hardoim, P.R., L.S. van Overbeek, G. Berg, A.M. Pirttilä, S. Compant, A. Campisano, M. Döring, A. Sessitsch. 2015. The hidden world within Plants: Ecological and evolutionary considerations for definingfunctioning of microbial endophytes. *Microbiol. Mol. Biol*. 79. 293–320.

[11] Glick, B.R. 2014. Bacteria with ACC deaminase can promote plant growth and help to feed the world. *Microbiol. Res*. 169. 30–39.

[12] Khan, A.L., A.H. Boshra, A. Elyassi, A. Sajid, K. Al-Hosni, J. Hussain, A. Al-Harassi, I.J. Lee. 2016. Indole acetic acid and ACC deaminase from endophytic bacteria improves the growth of Solanum lycopersicum. *Electron. J. Biotechn*. 21. 58–64.

[13] Khan, Z., S.L. Doty. 2009.Characterization of bacterial endophytes of sweet potato plants. *Plant Soil*. 322. 197-207.

[14] Teaumroong, N., K. Teamtaisong, T. Sooksa-ngun, N. Boonkerd. 2001. The diazotrophic Endophytic bacteria in thai rice. *Sustainable Rice Production*. 147-160.

[15] Vega, F.E, P.R. Monica, P. Francisco, S.B. Jeffrey. 2005. Endophytic bacteria in *Coffea arabica* L. *J. Basic Microbiol*. 45(5). 371–380.

[16] Rashid, S., T.C. Charles, B.R. Glick. 2012. Isolation and characterization of newplant growth-promoting bacterial endophytes. *Appl. Soil Ecol*. 61. 217–224.

[17] Dong, L., C. Ruiyang, X. Lina, W. Fugang, W. Guangfei, X. Jiang, W. Yong, G. Xiaotong, C. Zhongjian, C. Shilin. 2018. Diversity and composition of bacterial endophytes among plant parts of Panax notoginseng. *Chin Med*. 13. 41.

[18] Padder, S.A., A.B. Zahoor, Kuldeep. 2017. Isolation and characterization of indole-3-acetic acid producing bacterial root endophytes associated with brown sarson (*Brassica rapa* L.). *Int. J. Adv. Sci. Eng. Technol*. 5(3). 69-74.

[19] Chairhan, M., L. Saisamorn. 2011. Screening and optimization of indole-3-acetic acid production and phosphate solubilization from Rhizobacteria aimed at improving plant growth. *Curr. Microbiol*. 62. 173–181.

[20] Setia, I.N., Suharjono., Y. Nurani 2018. Plant growth-promoting properties of free-living diazotrophic rhizobacteria from Tangerine (*Citrus reticulate L.*) var Batu 55. *Malays. J. Microbiol.* 14(5). 364-371.

[21] Mihalache, G., M.Z. Maria, M. Marius, I. Iuliu, S. Marius, R. Lucian. 2015. Phosphate-solubilizing bacteria associated with runner bean rhizosphere. *Arch. Biol. Sci. Belgrade*. 67(3). 793-800.

[22] Rhoden, S.A., A. Garcia, M.C. Santos e Silva, J.L. Azevedo, J.A. Pamphile. 2015. Phylogenetic analysis of endophytic bacterial isolates from leaves of the medicinal plany *Trichilia elegans* A. Juss. (Meliaceae). *Genet. Mol. Res*. 14(1). 1515-1525.

[23] Kakade, P.D., R.C. Sushma. 2016. Phylogenetic analysis of endophytic bacteria from Nakshtra trees. *Int. J. Curr. Microbiol. App. Sci.* 5(12). 565-582.

[24] Bhutani, N., M. Rajat, N. Monika, S. Pooja. 2018. Optimization of IAA production by endophytic *Bacillus* spp for their potential use as plant growth promoters. *Isr. J. Plant Sci.* 65. 1-2.

[25] Khalid, A., M. Arshad, Z.A. Zahir. 2004. Screening plant growth-promoting rhizobacteria for improving growth and yield of wheat. *J. Appl. Microbiol.* 96. 473-480.

[26] Shaikh, A.A., P.R. Parmar, B.K. Rajkumar, D.H. Patel, H.R. Desai, B.G. Solanki. 2017. Bioprospecting potential of endophytic

ISSN. 2087-2852
E-ISSN. 2338-1655

bacteria from leaves of *Gossypium hirsutum*. *Int. J. Curr. Microbiol. App. Sci*. 6(10). 1718-1730.

[27] Vyas, P., A. Gulati. 2009. Organic acid production *In vitro* and plant growth promotion in maize under controlled environment by phosphate-solubilizing fluorescent Pseudomonas. *BMC Microbiol*. 9. 174 –188.

[28] Anzuay, M.S., F. Ornella, G.A. Jorge, M.L. Liliana, F. Adriana, T. Tania. 2013. Genetic diversity of phosphate-solubilizing peanut (*Arachis hypogaea* L.) associated bacteria and mechanisms involved in this ability. *Symbiosis*. 60(30). 143-154.

[29] Jha, C.K., B. Patel, M. Saraf. 2012. Stimulation of the growth ofJatropha curcas by the plant growth promoting bacterium *Enterobacter cancerogenus* MSA2. *World J. Microbiol. Biotechnol.* 28(3). 891-899.

[30] Duan, J., W. Jiang, Z. Cheng, J.J. Heikkila, B.R. Glick. 2013. The complete genome sequence of the plant growth-promoting bacterium *Pseudomonas* sp. UW4. *PLoS ONE*. 8(3). e58640.

[31] Zhao, L., Y. Xu, R. Sun, Z. Deng, W. Yang, G. Wei. 2011. Identification and characterization of the endophytic plant growth prompter *Bacillus cereus* strain mq23 isolated from *Sophora alopecuroides* root nodules. *Braz. J. Microbiol.* 42(2). 567–575.

[32] Hemida, K.A., M.M.R. Amany. 2019. Improvement salt tolerance of safflower plants by endophytic bacteria. *J. Hortic. Plant Res.* 5. 38-56.

[33] Paz, I.C.P., R.C.M. Santin, A.M. Guimarães, O.P.P. Rosa, A.C.F. Dias, M.C. Quecine, J.L. Azevedo, A.T.S. Matsumura. 2012. Eucalyptus growth promotion by endophytic *Bacillus* spp. *Genet. Mol. R*es. 11(4). 3711–3720.

[34] Afzal, I., I. Irum, K.S. Zabta, Y. Azra. 2016. Plant growth-promoting potential of endophytic bacteria isolated from roots of wild *Dodonaea viscosa* L. *Plant Growth Regul.* 81(3). 399–408.

[35] Kandel, S.L., A. Firrincieli, P.M. Joubert, P.A. Okubara, N.D. Leston, K.M. McGeorge, G.S. Mugnozza, A. Harfouche, S.H. Kim, S.L. Doty. 2017. An *in vitro* study of bio-control and plant growth promotion potential of salicaceae endophytes. *Front. Microbiol*. 8. 1–16.

[36] Kim, K.Y., J. Diann, B.K. Hari. 2006. *Rahnella aquatilis*, a bacterium isolated from soybean rhizosphere can solubilize hydroxyapatite. *FEMS Microbiol. Lett*. 153. 273-277.

[37] Laurentis, V.L., A.D.B. Sergio, A.P. Ricardo, M.V. Alessandra, C.P.V. Ana, P.D.B. Caroline, X.L.V. Haroldo. 2014. *Kluyvera ascorbata*: A Plant Growth-Promoting Bacteria (PGPB) to manage *Plutella xylostella* (L., 1758) (Lepidoptera: Plutellidae). *Int. J. Agric. Sci.* 1(5). 2348-3997.

ISSN. 2087-2852
E-ISSN. 2338-1655

Effect of Cold Storage Time (4°C) on Malondialdehyde (MDA) Level, Motility and Viability Spermatozoa of *Cyprinus carpio* L. Punten Strain

Rosyi Wirastuti[1], Agung Pramana Warih Marhendra[2] , Jantje Wiliem Souhaly[2], Sri Rahayu[2*]

[1]Master Program of Biology, Faculty of Mathematic and Natural Sciences, University of Brawijaya, Malang, Indonesia
[2]Department of Biology, Faculty of Mathematics and Natural Sciences, University of Brawijaya, Malang, Indonesia

Abstract

The aim of this research is to know the level of MDA, motility, and viability of spermatozoa of *Cyprinus carpio* L. in cold storage time at 4°C. This study used treatment extenders that were NaCl 0.9% as control, diluent of egg yolk with concentrate 0%, 5%, 10%, 15%, and storage in 0 h, 24 h, 48 h, 72 h, and 96 h at 4°C. The data were analyzed using ANOVA ($P<0.05$). The results showed that the quality (motility and viability) of spermatozoa *C. carpio* L. Punten strain in cold storage could be maintained at 96 h. The optimum storage for motility was found in a diluent of egg yolk concentrate 5% at 48 h. MDA levels of semen from *C. carpio* L. Punten strains after being stored at cold temperatures increased at 0 h to 24 h, then decreased after 48 h of storage and increase at 72 h - 96 h stored. Egg yolk concentration and storage time had a significant effect on MDA levels. There is a negative correlation between MDA levels and motility. There was no correlation between MDA levels and the viability of spermatozoa *C. carpio* L. Punten strain.

Keywords: *Cyprinus carpio* L**,** Egg yolk**,** Malondialdehyde, Motiliy, Viability.

INTRODUCTION

Cyprinus carpio L is classified as a type of fish that has high economic value [1]. One of the main factors needed to increase the cultivation and production of *C. carpio* L is created as the best quality of parental fish to produce good quality seeds. The process of producing the best quality of parental fish required a long time and high cost. Therefore, it must be utilized optimally. During the reproductive season, parental fish sperm can be stored and can be used when required.

The advantage of sperm storage is can be stored for a long time and can be used when necessary [2]. Sperm storage at low temperatures can cause cold shock [3], which can produce ROS (Reactive Oxygen Species) [4]. ROS is highly reactive, resulting in lipid peroxidation. Malondyladehid (MDA) is the final result of the lipid peroxidation process, which is toxic to cells. MDA can cause damage and decrease the integrity of the spermatozoa membrane, resulting in decreased sperm quality [5]. Sperm storage required diluent which protects sperm from low temperatures and provides an energy source during the storage process, and also to keep sperm from damaged and die during storage. The quality of sperm during storage is maintained using a good medium. The use of storage media can inhibit sperm movement, stabilize the physiology of sperm, and maintain the viability of sperm [6].

The diluent of sperm was supply nutrients and maintained the osmotic pressure and electrolyte balance to protected viability sperm. One of the diluents that can be used is egg yolk. Since 60 years ago, egg yolk has been shown to be an effective medium for storing sperm in various species, for example, the storage of salmon (*Salmon salar*) and rainbow trout (*Oncorhynchus mykiss*) [7].

Egg yolk contains LDL (Low-Density Lipoprotein), which can maintain sperm at low temperature, increase motility during storage, and binding to the sperm membrane to preserving the membrane from protein damage [8]. The content of egg yolks such as cholesterol, fatty acids, phospholipids, progesterone, and antioxidant compounds have the quality as a protective agent [9,10,11]. Therefore, it is necessary to choose a suitable and efficient medium storage of egg yolk. The research aimed to determine the quality and spermatozoa MDA levels of *C. carpio* L. Punten strain after cold stored at temperature 4°C with diluent of egg yolk, and evaluate the interaction between MDA levels with motility and viability of spermatozoa.

MATERIAL AND METHOD

Semen Collection

Semen was collected from six male *C. carpio* L. Punten strain aged one year and the weight ± 700 g by manual abdominal stripping.

Correspondence address:
Sri Rahayu
Email : srahayu@ub.ac.id
Address : Faculty of Mathematic and Natural Science, Brawijaya University, Malang, 65145

ISSN. 2087-2852
E-ISSN. 2338-1655

Analysis of Spermatozoa Quality

Analysis of sperm quality performed by dripping 10 µL of semen, then added 10 µL of distilled water on the preparation object glass and then observed using a microscope. Sperm used in this research had a motility of more than 50%. Treatment extender that was NaCl 0.9% as control, Egg yolk with concentrate 0%, 5%, 10%, 15%. Sperm and extender ratio were 1:9 (100 µL : 900 µL) [12,13], and then antibiotic penicillin-streptomycin was added. The sample was applied in five different cold storage times i.e., 0 h, 24 h, 48 h, 72 h, and 96 h at 4°C. Motility, Viability, and MDA level of sperm were observed.

Motility evaluation was performed by dripping 10 µL semen, and 10 µL distilled water semen on the preparation object glass and then observed using a microscope. Viability evaluation was carried out by dripping 10 µL semen and 10 µL eosin-nigrosin on the preparation object-glass, and then it was mixed, swabbed, and then observed using a microscope. Spermatozoa that absorbed the color was dead, whereas the sperm that did not absorb color was alive. the observation was performed by a light microscope (Olympus BX51) with magnification at 400x.

MDA Level Anaylsis

A solution of each treatment was taken 400 µl and added with 400 µL of Trichloroacetic acid (TCA) 20% into the TBA 0.5% then were mixed. 200 µL HCl 1N was added and 1000 µL distilled water and mixed, incubated at 95°C for 15 minutes, and centrifuged at 10000 rpm at 4°C for 10 minutes. The supernatant was read in absorbance 532 nm wavelength [14].

Data Analysis

Data were analyzed by one-way ANOVA. Kolmogorov-Smirnoff and homogeneity Levene's test were used for data normality. If there was significant differentiation, it was continued by Duncan.

RESULT AND DISCUSSION

The quality of Spermatozoa (Motility and Viability)

The quality of Spermatozoa has two parameters analysis, such as motility and viability. Motility spermatozoa have variated based on strength and duration [15]. The result of motility spermatozoa *C. carpio* L. Punten strain has shown in Table 1. Diluent of egg yolk concentrate 0%, 5%, 10%, and 15% have decreased after storage at 4°C. The time of storage 0 h and 24 h showed that the percentage of motility has more than 70% and decreased to 50% at 48 h – 72 h.

The time of cold treatment storage is significantly different from the percentage of motility spermatozoa with *a P-value* = 0.000. EYC 0% at time 0 h – 24 h has high percentage of motility 95.14% ± 4.84% and 82.74% ± 6.55%. Furthermore, motility at time 96 h has the lowest percentage 19.82% ± 8.34%. It was shown that cold storage time at 4°C would decrease the motility of spermatozoa. Motility spermatozoa of sturgeon fish *A. gueldenstaedtii* and *A. baerii* were decreased significantly after 72 h of storage at a cold temperature [16].

Viability spermatozoa can be observed by an eosin-negrosin dye. Living sperm did not absorb color caused it still has membrane function, whereas sperm absorbed color was died [17]. The result of viability spermatozoa *C. carpio* L. Punten strain has shown in Table 2. Percentage of viability shown that sperm has decreased by storage at 0 h – 96 h (Table 2). EYC 15% has a high percentage of viability spermatozoa and a significant difference with EYC 0% and 5%, whereas there was no significant difference between EYC 10% and EYC 15%. It was shown that EYC 10% and 15% have the ability to maintan viability of spermatozoa at 4°C compared to other concentrations.

The percentage of viability spermatozoa was significantly different at 0 h and 24 h with percentage viability at storage time 72 h and 96 h. However, the average percentage optimum of viability spermatozoa stored through 96 h ≥ 76.07% ± 7.50%.

The change in storage temperature influences the quality of spermatozoa. The level of ROS production in the population of sperm has a negative correlation with the quality of the sperm. Leukocytes can increase nitric oxide as free radical compounds in seminal plasma sperm of abnormal and dead [17].

The previous study has demonstrated that a concentration of 10% egg yolk medium has the ability to maintained spermatozoa compared with honey and glucose at the same concentration [7]. The current study was also shown that the percentage of viability spermatozoa, which stores in a diluent of egg yolk, keeps maintained.

Table 1. The average percentage of motility spermatozoa *C. carpio* L. Punten strain at cold storage 4°C used diluent of egg yolk

Storage Time (h)	Percentage of motility Spermatozoa (%)			
	EYC 0%	EYC 5%	EYC 10%	EYC 15%
0	91.83 ± 4.98	95.14 ± 4.84	88.82 ± 6.03	89.63 ± 5.83
24	88.24 ± 8.06	88.77 ± 8.03	84.40 ± 5.91	82.74 ± 6.55
48	65.82 ± 9.73	78.51 ± 4.60	73.25 ± 8.81	67.03 ± 10.64
72	52.69 ± 8.53	69.03 ± 5.53	65.88 ± 8.20	60.98 ± 14.74
96	19.82 ± 8.34	38.89 ± 7.91	41.80 ± 7.59	39.37 ± 7.21

Notes: EYC= Egg Yolk Concentration

Table 2. The average percentage of viability spermatozoa *C. carpio* L. Punten strain at cold storage 4°C used diluent of egg yolk

Storage Time (h)	Percentage of viability Spermatozoa (%)			
	EYC 0%	EYC 5%	EYC 10%	EYC 15%
0	92.68 ± 1.39	96.14 ± 2.04	96.64 ± 2.35	98.17 ± 0.79
24	92.17 ± 3.31	94.84 ± 3.92	96.09 ± 2.76	96.92 ± 2.30
48	84.63 ± 6.78	86.22 ± 2.98	95.08 ± 3.36	94.31 ± 5.34
72	76.35 ± 7.00	83.48 ± 5.22	85.87 ± 8.06	88.83 ± 3.58
96	76.07 ± 7.50	80.61 ± 8.73	82.55 ± 7.95	87.19 ± 5.15

Notes : EYC= Egg Yolk Concentration

Level of Malondialdehyde (MDA)

Level of malondialdehyde was observed by thiobarturic acid reactive subtances (TBARS) method using spectrophotometer with absorbance wavelenght of 532 nm. Based on table 3 the result shown that the effect diluent of spermatozoa *C. carpio* L. punten strain EYC 0% was significantly different compared to MDA level in EYC 15%, while EYC 5%, 10% and 15% was not significantly different. EYC 15% had highest MDA level, while EYC 10%, 5% and 0% was in lowest position.

Egg yolk has low density lipoprotein to protect the membrane of sperm from heat shock [8,18,19]. The treatment of storage time in this study had a significant effect on percentage MDA levels. The storage time of 48 hours had the lowest levels 119.88 ± 36.11 ng/ml - 137.82 ± 39.49 ng/ml, while the storage time of 96 hours had the highest levels 137.24 ± 25.07 ng/ml - 164.44 ± 29.36 ng/ml). The effect of storage time was increased MDA levels of spermatozoa C. *carpio* at 0 h to 24 h. Furthermore, there was decreased in MDA levels at 24 h to 48 h. Then the MDA levels increase at 72 h to 96 h (Table 3).

Table 3. The average percentage of MDA level *C. carpio* L. punten strain at cold storage 4°C used diluent of egg yolk

Storage Time (h)	Percentage of MDA Level (ng/ml)			
	EYC 0%	EYC 5%	EYC 10%	EYC 15%
0	139.74 ± 31.03	138.71 ± 26.07	142.68 ± 25.29	156.06 ± 36.09
24	150.91 ± 56.38	162.38 ± 49.12	165.03 ± 38.09	171. 50 ± 50.55
48	119.88 ± 36.11	120.03 ± 23.47	122.68 ± 27.78	137.82 ± 39.49
72	133.71 ± 32.49	139.44 ± 25.70	140.62 ± 34.17	140.47 ± 30.65
96	137.24 ± 25.07	141.21 ± 22.50	149.88 ± 29.10	164.44 ± 29.36

Notes : EYC : Egg Yolk Concentration

Table 4. Pearson Correlation Coefficient Analysis-SPSS

		MDA	Motility	Viability
MDA	Pearson Correlation	1	-.263**	-.015
	Sig. (2-tailed)		.004	.870
	N	120	120	120
Motility	Pearson Correlation	-.263**	1	.567**
	Sig. (2-tailed)	.004		.000
	N	120	120	120
Viability	Pearson Correlation	-.015	.567**	1
	Sig. (2-tailed)	.870	.000	
	N	120	120	120

**. Correlation is significant at the 0.01 level (2-tailed).

ISSN. 2087-2852
E-ISSN. 2338-1655

In this research, the high concentration of egg yolk indicated that the level of MDA was high (15% egg yolk). Egg yolk contains lipid macromolecules and proteins, which are the target of lipid peroxidation by free radical compounds. Free radical compounds are reactive and can modify the structure of several biomolecules such as lipids, proteins, and nucleic acids. Lipid peroxidation products may cause an oxidation reaction cycle, which affects the pH. Furthermore, the amount of egg yolk is assumed to cause the diluent medium to become more concentrated and decrease the pH. Production of MDA was increased at low pH by lipid peroxidation chain reactions [20].

Interaction of Malondialdehyde (MDA) with Motility and Viability Spermatozoa

This research was found that MDA levels have a negative correlation with spermatozoa motility and viability percentage of *C. carpio* L. Punten strain. A significant correlation occurs in MDA levels with the percentage of motility (correlation coefficient = -0.263) (Table 4).

There is a positive correlation of motility with significant viability (correlation coefficient = 0.567), and it is classified as a strong correlation. Meanwhile, there was no significant correlation between MDA levels and viability (p = 0.870> 0.05). It indicates that when the MDA level increases, the motility of the sperm would be decreased. Furthermore, there is no correlation between MDA levels and viability spermatozoa. It indicated that MDA levels with a storage at 96 h have not provided a significant correlation. In addition, the interaction between motility and viability shows that when the motility of the sperm decreases, the viability would be also decreased.

Malondialdehyde is a marker of oxidative stress caused by ROS [21] and a marker of lipid peroxidation [16]. The results of this study were related to a previous study [22], which show that increased levels of ROS were negatively correlated with sperm concentration, motility, morphology, and parameters of semen. ROS may cause oxidative damage to the membrane, midpiece, axonema, and DNA of sperm, which leads to apoptosis [23,24]. Polyunsaturated Fatty Acid (PUFA) is able to cause lipid peroxidation of membrane spermatozoa [25]. Lipid peroxidation increases the membrane integrity of sperm, so it can increase cell permeability and enzyme inactivation [16]. ROS will increase the expression of lipid peroxidation were affect the MDA that causes the death of the sperm cell. It caused a decrease in motility, so that level of MDA was high.

This research has shown that egg yolk has the ability to preserve sperm in cold storage time at 0 h – 96 h. Egg yolk diluent is appropriate to use as an applicative diluent caused it was easy and cheap. Also, the quality (motility and viability) of the sperm of *C. carpio* L. Punten strain was maintained by the addition of egg yolk during cold storage at 0 h - 48 h and also suitable to management and breeding of *C. carpio* L. Punten strains by providing transfer of male gametes to reducing the risk of death or stress of male parental *C. carpio* L. Punten strain fish species.

CONCLUSION

The quality (motility and viability) of spermatozoa fish *C. carpio* L. Punten strain was maintained at 96 h during cold storage. The optimum storage for motility was found in egg yolk diluent 5% at 48 hours. The MDA level of the semen of *C. carpio* L. Punten strain stored at cold temperatures increased at 0 h - 24 h, then decreased at 48 h of storage and increased at stored 72 h - 96 h. There is a negative correlation between MDA levels and motility. There was no correlation between MDA levels and the viability of spermatozoa *C. carpio* L. Punten strain.

REFERENCES

[1] Eveline., J. Santoso, M. Huangdinata. 2019. Utilization of carp (*Cyprinus carpio*) as surimi of sausage manufacturing. *Jurnal Pengolahan Hasil Perikanan Indonesia*. 22(22). 366-374.

[2] Toelihere, M.R. 1981. Inseminasi buatan pada ternak. Angkasa.

[3] Watson, P.F. 2000. The causes of reduced fertility with cryopreserved semen. *Anim. Reprod. Sci*. 60. 481-492.

[4] Nebel, R.L. 2007. Techniques for artificial insemination of cattle with frozen thawed semen. in: Current Therapy In Large Animal Theriogenol, 2nd Ed. Saunders Elselvier. Missouri.

[5] Sanocka, D., M. Kurpisz. 2004. Reactive oxygen species and sperm cells. *Reprod. Biol. Endocrinol*. 2. 12-19.

[6] Maria, A.N., A.T.M. Viveiros, L.H. Orfão,, A.V. Oliviera, G.F. Moraes. 2006. Effect of cooling and freezing on sperm motility of the endangered fish Piracanjuba *Brycon*

orbignyanus (Characiformes, Characidae). *Anim. Reprod*. 3(1). 55-60.

[7] Muchlisin, Z.A., W.N. Nadiah, N. Nadiya, N. Fadli, A. Hendri, M. Khalil, M.N Siti-Azizah. 2015. Exploration of natural cryoprotectans for cyropreservation of African catfish, *Clarias gariepinus*, Burchell 1822 (Pisces: Clariidae) Spermatozoa. *Czech J. Anim. Sci*. 60(1). 10-15. doi: 10.17221/115/2013-CJAS.ity.

[8] Moussa M., V. Martinet, A. Trimeche, D. Tainturier, M. Anton. 2002. Low density lipoproteins extracted from hen egg yolk by an easy method: cryoprotective effect on frozen-thawed bull semen. *Theriogenology*. 57. 1695-1706.

[9] Bozkurt Y., I. Yavas, C. Yildiz. 2014. Effect of different avian egg yolk types on fertilization ability of cryopreserved common carp (*Cyprinus carpio*) spermatozoa. *Aquac. Int*. 22. 131-139.

[10] Mostl, E., H. Spendier, K. Kotrschal. 2001. Concentration of immunoreactive progesterone and androgens in the yolk of hen's eggs (Gallus domesticus). *Wiener Tierarztliche Monatsschrift*. 88. 62-65

[11] Sakanaka, S., Y. Tachibana, N. Ishihara, L.R. Juneja. 2004. Antioxidant activity of egg-yolk protein hydrolysates in a linoleic acid oxidation system. *Food Chem*. 86. 99-103.

[12] Sultana M., M. Nahiduzzaman, M.M. Hassan, M.U.H. Khanam, M.A.R. Hossain. 2010. Fertility of cryopreserved common carp (*Cyprinus carpio*) spermatozoa. *Univ. J. Zool. Rajshahi. Univ*. 28. 51-55.

[13] Lehninger, A.L., M.C. Michael. 2004. Principles of biochemistry 3rd. W.H. Freeman and co. Virginia USA. 549-542.

[14] Zhang, Z., R. Huang. 2013. Analysis of malondialdehyde, chlorophyll proline, soluble sugar, and glutathione content in arabidopsis seedling. *Bio-Protocol*. 3(14). doi: 10.21769/BioProtoc. 817.

[15] Billard, R. 1986. Spermatogenesis and spermatology of some teleost fish species. *Reprod. Nutr. Develop*. 26(4). 877-920.

[16] Shaliutina, A., M. Hulak, L. Gazo, P. Linhartova, O. Linhart. 2013. Effect of short-term storage on quality parameters, DNA integrity, and oxidative stress in Russian (*Acipenser gueldenstaedtii*) and Siberian (*Acipenser baerii*) sturgeon sperm. *Anim. Reprod Sci*. 139. 127-135.

[17] Ducha, N., T. Susilaeati., Aulanni'am., S. Wahyuningsih, M. Pangestu. 2012. Ultrastucture and fertilizing ability of *Limousin* bull sperm after storage in Cep-2 extender with and without egg yolk. *Pak. J. Biol. Sci.* 15(20). 979-985.

[18] Leeuw, F.E., A.M. Leeuw, J.H.G. Daas, B. Colenbrander, J. Verkleij. 1993. Effects of various cryoprotective agents and membrane integrity after cooling and freezing. *Cryobiology*. 30. 32-44.

[19] Lima, I.C.S., I.R.A. Andrade, G.V. Aguiar, M.M. Silva, A.G.V. Catunda, G.A. Martins, C.R.F. Gadelha, A.C.N. Campos. 2013. *In vitro* evaluation of goat cauda epididymal sperm cooled in different extenders at 4°C. *Arch. Zootec*. 62(239). 429-437.

[20] Aitken, R.J., M.A. Baker. 2006. Oxidative stress, sperm survival and fertility control. *Moll. Cell Endrocrinol*. 16. 250(1-2). 66-69.

[21] Held, P. 2015. An introduction of reactive oxygen species. White Paper: BioTech Instruments, Inc.

[22] Agarawal, A., S.A. Prabakaran, T.M. Said. 2005. Prevention of oxidative stress injury to sperm. *J. Androl.* 26. 654-660.

[23] Beirao, J., F. Soares, P. Pousao-Ferreira, P. Diogo, J. Dias, M.T. Dinis, M.P. Herraez, E. Cabrita. 2014. The effect of enriched diets on *Solea senegalensis* sperm quality. *Aqua Culture.* 435. 187-194

[24] Chromcova, L., J. Blahova, D. Zivna, L. Plhalova, F. Casuscelli, D. Tocco, L. Divisova, M. Prokes, C. Faggio, F. Tichy, Z. Svobodova. 2015. NeemAzal T/S – toxicity to early life stages of common carp (*Cyprinus carpio* L.). *Veterinarni Medicina*. 60(1). 23-30.

[25] Trenzado, C., M.C. Hidalgo, M. García-Gallego, A.E. Morales, M. Furné, A. Domezain, J. Domezain, A. Sanz. 2006. Antioxidant enzymes and lipid peroxidation in sturgeon *Acipense naccarii* and trout *Oncorhynchu mykiss*: A comparative study. *Aquaculture*. 254. 758–767.

ISSN. 2087-2852
E-ISSN. 2338-1655

Isolation and Identification of Indigenous Cellulolytic Bacteria from Sago Pith Waste at Palopo, South Sulawesi, Indonesia

Mamluatul Faizah[1*], Tri Ardyati[2], Suharjono[2]

[1]Master Program of Biology, Department of Biology, Faculty of Mathematics and Natural Sciences, University of Brawijaya, Malang, Indonesia
[2]Department of Biology, Faculty of Mathematics and Natural Sciences, University of Brawijaya, Malang, Indonesia

Abstract

Palopo, South Sulawesi, is one of the traditional industrial centers of sago processing. The accumulation of sago pith waste around industrial sites can pollute the environment. Some microorganisms can degrade the cellulose in sago pith waste. This study was aimed to evaluate the indigenous cellulolytic bacteria from sago pith waste as a biodegradation agent. Bacteria were isolated from sago pith waste and grown on a 1% Carboxyl methyl cellulose (CMC) agar medium. The cellulolytic activity was analyzed semiquantitatively using 1% Congo red and quantitatively using the 3,5-Dinitrosalicylic Acid (DNS) method at pH variations of 4, 5, and 6. The potential isolate was identified based on 16S rDNA sequence similarity. This study obtained 21 bacterial isolates where six isolates were A1D, A1E, A1I, A1K, A2A, and B1A had the highest cellulolytic index at 0.82 – 1.13. Among those six isolates, the A1E isolate had the highest cellulolytic activity, 0.54 U.mL^{-1} at pH 6. The isolate A1E was identified as *Burkholderia cepacia* JCM 2799 with 99.73% similarity of 16S rDNA sequence.

Keywords: *Burkholderia cepacia*, cellulolytic bacteria, cellulase enzyme, sago waste.

INTRODUCTION

Sago (*Metroxylon sago* Rott.) is a native plant in Southeast Asia. Indonesia has the largest sago plantation in the world. South Sulawesi, especially Palopo City, is one of the traditional industrial centers of sago processing in Indonesia, which contributes significantly to the production of sago waste. In 2018, the area of sago plantations in South Sulawesi reached 4,383 ha with a productivity of 2,626 tons of sago [1]. Sago trees contain 20-30% starch and 70-80% pith [2]. Thus, the sago waste produced annually ranges from 1,838 - 2,100 tons.year^{-1}.

In general, the sago pith waste in the sago processing industry is not handled properly. It is only allowed to accumulate on the ground that causing acidity in the soil, polluting the environment and causing unpleasant odors [3]. Soil contamination caused by the sago pith waste requires serious attention, so it is important to degrade it by utilizing microorganisms. Sago pith waste contains 20% of cellulose [4]. Cellulose is a major component of plant cell walls, unbranched linear chains consisting of several thousand glucose units with β-1,4 glycosidic bonds. Cellulose is insoluble in water and has high mechanical strength, making it difficult to degrade [5].

Cellulolytic bacteria can degrade cellulose by producing extracellular cellulase enzymes. Cellulase is an enzyme that catalyzes the cellulolysis process (hydrolysis of cellulose) to be glucose, cellobiose, and cellooligosaccharides [6]. Cellulase enzymes produced by microorganisms play an important role in the biodegradation of cellulose and lignocellulose wastes to be more simple compounds. The hydrolysis of cellulose into glucose by cellulase enzymes acts synergistically including three enzymes, namely endo-β-1,4-glucanase, Cellobio-hydrolase, and β-glucosidase. Endo β-1,4-glucanase (EG; EC 3.2.1.4) attack amorphous regions and cleave the internal glycosidic bonds. Cellobiohydrolase (CBH; or Exo-β-1,4-glucanase, β-1,4-D-glucan-cellobiohydrolase, EC 3.2.1.91) attack the non-reducing cellooligosaccharide chain or crystalline regions and produce cellobiose, then the cellobiose will be hydrolyzed into glucose by β-glucosidase (BG; cellobiase, β-D-glucoside glucanohydrolase, EC 3.2.1.21) [7].

Several groups of bacteria such as *Cellulomonas, Pseudomonas, Thermoactino-mycetes*, and *Bacillus* [8], *Bacillus pumilis, B. licheniformis, B. cereus*, and *Pseudomonas aeruginosa* showing cellulolytic activity [9]. Meanwhile, *Serratia liquefaciens, Acinetobacter iwofii, Bacillus Licheniformis*, and *Bacillus cereus* were reported as indigenous bacteria from sago waste [10]. Therefore, this study is important to obtain bacterial isolates that have potency as biodegradation agents to solve the problem of sago pith waste.

* Correspondence address:
Mamluatul Faizah
Email : mamluatulfaizah7@gmail.com
Address : Dept. Biology, University of Brawijaya, Veteran Malang 65145

ISSN. 2087-2852
E-ISSN. 2338-1655

MATERIAL AND METHOD

Sago pith waste sampling

Sago pith waste was collected from the traditional industry of sago in Palopo, South Sulawesi at two locations, location A (2°53'34"S 120°10'18"E) and location B (3°2'20.20"S 120°12'33.77"E). The sample was taken from a pile of sago pith waste in the bottom, near the ground, and stored in a plastic bag in an isotherm box. The physicochemical parameter that measured including organic matter, C/N ratio, and pH of sago pith waste. The organic matter and C/N ratio were analyzed in Soil Laboratory, Faculty of Agriculture, Brawijaya University.

Isolation and Screening of Cellulolytic Bacteria

Twenty-five grams of sago pith waste was suspended in 225 mL of 0.85% NaCl solution, and we made serial dilution until 10^{-7}. The aliquot of sample suspension 0.1 mL was spread on a Petri dish containing 1% CMC-agar medium and incubated at 30°C for 72 hours. The CMC-agar medium ($g.L^{-1}$) consist of CMC 10, Yeast Extract 4, KH_2PO_4 4, Na_2HPO_4 4, $MgSO_4.7H_2O$ 0.2, $CaCl_2.2H_2O$ 0.001, $FeSO_4.7H_2O$ 0.004, and agar 15 at pH 6 [11].

The bacterial colonies that were grown on the CMC medium were observed and purified. The pure isolates were screened semi-quantitatively for cellulolytic producing enzymes using Congo red. The isolates then cultivate in 20 mL of 1% CMC-broth medium as much as 20 µL with equal cell density was 10^7 $cells.mL^{-1}$ was taken and inoculated on blank disc paper and placed onto 1% CMC-agar medium and incubated at 30 °C for 72 hours. After incubation was completed, then flooded with 1% Congo Red solution for 15 minutes and it washed with 1M NaCl solution [12]. The cellulolytic index (CI) was determined with the formula 1.

$$CI = \frac{clear\ zone\ diameter - colony\ diameter}{colony\ diameter} \ldots\ldots\ldots\ldots (1)$$

Growth Curve and Crude Enzyme Production of Selected Bacteria

Broth culture of selected bacterial isolates (10%) were inoculated into 100 mL of 1% CMC-broth medium and incubated in a rotary shaker at 30°C, 120 rpm for 72 h. The bacterial culture as much as 5 mL were taken every 4 h for 7 days and optical density (OD) was measured using a spectrophotometer at 540 nm wavelength. The production of crude cellulase of each bacterium was determined at the exponential growth phase. The crude enzyme was obtained by centrifugation of culture medium at 4°C, 10.000 rpm for 10 minutes. The supernatant was defined as a crude cellulase enzyme [13].

Cellulolytic Activity Assay

Cellulolytic activity of each selected bacteria was assayed quantitatively by incubated substrate of 1% CMC in the 1800 µL 20 mM buffer citrate (pH 4, 5, and 6) with 200 µL crude enzyme extract at 30°C for 30 minutes. The reaction was stopped by added 2 mL of DNS then boiled in a water bath at 100°C for 5 minutes. The sample was cooled at room temperature and its absorbance was measured at 540 nm. One unit of cellulase enzyme activity is defined as the amount of enzyme that releases 1 µmol glucose per mL per minute. The values of the cellulolytic activity were determined based on the glucose standard curve [13].

Identification of Bacteria Based on 16S rDNA

Bacterial chromosomal DNA was extracted using a Quick-DNA™ Fungal/Bacterial Miniprep Kit (ZYMO RESEARCH, USA). The 16S rDNA sequence was amplified by Polymerase Chain Reaction (PCR) using universal primer 27f (5'-AGAGTTTGATCCTGGCTCAG3') and 1492r (5'-GGTTACCTTGTTACGACTT-3') with PCR program: pre-denaturation at 94°C for 5 min, followed by denaturation at 94°C for 30 s, annealing at 55°C for 30 s, and extension at 72°C for 30 s over 35 cycles and a final extension at 72°C for 5 min. The amplicon of 16S rDNA was confirmed by 1.5% agarose gel electrophoresis and visualized using a UV transilluminator. An amplicon of 16S rDNA was purified and sequenced in First BASE, Malaysia. The 16S rDNA sequences of bacteria were aligned with reference strains from the GenBank database using the MEGA V.6 program, and the phylogeny tree was constructed and inferred according to the Neighbor-joining algorithm and Tamura-Nei model [14].

Data Analysis

Semiquantitative data of cellulolytic activity was variance analyzed based on One-Way ANOVA. Meanwhile, quantitative data of cellulolytic activity were analyzed based on Two-Way ANOVA followed by Tukey test using SPSS 16 program.

RESULT AND DISCUSSION

Potential Isolates of Cellulolytic Bacteria

The study of cellulolytic bacteria from the sago pith waste was obtained 21 isolates where 16 isolates from location A and 5 isolates from location B. The density of cellulolytic bacteria at

ISSN. 2087-2852
E-ISSN. 2338-1655

location A 25 x 10^5 CFU.g^{-1} was higher than location B 19.3 x 10^5 CFU.g^{-1}. The low bacterial density at location B is due to the lower organic carbon, nitrogen, C/N ratio, and organic matter in sago pith waste samples (Table 1). Organic matter plays an important role in microorganism density and pH [15]. The low pH in sago pith waste is due to the fermentation activity of microorganisms to form organic acids (acetic acid, pyruvic acid, and lactic acid) [16,17]. Carbon and nitrogen are macromolecules that have structural and functional roles in bacteria's cell components [18]. Based on similar research, the physicochemical parameter of sago pith waste contained 33.01% C-organic, 1.66% N-total, 20% C/N ratio [19], and pH 6 [17].

Table 1. Physicochemical parameter of sago pith waste

Parameter	Location A	Location B
C-organic (%)	38.9 ± 1.22	31.5 ± 3.25
N-total (%)	0.2 ± 0.06	1.2 ± 0.69
C/N ratio	179.7 ± 37.07	37 ± 28.69
Organic matter (%)	67.3 ± 2.10	54.5 ± 5.62
pH	5.9 ± 0.66	4.7 ± 0.35

Based on the cellulolytic index, there were six potential isolates consist of A1E, A1K, A1D, A2A, A1I, and B1A with cellulolytic index were 1.13, 0.97, 0.93, 0.88, 0.82, and 0.82, respectively (Fig. 1). The clear zone indicates the ability of bacteria to produce cellulase enzymes to hydrolyze cellulose substrates [20]. The similar research from sago waste reported that *Serratia liquefaciens*, *Acinetobacter iwofii*, *Bacillus licheniformis*, and *Bacillus cereus* had cellulolytic index were 1.019, 2.009, 1.031, and 1.195, respectively [10]. Based on this study, the cellulolytic index of the A1E isolate was similar to the cellulolytic index of *Serratia liquefaciens*, *Bacillus licheniformis*, and *Bacillus cereus*.

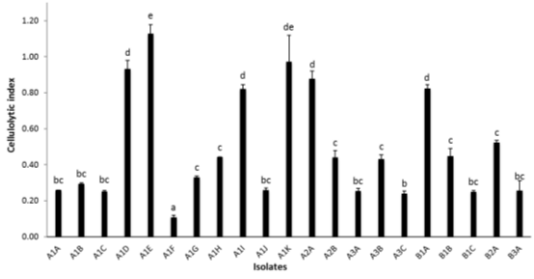

Figure 1. Cellulolytic index of bacteria

Growth Curve of Selected Cellulolytic Bacteria

The growth curve of six cellulolytic bacterial isolates (Fig. 2), whole isolates were not showed an adaptation phase. The cell density of those isolates was increased significantly at the logarithmic/exponential growth phase from initial incubation until 24 h. In the exponential growth phase, bacteria perform constantly at a maximum growth rate of cell division [13]. The bacterial cells had an optimal production of cellulase at the exponential growth phase [21]. It is due to cellulase as primary metabolites that have an important role in decomposing cellulose to be glucose as the carbon source for bacterial growth [22]. The stationary growth phase of cellulolytic bacteria occurred from 24 h until 64 h for A1D, A1I, A2A, and B1A, then followed by the death phase at 72 h, whereas A1E and A1K still in the stationary growth phase at 72 h. In the stationary growth phase, there is a balance between the number of live cells and dead cells [23].

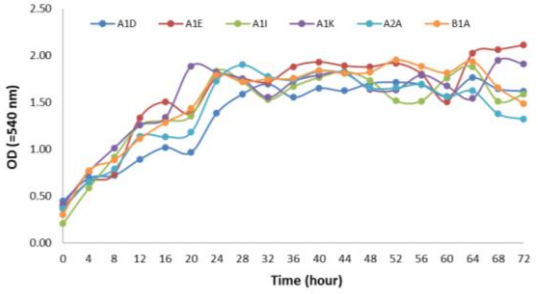

Figure 2. Growth curve of cellulolytic bacteria

Each bacterial isolate with a density of 10^7 cells.mL^{-1} at exponential growth phase (24 h incubation) had the highest potency for the production of cellulase enzymes A similar study showed the exponential growth phase of cellulolytic bacteria occurs at 4 – 24 h incubation [13]. Another research was reported that the production of cellulase enzymes at 24 h incubation [24]. The exponential growth phase was considered at the incubation time of 36 h. Bacterial cultures have a significant cell mass at the exponential phase that can be expected the cellulase enzymes production more quickly [25].

Cellulolytic Activity of Bacterial Isolates

The A1E isolate at optimum pH 6 had the highest cellulolytic activity for 0.54 U.mL^{-1} (Fig. 3). The isolate A1K, A1D, and A1I at optimum pH 6 had a cellulolytic activity for 0.35 U.mL^{-1}, 0.27 U.mL^{-1}, and 0.22 U.mL^{-1}, respectively. While A2A and B1A isolates at optimum pH 5 had cellulase activity for 0.31 U.mL^{-1} and 0.33 U.mL^{-1}, respectively. A similar study was reported that *Cerenna* sp. and *Pseudomonas aeruginosa* at optimum pH 6 had cellulase activity 0.928 U.mL^{-1} and 1.554 U.mL^{-1}, respectively [26]. *Bacillus subtilis, B. brevis, Paenibacillus* sp., and

ISSN. 2087-2852
E-ISSN. 2338-1655

Cellulomonas sp. are active at optimum pH 5.5 – 7 [24]. The Cellulase activity of *Citrobacte*r sp. from pretreated bagasse was optimum at pH 6 [27].

The pH is a factor that has a significant effect on the stability of enzymatic reaction [28]. The enzymes that are produced from different bacteria allow them to have different optimum pH for their activity. When the pH changes, the enzyme's active site, and the substrate can alter because of the ionization. It influences the rate of the binding substrate to the active site of the enzyme [29]. Based on this research, at pH 6 and pH 5, the active site of the cellulase can be ionized optimally. Therefore, its activity can be optimal, as well.

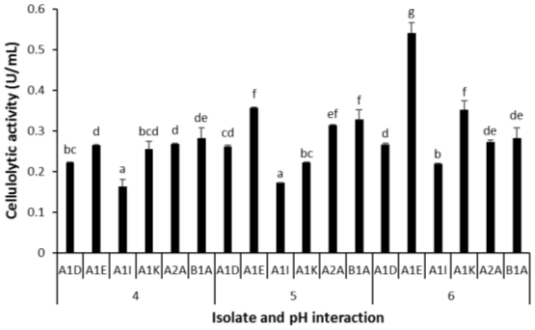

Figure 3. Cellulolytic activity of bacteria at pH variation

Species of Potential Cellulolytic Bacteria

Potential cellulolytic bacteria A1E isolate from sago pith waste was identified phylogenitically based on 16S rDNA sequence similarity. Figure 4 showed that the A1E isolate was identified as *Burkholderia cepacia* JCM 2799 with 99.73% similarity of 16S rDNA sequence (Fig. 4). Previous studies also reported that *Burkholderia cepacia* from banana peel waste was potential as a cellulose decomposer with cellulolytic index 1.36 [30].

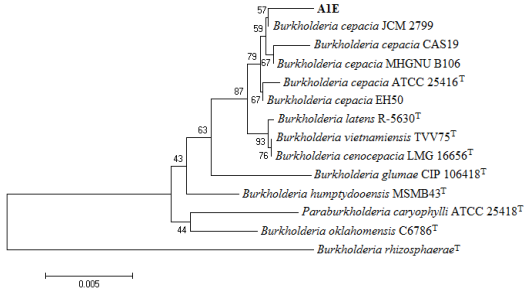

Figure 4. Phylogeny tree that showed relationship of A1E isolate and reference bacterial strains based on 16S rDNA sequence according Neighbor-joining algorithm

Burkholderia is a genus of lignocellulolytic bacteria [31, 32], and it is known to have cellulolytic activity [33]. *Burkholderia cepacia* from the soil in Xiling mountain has a cellulolytic activity of 2.76 $U.mL^{-1}$ at optimum temperature 60°C and pH 5 [34]. The different enzyme activity of bacteria can be influenced by the different conditions in the medium such as temperature, pH, carbon source, nitrogen source, enzymes, and substrate concentration [29].

CONCLUSION

The A1E indigenous isolate of sago pith waste from Palopo, South Sulawesi, had the highest potency as cellulolytic bacteria. The cellulase activity 0.54 $U.mL^{-1}$ was optimum at pH 6. The A1E isolate was identified as *Burkholderia cepacia* JCM 2799 with 99.73% similarity.

REFERENCES

[1] Directorate General of Plantations. 2017. Plantation statistic Indonesia. Secretariat Directorate of Plantations. Jakarta.

[2] Yanti, N.A., A. Munir. 2014. Screening bakteri amilolitik dan selulolitik dari limbah sagu. *Biowallacea.* 1(1). 1-6.

[3] Awg-Adeni, D.S., S. Abd-Aziz., K. Bujang, M.A. Hassan. 2010. Bioconversion of sago residue into value added products. *Afr. J. Biotechnol.* 9(14). 2016-2021.

[4] Kiat, L.J. 2006. Preparation and characterization of carboxymethyl sago waste and its hydrogel. Master Thesis. Universiti Putra Malaysia. Malaysia.

[5] Omoniyi, O., O.A. Okwa, O.O. Junaid, I.O. Ikuoye , A. Oyebola. 2016. Sustainable solid waste management: isolation of cellulolytic microorganisms from dumpsites in Lagos, Southwest Nigeria. *Int. J. Curr. Microbiol. App. Sci.* 5(11). 842-853.

[6] Irfan, M., A. Safdar, Q. Syed, M. Nadeem. 2012. Isolation and screening of cellulolytic bacteria from soil and optimization of cellulase production and activity. *Turk. J. Biochem*. 37(3). 287–293.

[7] Behera, B.C., B.K. Sethi, R.R. Mishra, S.K. Dutta, H.N. Thatoi. 2017. Microbial cellulases - diversity & biotechnology with reference to mangrove environment: A review. *J. Genet. Eng. Biotechnol*. 15. 197–210.

[8] Lokhande, S., M. Musaddiq. 2015. Isolation of cellulolytic bacterial strains for bioconversion of municipal solid waste. *Int. J. Appl. Res*. 1(11). 902-905.

[9] Chaudhary, N., J.I. Qazi, M. Irfan. 2017. Isolation and identification of cellulolytic and ethanologenic bacteria from soil. *Iranian J. Sci. Technol*.

[10] Hastuti, U.S., P. Yakub, H.N. Khasanah. 2014. Biodiversity of indigenous amylolytic and cellulolytic bacteria in sago waste product at Susupu, North Moluccas*. J. Life Sci.* 8. 920-924.

[11] Thomas, L., H. Ram, V.P. Singh. 2018. Inducible cellulase production from an organic solvent tolerant *Bacillus* sp. SV1 and evolutionary divergence of endoglucanase in different species of the genus *Bacillus*. *Braz. J. Microbiol*. 49. 429-442.

[12] Rawway, M., S.G. Ali, A.S. Badawy. 2018. Isolation and identification of cellulose degrading bacteria from different sources at assiut governorate (Upper Egypt*). J. Eco. Heal. Env*. 6(1). 15-24.

[13] Jannah, A., Aulanni'am., T. Ardyati, Suharjono. 2018. Isolation, cellulase activity test and molecular identification of selected cellulolytic bacteria indigenous rice bran. *Indones. J. Chem*. 18(3). 514 – 52.

[14] Potprommanee, L., X.Q. Wang, Y.J. Han, D. Nyobe, Y.P. Peng, Q. Huang, J.Y. Liu, Y.L. Liao, K.L. Chang. 2017. Characterization of a thermophilic cellulase from *Geobacillus* sp. HTA426, an efficient cellulase-producer on alkali pretreated of lignocellulosic biomass. *PLoS ONE*. 12(4). 1-16.

[15] Garbeva, P., J.A. van Veen, J.D. van Elas. 2004. Microbial diversity in soil: selection of microbial population by plant and soil type and implications for disease suppressiveness. *Annu. Rev. Phytopathol.* 42. 243-270.

[16] Indrayati, S., Y.M. Nur, Periadnadi., Nurmiati. 2017. Pemanfaatan ampas sagu (*Metroxylon sago* Rottboel.) hasil fermentasi *Trichoderma harzianum* Rifai dan penambahan microflora alami pencernaan ayam broiler dalam pembuatan pakan ayam konsentrat berprobiotik. *Jurnal Bibiet.* 2(2). 68-74.

[17] Uhi, Harry T. 2007. Peningkatan nilai nutrisi ampas sagu (*Metroxylon* sp.) melalui bio-fermentasi. *Jurnal Ilmu Ternak*. 7(1). 26-31.

[18] Widadri., W. Mangunwardoyo., H. Ambarsari. 2019. Effect of C/N ratio variations on the capability of microbes from Muara Karang river sediment in the production of biogas and identification using VITEK 2. *IOP Conf. Series: Earth and Environmental Science*. 308. 1-8.

[19] Hammado, N., Budiyono., S. Utomo. 2018. Physicochemical characteristic of sago hampas and sago wastewater in Luwu regency. *E3S Web of Conferences*. 73. 1-3.

[20] Khotimah, S., Suharjono., T. Ardyati, Y. Nurani. 2020. Isolation and identification of cellulolytic bacteria at fibric, hemic and sapric peat in Teluk Bakung Peatland, Kubu Raya District, Indonesia. *Biodiversitas.* 21(5). 2103-2112.

[21] Seo, J.K., T.S. Park, I.H. Kwon, M.Y. Piao, C.H. Lee, J.K. Ha. 2013. Characterization of cellulolytic and xylanolytic enzymes of *Bacillus licheniformis* JK7 isolated from the rumen of a native Korean goat. *Asian-Australas J Anim Sci.* 26(1). 50-58.

[22] Sanchez, S., A.L. Demain. 2008. Review: metabolic regulation and overproduction of primary metabolites. *Microbial Biotechnology*. 1(4). 283–319.

[23] Maier, R.M. 2009. Bacterial growth. In: Environmental Microbiology. Elsevier Inc. UK. 37-54.

[24] Meng, F., L. Ma, S. Ji, W. Yang, B. Cao. 2014. Isolation and characterization of *Bacillus subtilis* strain BY-3, a thermophilic and efficient cellulase-producing bacterium on untreated plant biomass. *Lett. Appl. Microbiol.* 59(3). 306-312.

[25] Munifah, I., T.C. Sunarti, H.E. Irianto, A. Meryandini. 2015. Biodiversity of cellulolytic bacteria isolated from the solid wastes of agar seaweed processing industry. *Squalen Bull. Mar. Fish. Postharvest Biotech*. 10(3). 129-139.

[26] Obidi, O.F., O.O Awe, F.O. Okekunjo, M.N. Igwo-ezsikpe. 2018. Studying the cellulolytic activity of microorganisms isolated from stained painted walls with reference to certain factors: a cross sectional study. *Int. J. Environ. Sci*. 1-10.

[27] Jones, J.A., R.G. Kerr, B.A. Haltli. W.F. Tinto. 2018. Temperature and pH effect on glucose production from pretreated bagasse by a novel species of *Citrobacter* and other bacteria. *Heliyon*. 4. 1-16.

[28] Kiio, I.K., M.F. Jackim, W.B. Munyali, E.K. Muge. 2016. Isolation and characterization of a thermostable cellulase from *Bacillus licheniformis* strain Vic isolated from geothermal wells in the Kenyan Rift Valley. *Open Biotechnol. J*. 10. 198-207.

ISSN. 2087-2852
E-ISSN. 2338-1655

[29] Robinson, P.K. 2015. Enzymes: principles and biotechnological applications. *Essays Biochem*. 59. 1-41.
[30] Grevitara, Y.P., B. Rahma, H. Septirangga, I. Dahlia, E. Suarsini. 2018. Isolation and identification of cellulose degrading bacteria from banana peel compost. *El-Hayah*. 7(1). 6-11.
[31] Woo, H.L., T.C. Hazen, B.A. Simmons, K.M. DeAngelis. 2014. Enzyme activities of aerobic lignocellulolytic bacteria isolated from wet tropical forest soils. *Syst. Appl. Microbiol.* 37.
[32] Akita, H., Z. Kimura, M.Z.M. Yusoff, N. Nakashima, T. Hoshino. 2017. Identification and characterization of *Burkholderia multivorans* CCA53. *BMC Res. Notes*. 10(249). 2-6.
[33] Guerrero, E.B., J. Arneodo, R.B. Campanha, P.A. de Oliveira, M.T.V. Labate, T.R. Cataldis, E. Campos, A. Cataldi, C.A. Labate, C.M. Rodrigues, P. Talia. 2015. Prospection and evaluation of (Hemi) cellulolytic enzymes using untreated and pretreated biomasses in two Argentinean Native Termites. *PloS ONE*. 10(8). 1-23.
[34] Lichun, M., X. Lihui, H. Gang. 2018. Isolation and identification of cellulase-producing bacteria and optimization of their enzyme-producing conditions. *China Brewing*. 04.

ISSN. 2087-2852
E-ISSN. 2338-1655

The Use of Food Coloring Dyes in Bacterial Staining

Rio Risandiansyah[1*], Arniyati Arniyati[1], Nofie Irmalia Nurita[1], Natasya Hana Gionika[2]

[1]Central Laboratory of Medical Research, Faculty of Medicine, University of Islam Malang, Indonesia
[2] Study Program of Pharmacy, Faculty of Medicine, University of Islam Malang, Indonesia

Abstract

Staining creates a contrast between the cells and its surrounding, and enables the microscopic characteristics of bacterial cells to be easily visible and distinguished. However, staining often relies on dyes which are expensive, not readily available, or toxic. In this study, the use of food coloring dyes to stain bacteria was explored. We stained Gram-positive bacteria (*Bacillus sp*. and *Staphylococcus aureus*) and Gram-negative bacteria (*Escherichia coli*) using several food coloring dyes of different colors, which were purchased locally. After slide fixation, the dye was flooded on the bacterial smear and air-dried for up to 30 minutes and observed by using microscope before and after washing with water. The results of this study show that prior to washing, most food coloring dyes were able to stain bacterial cells. However, after washing, only pink and purple food coloring dyes were retained, showing pink colored cells. We suspected that erythrosine was the agent responsible for this result, and was able to show similar characteristics with erythrosine alone. This study concludes that food coloring dyes containing erythrosine can be used to stain bacterial cells indiscriminately.

Keywords: Bacterial cell staining, erythrosine, food coloring dyes, resource-limited.

INTRODUCTION

Staining is a basic technique in microscopy, crucial in determining the basic morphological structure and characteristics to separate and identify one cell to another. Cell staining relies on specific dyes capable to bind to specific structures of a cell (such as nucleic acids or cytoplasm) and retains within these structures [1]. It creates a contrast between the cells and its surrounding and enables the cells to be visualized and characterized. Gram staining, in which its discovery is an important milestone in medical microbiology [2], for instance, a bacterial cell can be separated into Gram positive or negative based on the components of its cell wall and its ability to retain stain after alcoholic washing [3].

Cell staining is particularly useful in histology, pathology, and microbiology [4,5], and few studies exist which explores new staining method and techniques within the last decade [6,7]. However, the difficulty of the discovery of novel stains, such as in the case of the discovery of Gram staining, often relies on trial and error and has a degree of serendipity involved [3]. It is a common perception that diagnosis requires techniques with higher sensitivity and specificity, such as nucleic acid amplification techniques or fluorescent microscopy. However, even in these techniques, there is a demand for novel stains that are safer for the environment, less toxic, readily available, and less expensive, yet having similar efficacy with current stains [8].

Staining techniques are important in the field of medical microbiology. Bacterial staining, usually Gram staining, is often used to guide therapy in patients with infections [9], and particularly considering increased antibiotic resistance [10]. Other stainings, such as simple staining and vital staining, may be used to rapidly detect the presence of bacteria or even pathogenic bacteria using a single stain method [7,11,12]. Point-of-care in rural or underdeveloped areas, however, provide logistical challenges in obtaining a Gram kit, or any other staining kits, and may be a barrier to the technique. Furthermore, some compounds used in several single staining procedures are considered to be toxic to humans and the environment and, in the case of crystal violet, may even be considered to be carcinogenic [13,14].

Food coloring, unlike chemical staining kits, are often easier to find as well as being less toxic to human health, although some has reported the compounds contained in food coloring to be unsafe for consumption if taken chronically [15]. Food coloring often contains chemicals, which are also known to be bacterial stains, such as erythrosine [16], brilliant blue FCF [17], and sunset yellow [7]. However, previous research has used those substances in controlled concentrations, and not when they are packaged in a food coloring product.

In this paper, we explore the use of food-grade food coloring to stain Gram-positive and

* Correspondence address:
Rio Risandiansyah
Email : risandiansyah@gmail.com
Address : Faculty of Medicine, University of Islam Malang
Jl. Mayjen Haryono No. 193 Malang 65144

ISSN. 2087-2852
E-ISSN. 2338-1655

Gram-negative bacteria. We then evaluate the ability after each stain to evaluate the basic microscopic characteristic of each bacteria, whether the stain can stain bacteria with different characteristics, and whether the stain is retained after washing. On successful stains, a food-grade pure compound was used and tested for the concentration with the best bacterial visualization.

MATERIAL AND METHOD

Bacteria preparation

Bacteria (*Bacillus sp., Escherichia coli, and Staphylococcus aureus*) were obtained from the Laboratory of Microbiology, Department of Biology, University of Brawijaya, Malang. Prior to staining, bacteria were subcultured in nutrient agar plates (Merck, peptone 5 $g.L^{-1}$, Meat extract 3 $g.L^{-1}$, and Agar 12 $g.L^{-1}$) and incubated at 37°C for at least 20 hours. The bacteria stained in this study were a Gram-positive bacillus (*Bacillus sp*.), a Gram-negative bacillus (*Escherichia coli*), and a Gram-positive coccus (*Staphylococcus aureus*).

Bacteria fixing for staining

Prior to any staining method, bacteria were fixed on a glass microscope slide by the following method, based on established literature. A sterile loop of bacteria from the aforementioned plates was mixed with a small drop of normal saline from a glass pipette on a glass slide under a biosafety cabinet. The slides were left to dry inside the biosafety cabinet for approximately 10 minutes, and fixated by passing the slides through an open flame. These slides were then used directly for staining. All staining was performed on a staining tray.

Staining method using water-based food coloring

Food coloring was purchased from a local bakery material store. The brand of the food color was chosen randomly, however, the color chosen was determined by its constituent. For this study, several food colorings were used in the initial food stain. A dark red food color (HakikiTM; ingredients: Sorbitol, Ponceau 4R Cl No. 16255, Carmoisine Cl No. 14720, and Tatrazine Cl No. 19140), blue food color (R&WTM; ingredients: Sorbitol, Brilliant Blue Cl No. 42090), pink food color (R&WTM, ingredients: Sorbitol, Erythrosine Cl No. 45430, Carmoisine Cl No. 14720), and purple food color (HAKIKITM; ingredients: Erythrosine Cl No. 45430, Brilliant Blue No. 42090) were tested in this study. The bacterial smear on slides was flooded with the food coloring and left for 1 minute, and drained without washing. The slides were then left at least 30 minutes before observation under a microscope. After the images were taken, the slides were washed under running water, left to dry for 10 - 30 minutes, and the images were taken again using the same method.

Staining method using Erythrosine

Erythrosine was purchased from a local chemical store and was oil-based food grade erythrosine (PT. Subur Kimia Jaya). The erythrosine obtained was in the form of a maroon-colored powder. Erythrosine was mixed with distilled water at 1 $mg.mL^{-1}$, 0.1 $mg.mL^{-1}$, 0.01 $mg.mL^{-1}$, and 0.001 $mg.mL^{-1}$and prepared at a volume of approximately 25 mL. The staining method was similar to the previous method, whereas the slides were flooded with the stain, left for 1 minute, drained without washing, and left for an additional 30 minutes to 1 hour before observation by a microscope.

Microscope image capturing

A trinocular microscope was used to obtain images of the preparation with 1000x magnification, medium light, the diaphragm set accordingly, and using a drop of immersion oil. After focusing, the images were obtained using the ocular camera and cropped for similar dimensions.

RESULT AND DISCUSSION

Unwashed single staining of bacteria using various food coloring dyes

Samples of bacteria obtained from nutrient agar plates were fixated and single stained, as described in the methodology section. Based on the images in Fig. 1, the microscopic characteristics of the bacterial cells were mostly clearly observable after food coloring application. Red food coloring resulted in outlining the cell borders, with clear and colorless area internal to the bacterial cells on all Gram-positive and Gram-negative bacteria, as with purple food coloring in *Bacillus sp*. bacteria. However, in several stains, the cells appear more visible, having a darker hue, such as observed in blue food color, pink food color in all bacterial Gram types, and purple food color in *E. coli*. The results of purple coloring in *S. aureus* were not visible, resulting in no staining patterns that were easily observable in Gram-positive or Gram-negative bacteria. However, bacilli bacteria were easier to observe and differentiate compared to cocci bacteria.

ISSN. 2087-2852
E-ISSN. 2338-1655

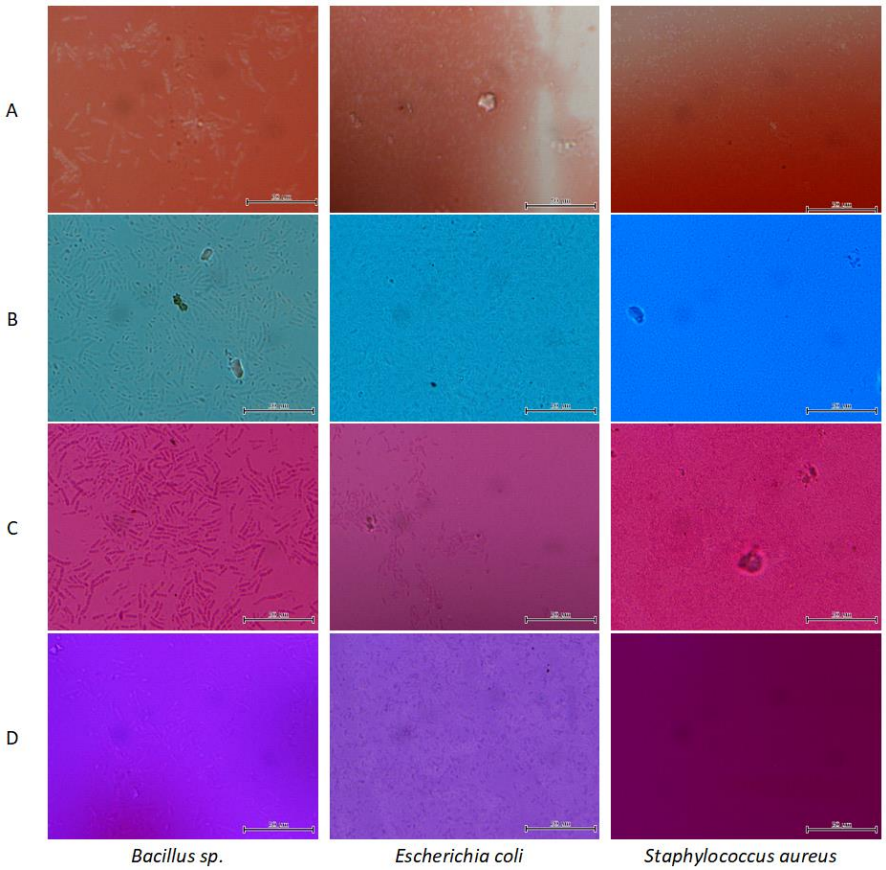

Figure 1. Cell images of various Gram positive and negative bacteria stained using various water-based food coloring without washing. The cells were stained using A. red food coloring, B. blue food coloring, C. pink food coloring, and D. purple food coloring. The basic cell morphology was clearly observable using these staining methods, however, no differentiation in Gram type was possible. The scale line was 50 µm.

Washed single staining of bacteria using various food coloring dyes

During washing, it was observed that the food color was washable using running water. However, observation under a microscope revealed that each food coloring was retained differently (Fig. 2). As shown in the images in Figure 2, food coloring was retained differently after washing. Red food coloring was not retained or faintly retained in *Bacillus sp.* and *S. aureus*, but was more clearly retained in *E. coli*.

Other food colorings were retained in most bacterial cells, regardless of their Gram type, with the most clearly retained food coloring in pink food coloring and purple food coloring. Furthermore, cell morphology and a staphylo type configuration were observable under pink food coloring staining in *S. aureus*.

Staining of bacteria using erythrosine with various concentrations

Cell visualization after staining with erythrosine was shown in Figure 3. Erythrosine used in this study was found to have low solubility with water, resulting in patches of stain debris across all bacterial slides. Erythrosine was found to stain bacteria regardless of Gram type with varying degrees depending on the concentration used. However, the images were accompanied by an amount of staining debris the higher the concentration of the erythrosine used.

At the lowest concentration of erythrosine, the cells, in particular *S. aureus*, were only faintly stained. However, it also had a relatively lower amount of staining debris. *S. aureus* was only clearly visible on the highest concentration of erythrosine. On the other hand, *Bacillus sp.* And *E. coli* was visible using erythrosine even up to a concentration as low as 0.01 mg.mL^{-1}.

ISSN. 2087-2852
E-ISSN. 2338-1655

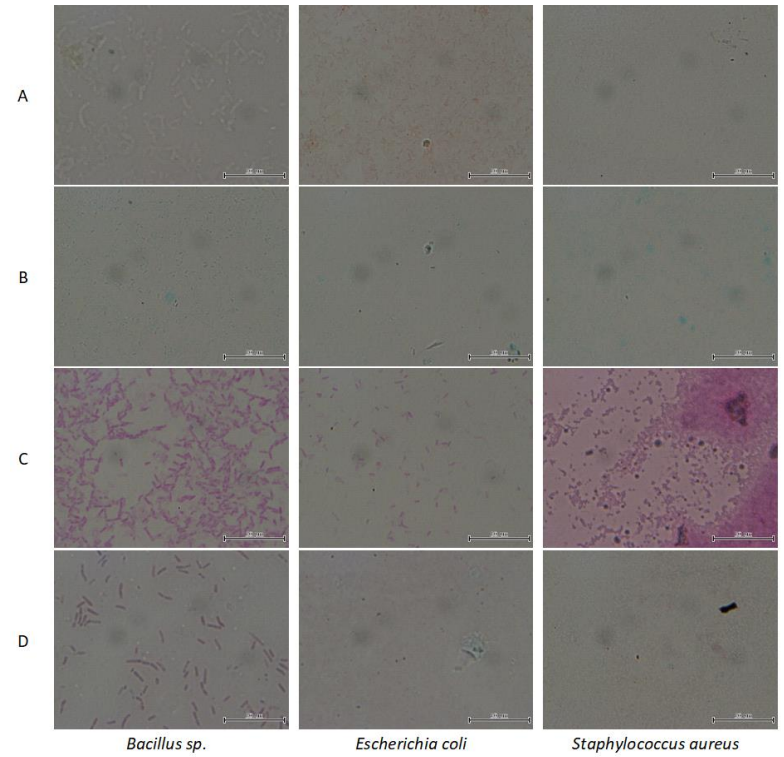

Figure 2. Cell images of various Gram positive and negative bacteria stained using various water-based food coloring and washed after staining. The cells were stained using A. red food coloring, B. blue food coloring, C. pink food coloring, and D. purple food coloring. Stains were retained differently between each bacterial type, but no differences were observed within different Gram types. The scale line was 50 µm.

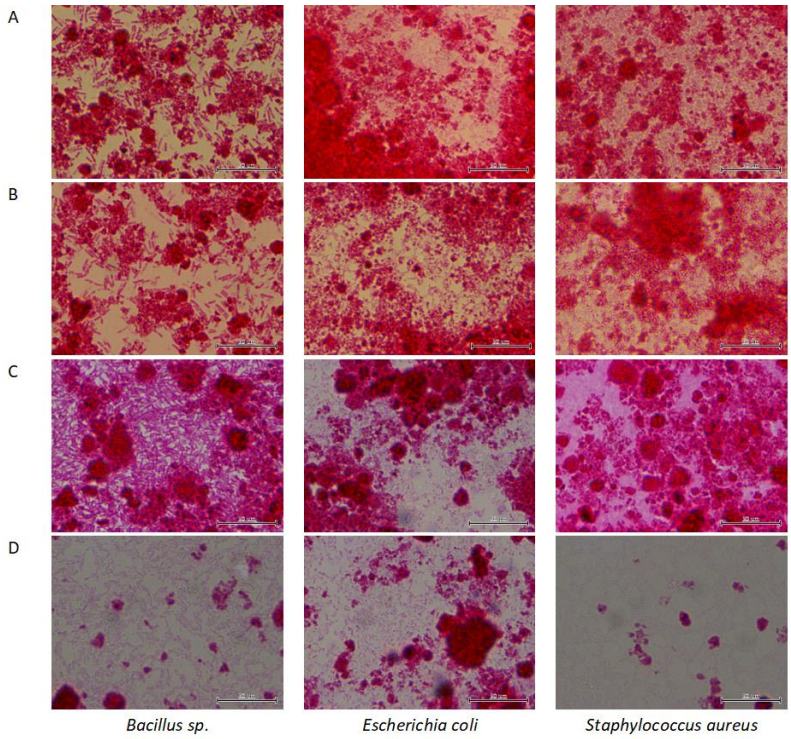

Figure 3. Cell images of Gram positive and negative bacteria using various concentrations of erythrosine. The cells were stained using erythrosine at A. 1 mg.mL^{-1}, B. 0.1 mg.mL^{-1}, C. 0.01 mg.mL^{-1}, and D. 0.001 mg/ml. erythrosine was found to be able to stain all cells, regardless of Gram type. The scale line was 50 µm.

ISSN. 2087-2852
E-ISSN. 2338-1655

DISCUSSION

Bacterial staining has many applications in the medical field or in even microbiology science, either to show the cell shape and formation, to pinpoint specific structures, and even used as a golden standard for some the determination of pathogens. For example, Gram stains can pinpoint the basic microscopic characteristics of a cause of an infectious disease. Positive results in an acid-fast stain, using a red color carbol-fuchsin, can indicate the presence of acid-resistant bacteria having a mycolic cell wall. Special characteristics of the bacteria can be stained using negative staining, capsule staining, spore staining, flagellar staining, as well as other methods.

Modification of Gram-stain is rarely done, but discoveries for alternatives have been done in several recent researchers by using different dyes or stains, which result in higher contrast [6]. In other cases, novel staining methods were developed in dentistry to detect the presence of oral biofilm in the teeth and gums [10,18]. However, the experiments tend to use pure compounds and do not generally use food-coloring dyes directly.

In this experiment, food-coloring dyes used contain a mixture of sorbitol and one or two coloring agents. It was observed that staining was retained after washing when using dyes containing erythrosine. Previous use of erythrosine found it to be taken up and able to inhibit *Streptococcus mutans* biofilm and therefore used as photodynamic therapy (PDT) for gingivitis [19]. Erythrosine was already classified as a biological stain [20], and recently, erythrosine has been shown to be able to stain several Gram-positive and Gram-negative bacteria indiscriminately, including *Bacillus cereus*, *Escherichia coli*, *Klebsiella pneumoniae*, *Pseudomonas flourescens*, *Serratia marcesans*, *Streptomyces albus*, *Streptococcus mutans*, *Proteus mirabilis*, *Staphylococcus aureus*, and *Enterococcus faecalis* [16].

This study also showed the efficacy of several different food coloring in staining bacteria. Our findings suggest that pink and purple food coloring was found to not only be taken by the bacterial cells, thus enabling the cells to be visible, because the stains were retained after washing. A common ingredient in both the pink and purple food coloring tested was erythrosine. Thus, we then tested using a purer form of erythrosine in a further test. This result supports other studies [15,16] and can report that erythrosine can also, in fact, stain the bacterial cells, albeit non-discriminatory. Erythrosine is reported as a membrane-impermeable stain and only taken by non-viable cells, such as after heat treatment [21]. As heat fixation was employed in this method, a similar process could explain how the food-colors containing erythrosine was able to stain the bacterial cells.

The advantages of using food coloring as a way to stain bacteria is that food coloring is relatively less toxic compared to several compounds used in *conventional* stains. Crystal violet, a component in Gram staining and also can be used in simple staining procedures [11], is reported to be mutagenic, a potent carcinogen and potent clastogenic, as well as persisting in the environment for a long period [13]. This study shows the possibility of unconventional methods to be used in the development of bacterial staining methodology.

CONCLUSION

Food coloring containing erythrosine can be used to stain bacterial cells indiscriminately.

ACKNOWLEDGEMENT

We would like to thank the Medical Faculty, University of Islam Malang, for providing us with the equipment required to do the experimentation.

REFERENCES

[1] Baskin, D. G. 2015. A historical perspective on the identification of cell types in pancreatic islets of langerhans by staining and histochemical techniques. *J. Histochem Cytochem*. 63(8). 543–58. doi: 10.1369/0022155415589119.

[2] Alturkistani, H.A., F.M. Tashkandi, Z.M. Mohammedsaleh. 2015. Histological stains: a literature review and case study. *Glob J. Health Sci*. 8(3). 72.

[3] Bartholomew, J.W., T. Mittwer. 1952. The Gram stain. *Microbiol. Mol. Biol. Rev*. 16(1). 1–29.

[4] Braak, H., S. Feldengut, J. Kassubek, D. Yilmazer-Hanke, K. Del Tredici. 2018. Two histological methods for recognition and study of cortical microinfarcts in thick sections. *Eur J. Histochem.* 62(4). 313–317.

[5] Ergün, E., L. Ergün, R.N. Asti, A. Kürüm. 2003. Light and electron microscopic morphology of Paneth cells in the sheep small intestine. *Rev. Med. Vet. (Toulouse)* 154(5). 351–355.

[6] Salleh, F.M., A.M. Al-Mekhlafi, A. Nordin, M.

ISSN. 2087-2852
E-ISSN. 2338-1655

Yasin 'Azlin, H.M. Al-Mekhlafi, N. Moktar. 2011. Evaluation of gram-chromotrope kinyoun staining technique: Its effectiveness in detecting microsporidial spores in fecal specimens. *Diagn. Microbiol. Infect. Dis*. 69(1). 82–85.

[7] Gao, P., C. Sun, Y. Li, X. Zou, X. Wu, Y. Ling, et al. 2011. Vital staining of bacteria by sunset yellow pigment. *Polish J. Microbiol*. 66(1). 113–117.

[8] Kim, S.I,, H.J. Kim, H.J. Lee, K. Lee, D. Hong, H. Lim, et al. 2016. Application of a non-hazardous vital dye for cell counting with automated cell counters. *Anal Biochem*. 492(3). 8–12. doi: 10.1016/j.ab.2015.09.010

[9] Tokuda, Y., M. Koizumi, G.H. Stein, R.B. Birrer. 2009. Identifying Low-risk patients for bacterial meningitis in adult patients with acute meningitis. *Intern. Med*. 48(7). 537–543.

[10] Becerra, S.C., D.C. Roy, C.J. Sanchez, R.J. Christy, D.M. Burmeister. 2016. An optimized staining technique for the detection of Gram positive and Gram negative bacteria within tissue. *BMC Res Notes* 9(1). 216. doi: 10.1186/s13104-016-1902-0

[11] Moyes, R.B., J. Reynolds, D.P. Breakwell. 2009. Preliminary staining of bacteria: simple stains. *Curr. Protoc. Microbiol*. Appendix 3: Appendix 3E.

[12] Cluss, R.G., N.L. Somerson. 1984. Simple staining procedure permits rapid counting of mycoplasma colonies. *J. Clin. Microbiol*. 19(4). 543–545.

[13] Mani, S., R.N. Bharagava. 2016. Exposure to crystal violet, its toxic, genotoxic and carcinogenic effects on environment and its degradation and detoxification for environmental safety. In: Reviews of environmental contamination and toxicology. United States. 71–104.

[14] Gillman, P.K. 2010. Methylene blue and serotonin toxicity: definite causal link. *Psychosomatics.* 51. 448–449.

[15] Merinas-Amo, R., M. Martínez-Jurado, S. Jurado-Güeto, Á. Alonso-Moraga, T. Merinas-Amo. 2019. Biological effects of food coloring in *in vivo* and *in vitro* model systems. *Foods*. 8(5). 176.

[16] Franke, J.D., A.L. Braverman, A.M. Cunningham, E.E. Eberhard, G.A. Perry. 2020. Erythrosin B: a versatile colorimetric and fluorescent vital dye for bacteria. *Biotechniques*. 68(1). 7–13. doi: 10.2144/btn-2019-0066

[17] Chau, H., Y. Goh, B. Si, V. Vujanovic. 2011. An innovative brilliant blue FCF method for fluorescent staining of fungi and bacteria. *Biotech. Histochem*. 86(4). 280–287. doi: 10.3109/10520295.2010.492733

[18] Ishiyama, K., K. Nakamura, T. Kanno, Y. Niwano. 2016. Bactericidal action of Photodynamic Antimicrobial Chemotherapy (PACT) with photosensitizers used as plaque-disclosing agents against experimental biofilm. *Biocontrol Sci*. 21(3). 187–191.

[19] Wood, S., D. Metcalf, D. Devine, C. Robinson. 2006. Erythrosine is a potential photosensitizer for the photodynamic therapy of oral plaque biofilms. *J. Antimicrob. Chemother*. 57(4). 680–684.

[20] Penney, D.P., J.M. Powers, M. Frank, C. Willis, C. Churukian. 2002. Analysis and testing of biological stains-- The Biological Stain Commission Procedures. *Biotech. Histochem*. 77(5–6). 237–275. doi: 10.1080/bih.77.5-6.237.275

[21] Krause, A.W., W.W. Carley, W.W. Webb. 1984. Fluorescent erythrosin B is preferable to trypan blue as a vital exclusion dye for mammalian cells in monolayer culture. *J. Histochem. Cytochem.* 32(10). 1084–1090.

ISSN. 2087-2852
E-ISSN. 2338-1655

The Effect of Gamma Irradiation on the Growth and Multiplication of the *In Vitro* Shoot of Patchouli (*Pogostemon cablin* Benth.)

Yunia Efrice Banyo, Serafinah Indriyani, Wahyu Widoretno*

Department of Biology, Faculty of Mathematics and Natural Sciences, University of Brawijaya, Malang

Abstract

The objective of this research was to evaluate the effect of gamma irradiation on shoot growth and multiplication of Patchouli (*Pogostemon cablin* Benth.) Two weeks-old in vitro shoots were irradiated gamma-ray, at doses of 0, 15, 30, 45, 60, and 75 Gy. The control shoot was not irradiated. The irradiated shoots were cultured on Murashige and Skoog (MS) medium supplemented with 0.1 mg.L^{-1} NAA and 0.3 mg.L^{-1} BA and incubated in a growth room for eight weeks at a temperature of 25±2°C. The results showed that the gamma irradiation inhibited the growth and multiplication of shoots. Explants irradiated with high-dose gamma-ray (45-75 Gy) had not formed shoot in four weeks of culture, while 58.3-83.3% of the explants without irradiation or irradiated at low doses 15 and 30 Gy formed shoots. The higher irradiation doses increased percentage of browning explants and reduced the percentage of forming shoots. Within the eight weeks of culture, explant without irradiation was able to form shoots at the percentage of 100% with 24 shoots per explant, while explants irradiated at 15-45 Gy were able to grow form shoots at the percentage of 77.7-95.5%. The high doses-irradiated explants (60 and 75 Gy) were only able to form shoots less than 13-20%, with 2-3 shoots per explant.

Keywords: Gamma rays (Gy), *in vitro* shoot, *Pogostemon cablin* Benth.

INTRODUCTION

Patchouli (*Pogostemon cablin* Benth.) is one of the essential oil-producing plants. The oil is mostly found in its leaves [1]. Essential oil forms this plant is universally recognized as the best because it is the material for the food, pharmacy, and cosmetic industry [2]. Indonesian Plantation Service recorded that patchouli plantation in the country covers an area of 18,841 ha, producing 2,115 tons patchouli oil [3]. The annual demand for the oil is 60%, around 700-2,800 tons. Indonesian export is estimated to be 80% of the world's export [4].

Industrial development has made both domestic and international demand for Patchouli oil increase [5]. One of the ways to increase oil production is developing genetic variations for quality seeds through mutation induction; one of the techniques is gamma-ray mutagen treatment [6]. Successful experiments to increase essential oil content and secondary metabolites are those in *Boswellia carterii* [7], orange peel [8], and ginger (*Zingiber officinale Roscoe*) [9]. Gamma irradiation of 30-100 Gy on *in vitro* shoot explants can produce variations in *Eustoma grandiflorum* and banana (*Musa* spp.) [10,11]. Gamma-ray also affects shoot growth of Strawberry [12] banana [13] and inhibited root growth in *Rubus fraxinifolius* [14] under *in vitro* conditions. The objective of this research was to evaluate the effect of gamma irradiation on the growth and multiplication of *in vitro* patchouli shoot explants.

MATERIALS AND METHODS

Plant material

In vitro shoots of Patchouli cv. Lhokseumawe were derived from laboratory's collection. *In vitro* shoots were propagated on MS medium-supplemented 0.1 mg.L^{-1} NAA and 0.3 mg.L^{-1} BA. Two weeks old *in vitro* shoots were used as explant for gamma-ray irradiation.

Gamma irradiation of *in vitro* shoot cultures.

The gamma irradiation was carried out at National Nuclear Energy Agency, Jakarta, Indonesia. Two weeks old in vitro shoot of approximately 1 cm in length were exposed to gamma radiation at different doses of gamma-rays (0, 15, 30, 45, 60, and 75 Gy). These doses based on previous research on *Coleus blumei* to obtain new *Coleus* variances in a relatively short time [15]. The source of gamma rays was ^{60}Co gamma irradiator-Gamma Cell 220 at a dose rate of 4585.5 Grey/minute. After irradiation, treated shoots were immediately transferred to a fresh MS medium containing 0.1 mg.L^{-1} NAA and 0.3 mg.L^{-1} BA. Fives shoots were cultured in each culture bottle, and ten replicated were conducted for each gamma-ray dose (Fig. 1).

The culture was incubated at a temperature of 25±2°C and 16h day/8h dark photoperiod at the light intensity of 600 lux in a growth room for 8

* Correspondence address:
Wahyu Widoretno
Email : wahyu_widoretno@yahoo.com
Address : Dept. Biology, University of Brawijaya, Jl. Veteran Malang, 65145

ISSN. 2087-2852
E-ISSN. 2338-1655

weeks. Percentage of browning explants and shoot formation; number and length of shoot were observed every four-week. Analysis of variance (ANOVA) followed by the LSD test was used to determine the differences in mean number of all tested parameters between irradiation doses.

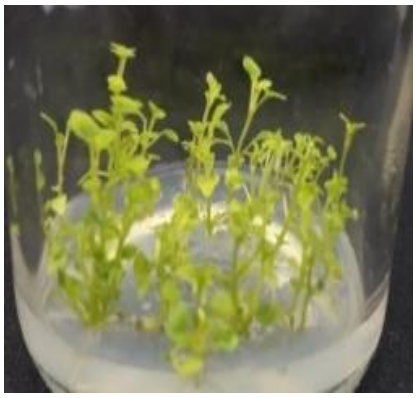

Figure 1. *In vitro* shoots used as explant for gamma ray irradiation

RESULTS AND DISCUSSIONS

The Gamma-irradiation on *in vitro* shoot explants affected the shoot growth and multiplication of patchouli. Irradiation at the doses 15-75 Gy caused browning on the shoot tip apical meristem and made the leaf yellowish. The higher the dose of irradiation, the higher was browning of explant. Gamma-ray irradiation on shoot explants also inhibited the growth of explants and the formation of new shoots. The inhibition of growth and multiplication of irradiated shoot increased as the gamma dose increased (Fig 2).

Gamma irradiation on *in vitro* shoot can increase the percentage of shoot browning and decrease shoot-forming explants. The effects of doses of gamma rays on shoot growth and formation of the new shoot during eight weeks in culture are shown in Figure 3. Gamma irradiation on shoot explant increased the percentage of shoot browning and decreased shoot-forming explant percentage, number, and length of the shoot. The browning percentage of irradiated shoot increased as the gamma dose increased.

The irradiation at the doses 15-75 Gy increased the percentage of browning 8.3-36.6% in four weeks of culture and 15.5-62% in eight weeks culture, while the shoot without irradiation (control) showed no browning (Fig. 3A). Gamma irradiation on shoot explant inhibited shoot growth and formation of a new shoot. Percentage of shoot formation and number shoot per explant of irradiated shoot explant decreased as the gamma dose increased (Fig. 3B and 3C). In four weeks of culture, the explant irradiated at higher doses of gamma rays (45-75 Gy) had not formed shoot, whereas more than 83.3% of non-irradiated explant (control) formed new shoot and 58.3-67% of irradiated explant at lower doses (15-30 Gy) formed shoot. The ability to form shoots of non-irradiated explants was ten shoots per explant, whereas at lower doses of gamma rays (15-30 Gy) was less than five shoots per explant.

Irradiation of gamma-ray also reduced the number of regenerated shoots per explant. The number of regenerated shoots reduced prominently with the increase in gamma irradiation dose. The number of regenerated shoots per explant was significantly lower at higher doses (60-75 Gy). However, at lower doses (15-45 Gy) was slightly decreased compared to control (Fig. 3C). In eight weeks of culture, 100% of non-irradiated explant produced shoot with 24 shoots per explant, while irradiated explant at lower doses of gamma rays (15-45 Gy) formed shoot was 67-77.7% with 7-20 shoots per explant.

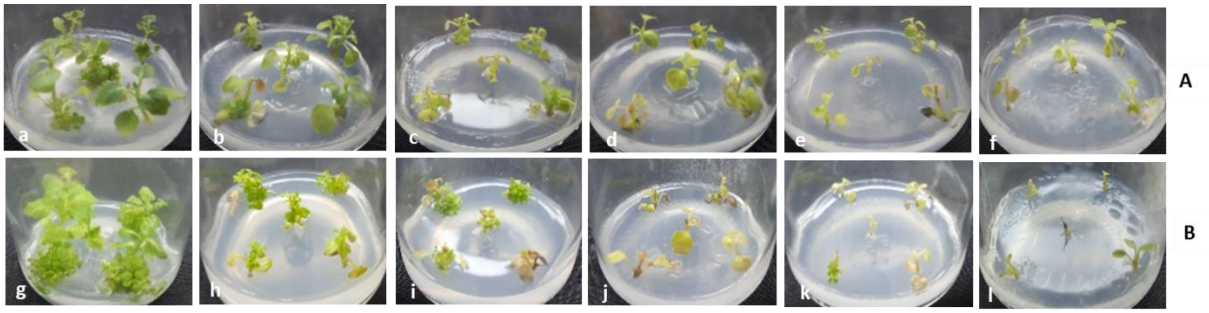

Figure 2. The responses of patchouli's *in vitro* shoot toward gamma irradiation. A. Explants were cultures for four weeks. B. Explants were cultures for eight weeks. **Description:** a,g: 0 Gy (control), b,h: 15 Gy, c,i: 30 Gy, d,j: 45 Gy, e,k: 60 Gy, f,l: 75 Gy.

ISSN. 2087-2852
E-ISSN. 2338-1655

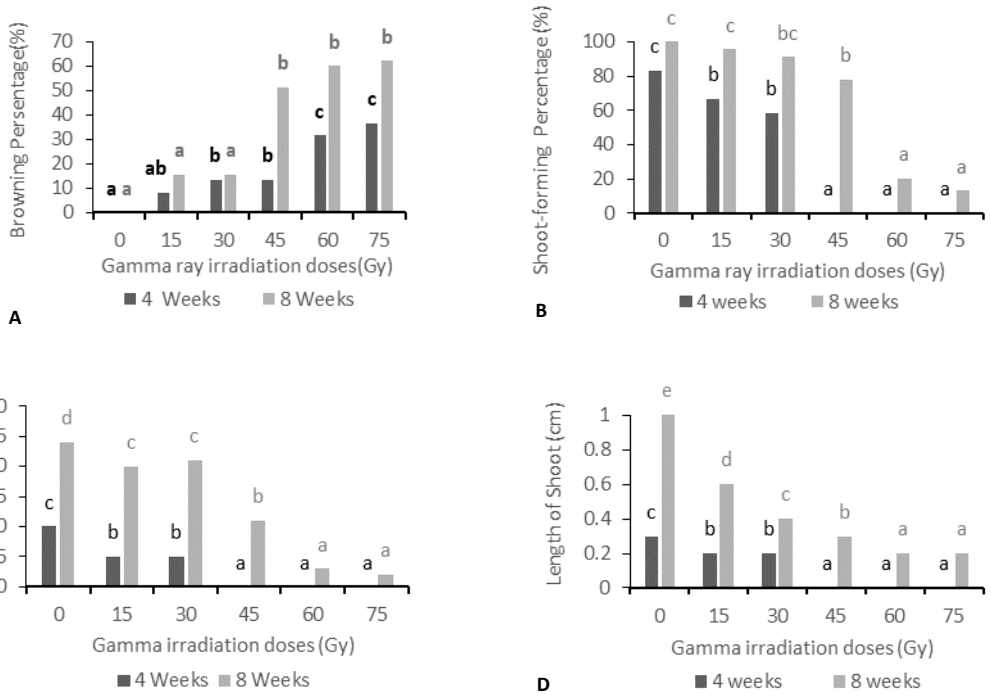

Figure 3. The effect of Gamma ray Irradiation on browning percentage, shoot-forming explant percentage, number and length of patchouli's *in vitro* shoots after 4-8 weeks of culture. **Notes:** the same letter in each observation parameter indicates insignificant difference according to 5% Duncan test.

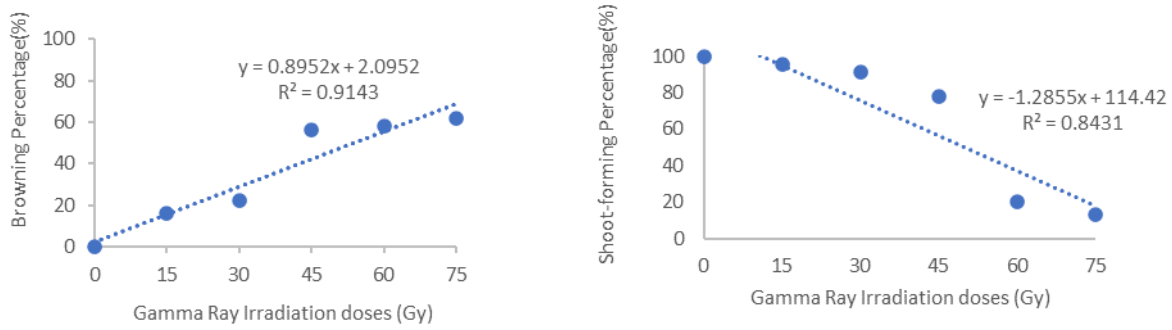

Figure 4. Correlation between gamma-ray irradiation doses and explant browning percentage and shoot-forming explant percentage

Shoot forming percentage of higher irradiated explant (60-75 Gy) was only 13-20%, with 2-3 shoots per explant (Fig. 3B and 3C). Beside shoot formed was lower, shoot growth of irradiated explant was also inhibited. The shoot length reduced with an increase in gamma irradiation doses (Fig. 3D). Shoot height growth at 8 weeks in the culture of explant without gamma-ray irradiation was about 1 cm, while shoot height growth of explant irradiated with gamma rays at doses of 15-45 Gy was between 0.3-0.6 cm. Shoot growth of explants that were irradiated by 60-75 Gy was only about 0.2 cm (Fig. 3D).

Analysis of the correlation between gamma-ray irradiation and the percentage of browning explant and the percentage of shoot forming obtained correlation coefficient R values of 0.9143 and 0.8431, respectively. There was a positive correlation between the dose of gamma-ray irradiation and the percentage of browning explants and a negative correlation between the dose of gamma-ray irradiation and the percentage

ISSN. 2087-2852
E-ISSN. 2338-1655

of shoot forming. This indicated that the increasing in the percentage of browning explant and the decreasing in the percentage of shoot formation were in line with the increase of gamma doses (Fig. 4). Gamma-ray irradiation on plant tissue caused browning and inhibited the growth and formation of a new shoot. Previous research found that explant browning caused by gamma irradiation was due to the degradation of indole acetic enzyme, which plays a role in the synthesis of IAA. The enzyme degradation produced browning of explants [16]. Browning is caused by phenol oxidation after cell membrane degradation or cell disorganization followed by chlorophyll degradation. This process is an indicator of the formation of quinones as a result of the enzyme activity [17]. Effect of gamma irradiation on explant browning also observed on shoot explant of *Colocasia esculenta* (L.) Schott [18], callus of *Ferula gummosa* [19], and plantlet of *Gerbera jamesonii* [20]. A previous study observed the effect of gamma irradiation on *in vitro* total phenolic content of *Ferula gummosa.* The research showed that the gamma irradiation-induced phenolic compound in *Ferula gummosa* callus and phenolic content increased with the increased gamma irradiation dose [19].

Cell damage from high doses of irradiation is thought to be the cause of the growth and development of Robusta BP 436 coffee to be inhibited. The inhibition of growth and development is indicated by the black callus, which indicates necrosis (cell death). High doses of gamma-ray irradiation produce free radicals in the hydroxyl form. Hydroxyl radicals or hydrogen peroxide will cause physiological damage in the form of inhibition of cell division and differentiation processes and gene damage if these hydroxyl radicals attach to the nucleotide chains causing DNA damage [21]**.**

Callus of Sugarcane (*Saccharum officinarum* L.) irradiated with gamma-ray doses 10-80 Gy cause browning at a dose of 40 Gy, and the extent of browning also increased with the increase of gamma irradiation dose [22]. Callus of Cucumis irradiated with a high-doses of 100-200 Gy experienced browning due to the absorption of gamma-ray irradiation that could increase free radicals, which damaged many cells in the callus [23]. High irradiation doses can change the ratio of the phytohormones auxin and cytokinin. It leads to the pattern change of cell differentiation, which could cause delays production of new shoots [24].

Irradiation-induced inhibition of shoot growth was caused by damage in meristem cells. The effect of irradiation was the inhibition of cell division, which results in inhibition of explant growth. Inhibition of shoot growth at higher doses of gamma rays is due to reduced mitotic activity in the meristematic tissue and reduced moisture contents of explants [25]. Chauduri also reported that irradiation at higher doses killed meristematic cells and result in the inability of the cells to absorb nutrients [26]. The inhibitory effect of the high dose of gamma rays on shoot growth was due to disruption of hormonal balance and enzymatic activities [27]. Irradiation does influence water intake to cells and the synthesis of endogenous hormones [20]. Inhibition of shoot growth due to the high dose of gamma rays was derived from cell cycle arrest at G/M phase during cell division and/or various damages in the entire genome [28].

Gamma irradiation inhibited in vitro shoot elongation of patchouli. Effect of gamma irradiation on inhibition of shoot length was observed in *Triticum aestivum* L. [29] Cicer [30], Corn [31], and Chrysanthemum [32]. Gamma irradiation prevented the shoot elongation of Cicer. The effect of gamma irradiation on shoot elongation was depending on the dose of gamma and genotype, respectively. The higher irradiation, shoot length was more affected [30]. Previous research found that gamma irradiation decreased the number of leaves and branches on Chrysanthemum [32]. Gamma-ray irradiation also had a significant impact on the shoot length of *Triticum aestivum* L. The shoot length decreased by 46% as the gamma dose increased [29]. It was observed that a decrease in shoot length is in proportion with increasing gamma dose in corn [31]. It was assumed that suppressed growth of explant tissue was caused by damage from irradiation treatment.

CONCLUSION

Gamma-ray irradiation on patchouli *in vitro* shoot inhibited shoot growth and multiplication. The irradiation of gamma rays at doses 15-75 Gy increased the browning percentage of explant and inhibited shoot formation. The percentage of shoot-forming explant, the numbers of shoots per explant, and shoot length decreased as the gamma-ray dose increased.

ISSN. 2087-2852
E-ISSN. 2338-1655

REFERENCES

[1] Ermaya, D., S.P. Sari, A. Patria, F. Hidayat, F. Razi. 2019. Identification of patchouli oil chemical components as the results on distillation using GC-MS. *IOP Conf. Earth and Environmental Science.* 365. 012039.

[2] Sufriadi, E., Y. Aisyah, F. Harahap, Y. Fernando, V.Mardina. 2020. A method for aseptic culture of bud explants *pogestemon cablin* Benth. Var Tapak Tuan, Aceh, Indonesia. *IOP Conf. Materials Science and Engineering.* 725. 012066.

[3] Suhesti, S., M. Susilowati, N. Sirait, Amalia, E. Hadipoentyanti. 2020. Morphological variations of putative patchouli mutants. *IOP Conf. Earth and Environmental Science.* 418. 012078.

[4] Lisma Y., L.M. Baga, Burhanuddin. 2018. Internal and external strategies in improving the value of patchouli agro industry case study of Koperasi Industri Nilam Aceh Barat. *Jurnal AGRISEP*. 17. 163-174.

[5] Habiburrohman, H., H.I. Agasi, L. Bernadetta. 2019. Preliminary design of high-yield patchouli (*Pogostemon cablin* Benth.) oil production system with phosphate fertilizer treatment and nutrient rich biomass production from black soldier flies (*Hermetia illucens*) larvae by applying a biorefinery concept. *UI Proceedings on Science and Technology.* 2. 48-52.

[6] Togatorop, E.R., S. I. Aisyah, M.R.M. Damanik. 2016. Effect of physical mutation by gamma ray irradiation on genetic variability and performance of *Coleus blumei*. *J. Hort. Indonesia*. 7. 187-194.

[7] Badr P., S. Daneshamouz, A.A. Mohammadi, A.R. Akbarizadeh, S. Afsharypuor. 2016. The effect of ^{60}Co-gamma radio-sterilization on *Boswellia carterii* essential oil composition. *Res. J. Pharmacogn*. 3. 67-74.

[8] Moussaid M., S. Caillet, J. Nketsia-Tabiri, C. Boubekri, M. Lacroix. Effects of irradiation in combination with waxing on the essential oils in orange peel. 2004. *J. Sci. Food Agric*. 84. 1657-1662.

[9] Magdy M.A., E.M. Fahmy, Abd EL-Rahman M.F. AL-Ansary, G. Awad. 2020. Improvement of 6-gingerol production in ginger rhizomes (*Zingiber officinale* Roscoe) plants by mutation breeding using gamma irradiation. *Appl. Radiat. Isot*. 162. 109-193.

[10] Abou-Dahab, A.M., A.A.M. Heikal, L.S. Taha., A.M.M. Gabr, S.A. Metwally, A.A.R. Ali. 2017. *In vitro* mutagenesis induction in *Eustoma grandiflorum* plant using gamma radiation. *J. Environ. Sci. Technol*. 10. 175-185.

[11] Due, M.S., A. Yunus, A. Susilowati. 2019. Banana diversity (*Musa* spp.) resulted from in vitro gamma ray irradiation based on morphological markers. *Proceeding of National Seminar of Masyarakat Biodiversitas Indonesia*. 5. 2407-8050.

[12] Gupta R., V.K. Wali, P. Bakshi, G. Singh, R.A. Shah, S. Rani. 2018. Effects of gamma irradiation on shoot, root and survival percent in strawberry cv. Chandler under *In vitro* Conditions. *Int. J. Curr. Microbiol. App. Sci*. 7. 1173-1182.

[13] Abdulhafiz F., F. Kayat, S. Zakaria. 2018. Effect of gamma irradiation on the morphological and physiological variation from In vitro individual shoot of banana cv. Tanduk (*Musa* spp.). *J. Plant Biotechnol*. 45. 140–145.

[14] Ismaini L., S. Normasiwi, M.I. Surya, Destri. 2018. Study on in vitro growth of *Rubus fraxinifolius* mutant (m1) resulted from gamma-ray irradiation (^{60}Co). *J. Agro Sci.* 6. 71-76.

[15] Aisyah S. I., Y. Marthin, M. Rizal, M. Damanik. *2015.* Improving performance of coleus through mutation induction by gamma ray irradiation. *J. Trop. Corp. Sci*. 2. 26-32.

[16] Lisdyayanti N.D., S. Anwar, A. Darmawati. 2019. Effect of gamma ray irradiation on callus induction and selection of rice tolerance level (*Oryza sativa* L.) on salinity stress by *In-Vitro*. *Berkala Bioteknologi.* 2. 67-75.

[17] Laukkanen, H., L. Rautiainen, E. Taulavuori, A. Hohtola. 2000. Changes in cellular structures and enzymatic activities during browning of Scots pine callus derived from mature buds. *Tree Physiol*. 20. 467–475.

[18] Brain, B., J. Stuar. 2019. Developing somaclonal variation of bogor taro to expand the diversity of character. *CCAMLR Sci*. 26. 50-55.

[19] Sheikhi A.A., H. Hassanpour, P. Jonoubi, M.G. Nohooji, M. Nadimifar. 2016. The effect of gamma irradiation on *In vitro* total phenolic content and antioxidant activity of *Ferula gummosa* Bioss. *J. Med. Plants.* 159. 122-131.

[20] Hasbullah N.A., R.M. Taha, A. Saleh, N. Mahmad. 2012. Irradiation effect on *in vitro* organogenesis, callus growth and plantlet

ISSN. 2087-2852
E-ISSN. 2338-1655

development of *Gerbera jamesonii*. *Hortic. Bras.* 30. 252-257.
[21] Ibrahim M.S.D., E. Randriani, L. Sari, A. Nuraini. 2019. Radiosensitivitas kalus embriogenik kopi robusta Bp 436 terhadap iradiasi sinar gamma. *J. Industrial Beverage Crops*. 6. 41-50.
[22] Nikam A.A., R.M. Devarumath, A. Ahuja, H. Babu, M.G. Shitole, P. Suprasanna. 2015. Radiation-induced in vitro mutagenesis system for salt tolerance and other agronomic characters in sugarcane (*Saccharum officinarum* L.). *The Crop Journal*. 1. 46-56.
[23] Venkateshwarlu, M. 2008. Effect of gamma rays on different explants of callus treatment of multiple shoots in Cucumis melo cv. Bathasa. *J. Environ. Biol*. 29. 789-792.
[24] RoostikaI., I. Darwati, Yudiwanti. 2013. Improvement of genetic variation of Pruatjan through gamma irradiation and *in vitro* selection. *Jurnal Littri.* 19. 88-98.
[25] Majeed, A., Muhammad, Z., Ahmad, H. and Khan, A. U. R.2009. Gamma Irradiation Effects on Some Growth Parameters of *Lepidium Sativum* L. *American-Eurasian J. Sustai. Agri*. 3. 424-427.
[26] Chauduri, K.S. 2002. A reliable and straightforward method to detect gamma irradiated lentil (*Lens culinaris* Medik.) seeds by germination efficiency and seedling growth test. *Radiat. Phys. Chem*. 64. 131-136.
[27] Wi, S.G., B.Y. Chung, J.S. Kim. 2007. Effects of gamma irradiation on morphological changes and biological responses in plants. *Micron*. 38. 553-564.
[28] Preussa, S.B., A.B. Britta. 2003. A DNA-damage-induced cell cycle checkpoint. *Arabidopsis Genetics.* 164. 323- 334.
[29] Borzouei, A., M. Kafi, H. Khazaei, B. Naseriyan, A. Majdabadi. 2010. Effects of gamma radiation on germination and physiological aspects of wheat (*Triticum aestivum* L.) seedlings. *Pak. J. Bot*. 42. 2281-2290.
[30] Toker C., B. Uzen, H. Canci, F.O. Ceylan. 2005. Effects of gamma irradiation on the shoot length of Cicer seeds. *Radiat. Phys. Chem*. 73. 365-367.
[31] Al-Salhi M, M.M. Ghannam, Al-Ayed, M.S. Al-Ayed, S.U. El-Kameesy, S. Roshdy. 2004. Effect of gamma irradiation on the biophysical and morphological properties of corn Nahrung. *Mol. Nutri. Food Res.* 48. 95-98.
[32] Dwimahyani, I., S. Widiarsih. 2010. The effects of gamma irradiation on the growth and propagation of *in-vitro* chrysanthemum shoot explants (cv. *Yellow Puma*). *Atom Indonesia.* 36. 45-49.

ISSN. 2087-2852
E-ISSN. 2338-1655

MANUSCRIPT SUBMISSION

FOCUS AND SCOPE

Journal of Experimental Life Science (JELS) is scientific journal published by Graduate Program of Brawijaya University as distribution media of Indonesian researcher's results in life science to wider community. JELS is published in every four months. JELS published scientific papers in review, short report, and life sciences especially nanobiology, molecular biology and cellular biology. JELS is scientific journal that published compatible qualified articles to academic standard, scientific and all articles reviewed by expert in their field.

Journal of Experimental Life Science (JELS) have vision to become qualified reference media to publish the best and original research results, and become the foundation of science development through invention and innovation on cellular, molecular, and nanobiology rapidly to community.

Journal of Experimental Life Science (JELS) have objectives to published qualified articles on research's results of Indonesian researchers in life science scope. JELS encompasses articles which discuss basic principles on nature phenomenon with cellular, molecular, and nanobiology approach.

PEER REVIEW PROCESS

Publication of articles by JITODE is dependent primarily on their validity and coherence, as judged by peer reviewers, who are also asked whether the writing is comprehensible and how interesting they consider the article to be. All submitted manuscripts are read by the editorial staff and only those articles that seem most likely to meet our editorial criteria are sent for formal review. All forms of published correction may also be peer-reviewed at the discretion of the editors. Reviewer selection is critical to the publication process, and we base our choice on many factors, including expertise, reputation, and specific recommendations. The editors then make a decision based on the reviewers' advice, from among several possibilities:

Accepted, with or without editorial revisions
Invite the authors to revise their manuscript to address specific concerns before a final decision

Rejected, but indicate to the authors that further work might justify a resubmission

Rejected outright, typically on grounds of specialist interest, lack of novelty, insufficient conceptual advance or major technical and/or interpretational problems

PUBLICATION FREQUENCY

JELS publish 2 Issues per year until 2017. JELS started to publish 3 Issues per year since 2018.

OPEN ACCESS POLICY

This journal provides immediate open access to its content on the principle that making research freely available to the public supports a greater global exchange of knowledge.

COPYRIGHT NOTICE

Authors who publish with this journal agree to the following terms:

Authors retain copyright and grant the journal right of first publication with the work simultaneously licensed under a Creative Commons Attribution License that allows others to share the work with an acknowledgement of the work's authorship and initial publication in this journal.

Authors are able to enter into separate, additional contractual arrangements for the non-exclusive distribution of the journal's published version of the work (e.g., post it to an institutional repository or publish it in a book), with an acknowledgement of its initial publication in this journal.

Authors are permitted and encouraged to post their work online (e.g., in institutional repositories or on their website) prior to and during the submission process, as it can lead to productive exchanges, as well as earlier and greater citation of published work (The Effect of Open Access).

PRIVACY STATEMENT

The names and email addresses entered in this journal site will be used exclusively for the stated purposes of this journal and will not be made available for any other purpose or to any other party.

ETHICS PUBLICATION

Research that using animal, human, and clinical testing is should already have ethical clearance certificate from authorized institution.

Title Typed in Bold, Capitalize each First Letter of Each Word, Except Conjunctive, *Scientific name* should not be Abbreviated (Calibri 14 Bold Center, should not exceed 12 words, except conjuctive)

First Author[1]*, Second Author[2], Third Author[3] (Calibri 12 Center, without title)

[1]First Author Affiliation, Correspondence author should be indicated by * symbol (Calibri 9 Center)
[2]Department of Biology, Faculty of Mathematics and Natural Sciences, University of Brawijaya, Malang, Indonesia
[3]Laboratorium of Physiology, Faculty of Medicine, University of Brawijaya, Malang, Indonesia

Abstract (Calibri 9 Bold Center)

This article illustrates preparation of your paper using MS-WORD (.doc or .rtf). Manuscript was numbered consecutively. Main text typed in two columns (67 characters), except title and abstract in one column. The manuscript should be written in English. The length of manuscript should not exceed 10 pages including table and figure in this format using A4 paper single space. The text should be in the margin of 3 cm up, down and left side, 2.5 cm on right side. Abstract includes the research purposes, research method and research results in one paragraph of *essay,* not *enumerative*. No citation in abstract. Abstract should not exceed 200 words. Keywords typed after abstract. (Calibri 9 Justify).

Keywords: manuscript, English, format, 5 words maximum (Calibri 9 Left)

INTRODUCTION* (Calibri 10 Bold, Left, Capslock)

All submitted manuscripts should contain original research which not previously published and not under consideration for publication elsewhere. Articles must be written in ENGLISH and manuscripts may be submitted for consideration as research report articles, short reports or reviews.

The introduction explains the background of the problem, the study of literature and research purposes. Some initial introduction paragraphs explain the problem and background to these problems [1]. The next few paragraphs explain the study of literature that contains recent knowledge development which is directly related to the issues. The last paragraph of the introductory section contains a description of the purposes of the study. (Calibri 10 Justify)

MATERIAL AND METHOD (Calibri 10 Bold, Left, Capslock)

This section describes the types of methods (qualitative, quantitative or mixed-method) with details of methods of data collection and data analysis [2]. This section also describes the perspective that underlying the selection of a particular method. (Calibri 10 Justify)

Correspondence address: (Calibri 8 Bold, Left)
Full name of correspondence author
Email : sapto@jurnal.ub.ac.id
Address : afiliation address include post code

Data Collection (Calibri 10 Bold, Left)

Explain the data collection methods, i.e. surveys, observations or archive, accompanied by details of the use of such methods. This section also describes the population, sampling and sample selection methods. (Calibri 10 Justify)

The use of English language should followed proper grammar and terms. Name of organism shoul be followed by its full scientific name in the first mention, in *italic* [3]. Author of the scientific name and the word of "var." typed regular. Example: *Stellaria saxatillis* Buch. Ham. First abbreviation typed in colon after the abbreviated phrase.

Author must use International Standard Unit (SI). Negative exponent used to show the denominator unit. Example: g l^{-1}, instead of g/l. The unit spaced after the numbers, except percentage [4]. Example: 25 g l^{-1}, instead of 25gl^{-1}; 35% instead of 35 %. Decimal typed in dot (not coma). All tables and figures should be mentioned in the text.

RESULT AND DISCUSSION (Calibri 10 Bold, Left, Capslock)

This section contains the results of the analysis and interpretation or discussion of the results of the analysis. Describe a structured, detailed, complete and concise explanation, so that the reader can follow the flow of analysis and thinking of researchers [5]. Part of the results study should be integrated with the results of the

analysis and the results and discussion are not separated.

Table

Table should be submitted within the manuscript and in separated file of *Microsoft Excel* (xls.). Table whould not exceed 8 cm (one column) and 17 cm (two columns). Table should be embedded in different page after references.

Table should be numbered in sequence. Table title should be brief and clear above the table, with uppercase in initial sentence. Vertical line should not be used. Footnote use number with colon and superscripted. Symbol of (*) or (**) was used to show difference in confidence interval of 95 and 99%.

Table 1. Example of the Table (Calibri 8.5 Left)

No	Point (Calibri 8.5 Justify)	Description
1		
2		
3		
4		
5		

Sources: Journal of PPSUB (Calibri 8.5 Left)

Figures

Figures should be in high resolution and well contrast in JPEG or PDF with the following conditions:

- Monochrome image (line art), figures of black and white diagram (solid/no shades of gray), resolution 1000-1200 dpi (dot per inch).
- Combination Halftone, combine figure and text (image containing text) and coloured graphic or in grayscale format. Resolution 600-900 dpi.
- Halftone, coloured figure or grayscale format without text. Resolution 300 dpi.
- Black and white figure should be in the grayscale mode, while coloured figures should be in RGB mode.
- Figure should not exceed the width of 8 cm (one column), 12.5 cm (1.5 columns) or 17 cm (two columns).
- Figures title typed clearly below the figure.
- Figure with pointing arrow should be grouped (grouping).
- Figures were recommended in black and white.
- Legend or figure description should be clear and complete. If compressed, the figure should be readable.
- Statistic graphic should be supplemented with data sources.
- If the figures come from the third party, it should have the copyright transfer from the sources.

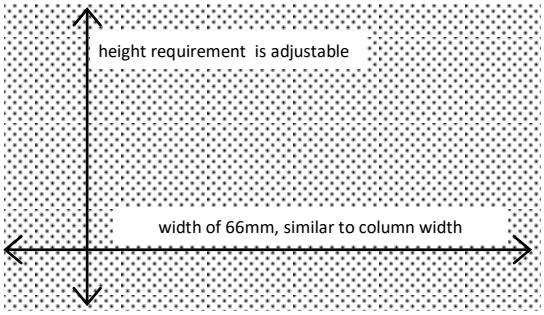

Figure 1. Illustration of Dimensional Figure of one column width. Figure dimension adjusted to the width of one column. Name the figure (diagram) written below the image. (Calibri 8.5 Justify)

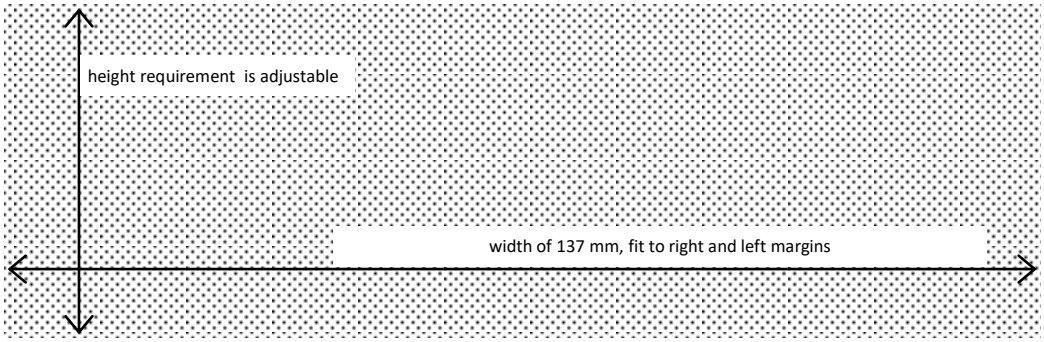

Figure 2. . Illustration of Dimensional Figure of two column width. Figure dimension adjusted to the width of two columns (137 mm). Figure were align top or bottom of the page. (Calibri 8.5 Justify)

References

1. Primary references include journal, patent, dissertation, thesis, paper in proceeding and text book.
2. Avoid self citation.
3. Author should avoid reference in reference, popular book, and internet reference except journal and private ana state institution.
4. Author was not allowed to use abstract as references.
5. References should been published (book, research journal or proceeding). Unpublished references or not displayed data can not be used as references.
6. References typed in numbering list (format number 1,2,3,…), ordered sequentially as they appear in the text (system of Vancouver or author-number style).
7. Citation in the manuscript typed only the references number (not the author and year), example: Obesity is an accumulation of fat in large quantities which would cause excessive body weight (overweight) [1]. Obesity is a risk factor of diabetic, hypertension dan atherosclerosis [2].

CONCLUSION (Calibri 10 Bold, Left, Capslock)

Conclusion of the study's findings are written in brief, concise and solid, without more additional new interpretation. This section can also be written on research novelty, advantages and disadvantages of the research, as well as recommendations for future research.(Calibri 10 Justify)

ACKNOWLEDGEMENT (Calibri 10 Bold, Left, Capslock)

This section describes gratitude to those who have helped in substance as well as financially. (Calibri 10 Justify)

REFERENCES (Calibri 10 Bold, Left, Capslock)

[1]. (Calibri 10 Justify, citation labelling by references numbering)
[2]. Vander, A., J. Sherman., D. Luciano. 2001. Human Physiology: The Mecanisms of Body Function. McGraw-Hill Higher Education. New York. (Book)
[3]. Shi, Z., M. Rifa'i, Y. Lee, K. Isobe, H. Suzuki. 2007. Importance of CD80/CD86-CD28 interaction in the recognation of target cells by $CD8^{+}CD122^{+}$ regulatory T cells. *Journal Immunology.* 124. 1:121-128. (Article in Journal)
[4]. Syafi'i, M., Hakim, L., dan Yanuwiyadi, B. 2010. Potential Analysis of Indigenous Knowledge (IK) in Ngadas Village as Tourism Attraction. pp. 217-234. In: Widodo, Y. Noviantari (eds.) Proceed-ing *Basic Science National Seminar 7* Vol.4. Universitas Brawijaya, Malang. (Article within conference proceeding)
[5]. Dean, R.G. 1990. Freak waves: A possible explanation. p. 1-65. *In* Torum, A., O.T. Gudmestad (eds). Water wave kinetics. CRC Press. New York. (Chapter in a Book)
[6]. Astuti, A.M. 2008. The Effect of Water Fraction of *Stellaria* sp. on the Content of TNF-α in Mice (*Mus musculus* BALB-C). Thesis. Department of Biology. University of Brawijaya. Malang. (Thesis)

Cover Image
3D Structure of EGCG (Epigallocatechin-3-Gallate)
Green Tea Component
Created by ::
Prof. Widodo, S.Si.,M.Si.,Ph.D MED Sc.

Address :
Building B, 1st Floor, Graduate Program Universitas Brawijaya
Jl. Mayor Jenderal Haryono 169, Malang, 65145,
East Java, Indonesia
Tel.: (+62341) 571260; Fax: (+62341) 580801
Email: jels@ub.ac.id
Web: jels.ub.ac.id

9 772087 285007